



**Politecnico
di Torino**

Politecnico di Torino

Laurea Magistrale in Ingegneria Biomedica
Orientamento Strumentazione Biomedica
A.A. 2021/2022
Sessione di Laurea di Luglio 2022

**Measuring the impact of a
twelve-week aerobic training
program on respiratory
parameters using Airgo™**

Relatore: Molinari Filippo
Correlatore: Kuller David

Candidata: Rigazio Sofia

Table of Contents

List of Figures	V
Abstract	1
Chapter 1 The Respiratory System	5
1.1 Anatomy and Physiology	5
1.1.1 Airways	5
1.1.2 Pulmonary pleurae	7
1.2 Ventilation Mechanics	8
1.2.1 Gas pressure and Boyle's law	8
1.2.2 Inspiration	8
1.2.3 Expiration.....	10
1.2.4 Dead space.....	10
1.3 Control of Ventilation.....	11
1.3.1 Dorsal respiratory group.....	12
1.3.2 Ventral respiratory group.....	12
1.3.3 Peripheral chemoreceptors.....	13
1.3.4 Central chemoreceptors.....	14
1.3.5 Lung receptors.....	15
Chapter 2 Monitoring Respiratory Health	17
2.1 Time Parameters.....	17
2.1.1 Respiratory rate	17
2.1.2 Inspiratory and expiratory time	18
2.1.3 Minute ventilation.....	18
2.2 Lung Volumes and Capacities.....	18
2.2.1 Spirometry.....	21
2.2.2 Gas dilution.....	22
2.2.3 Plethysmography.....	23
Chapter 3 Respiratory Variability	27
3.1 Nonrandom Variability	28

3.2 Sighs	29
3.2.1 Physiological factors influencing sighs	30
3.2.2 Sighs as resetters.....	30
Chapter 4 Airgo™	33
4.1 Device Description	34
4.1.1 Airgo™ Recorder	35
4.1.2 aWare strap belt.....	35
4.1.3 Device positioning.....	37
4.2 Software Description	39
4.2.1 Airgo™ app.....	39
4.2.2 Airgo™ Semantic Engine	39
4.3 Device Applications	41
4.3.1 Sleep quality assessment.....	41
4.3.2 Other applications.....	42
Chapter 5 Study Description	45
5.1 Participants	45
5.2 Methods	46
5.2.1 Study design	46
5.2.2 Home data collection	47
5.3 Results	48
5.3.1 Physicality.....	48
5.3.2 Cardiovascular fitness.....	48
5.3.3 Cognitive performance.....	48
5.3.4 Sleep analysis.....	49
Chapter 6 Airgo™ Data Analysis	51
6.1 Airgo™ Data	51
6.2 Methods	51
6.2.1 Breath vectors (CQBV).....	51
6.2.2 Calculation of parameters	52
6.2.3 Daytime and Nighttime isolation	54
6.2.4 Resting state detection	55
6.2.5 Sigh identification	55
6.2.6 Respiratory variability analysis	56
6.2.7 Sigh breath variability	59
6.3 Results	61
6.3.1 Time and Volume parameters.....	61

6.3.2	Sigh rate and amplitude.....	63
6.3.3	Respiratory variability.....	64
6.3.4	Sigh breath variability.....	67
6.4	Discussion.....	68
6.4.1	Respiratory parameters.....	68
6.4.2	Sigh rate and amplitude.....	68
6.4.3	Sigh breath variability.....	69
6.4.4	Sighs as nonrandom respiratory variability reseters.....	69
6.5	Limitations.....	69
6.6	Conclusion.....	70
	References.....	71
	Acknowledgements.....	85

List of Figures

- Figure 1.1:** The upper respiratory tract (left) consists of nose (or nostrils), nasal cavity, mouth, pharynx, and larynx. The lower respiratory tract (right) consists of trachea and, inside the lungs, bronchi, bronchioles, and alveoli. Source: [137] and [138]. 5
- Figure 1.2:** Lungs, bronchial tree and alveoli. Source: [135]. 6
- Figure 1.3:** Schematic illustration of the anatomy of an alveolus and a surrounding pulmonary capillary. Source: [134]. 6
- Figure 1.4:** Frontal (left) and transversal (right) view of the lower respiratory tract, with particular attention to pulmonary pleurae and pleural space. Source: [136]. 7
- Figure 1.5:** During inspiration (left), the diaphragm contracts and the external intercostal muscles contract, expanding the rib cage and causing air to flow into the lungs; during expiration (right), the diaphragm and the intercostal muscles relax, reducing the volume of the thoracic cavity and causing air to exit the lungs. Source: [139]. 9
- Figure 1.6:** Rib cage and intercostal muscles; intercostal muscles are located between the ribs. Source: [140]. 10
- Figure 1.7:** Schematic representation of the respiratory areas in the brain stem and spinal cord. Abbreviations: nA, nucleus ambiguus; nVII, facial nucleus; nXII, hypoglossal nucleus; nTS, nucleus of the solitary tract; DRG, dorsal respiratory group; PRG, pontine respiratory group; RVLN, rostral ventrolateral medulla; pFRG, para-facial respiratory group; VRG, ventral respiratory group; and C4, corresponding segment of the spinal cord. Source: [141]. 11
- Figure 1.8:** The aortic bodies are located near the aortic arch; the carotid bodies are located close to the carotid bifurcation on each side. Source: [26]. 13
- Figure 1.9:** Negative feedback loop induced by the effect of acidemia or hypercapnia on peripheral chemoreceptors in the control of ventilation. 14
- Figure 1.10:** Ventral view of the brain stem in which the three chemosensitive areas on each side of the ventral medulla are highlighted. Source: [12]. 14

Figure 2.1: Schematic representation of standard lung volumes and capacities on a volume-time spirogram. The four standard lung volumes are tidal (V_T or V_T), inspiratory reserve (IRV), expiratory reserve (ERV) and residual (RV) volumes. The four standard lung capacities are inspiratory (IC), functional residual (FRC), vital (VC) and total lung (TLC) capacities [144]. Source: [143].	19
Figure 2.2: Patient undergoing a spirometry test, assisted by a technician. Modified from [145].	21
Figure 2.3: Patient sitting in a body plethysmography chamber. Modified from: [147].	23
Figure 2.4: Elastic band placement for respiratory inductive plethysmography: the first band is placed at the level of the nipples, while the second one is placed at the umbilicus. Modified from: [148].	24
Figure 2.5: Example of marker placement for optoelectronic plethysmography. Source: [146].	25
Figure 3.1: Graph showing the growth of interest by the scientific community to respiratory variability over the last fifty years. Data source: [142].	28
Figure 4.1: The first prototype of the Conscious Clothing system, which won the 2013 US HHS / EPA “My Air, My Health Sensor Challenge”, and eventually evolved to become Airgo™. Source: [149].	33
Figure 4.2: Current (2022) external appearance of Airgo™. The wearable device consists of two parts: Airgo™ Recorder and aWare strap belt.	34
Figure 4.3: A close-up picture of the aWare strap belt. A silver coated yarn is interweaved in the nylon and spandex matrix.	35
Figure 4.4: SensorMedics’ normalized volumes and AirGo™’s normalized amplitudes in standing position for one of the subjects enrolled for the validation study. Source: [117].	36
Figure 4.5: Exemplary graph showing the non-linear relationship between the stretch of aWare belt and its electric resistance. The range of work should be in the “linear dynamic” region, between L1 and L2. LT is the length threshold and LM is the maximum length. Source: [115].	37
Figure 4.6: Schematic representation of the patented [115] belt placement of the Airgo™ device.	38

Figure 4.7: iOS version of the Airgo™ app for mobile devices. Source: [116].....	39
Figure 4.8: Example of Respiratory Instability Curve™.....	40
Figure 4.9: How the RIC™ is oriented with respect to the light blue Target area indicates the severity of the patient’s sleep disorders. The green curve represents a Risk Category of “None”, which in traditional PSG corresponds to AHI < 7; the blue curve represents a Risk Category “Mild”, which corresponds to AHI between 7 and 15; the orange curve represents a Risk Category “Moderate”, which corresponds to AHI between 15 and 30; the red curve represents a Risk Category “Severe”, which corresponds to AHI > 30.....	41
Figure 4.10: The cover of the sleep report provides an overview of the patient's sleep quality, showing the sleep quality index and the Respiratory Instability Curves™.	42
Figure 5.1: Summary of the study design. PSG, CPET, cognitive testing and blood draw were repeated before and after the twelve-week exercise program during which the participants were continuously monitored using screening devices at home.....	47
Figure 5.2: Comparison of cardiovascular fitness indicators (VO ₂ max, resting heart rate and sleeping heart rate) between the baseline (Pre-Ex) and the end of the twelve-week exercise program (Post-Ex). The asterisk is set as statistical significance (p < 0.05).	48
Figure 5.3: Comparison of sleep stage percentages between the baseline (Pre-Ex) and the end of the twelve-week exercise program (Post-Ex). W is for Wake, REM is for rapid eye movement and NREM is for non-rapid eye movement. Neither technique (PSG nor Home EEG) found statistically significant differences between Pre- and Post-Ex.	49
Figure 5.4: Comparison of traditional sleep quality measures between the baseline (Pre-Ex) and the end of the twelve-week exercise program (Post-Ex). WASO is for wake after sleep onset. Neither technique (PSG nor Home EEG) found statistically significant differences between Pre- and Post-Ex.	50
Figure 6.1: Two minutes of raw belt signal with superimposed tail and tip points of the computed CQBV's for a subject (BHE02).	51
Figure 6.2: Ten minutes of breath vectors, activity level, time and volume parameters calculated for a subject (BHE04).	53
Figure 6.3: Result of the resting state detection algorithm on the first day of a subject (BHE02). Blue represents the full activity level signal; superimposed in red is the activity level of the epochs detected by the algorithm as resting state.	55

Figure 6.4: Recapitulatory scheme about the procedures followed in the analysis of the autocorrelation sequences, described in subsection 6.2.6.....	57
Figure 6.5: Autocorrelation sequences calculated on respiratory rate, tidal volume and inspiratory time for a subject (BHE02) over the resting epochs of the first day of acquisition (5 th December 2019). Data is mean \pm standard error.	58
Figure 6.6: Autocorrelation sequences (ACSs) obtained averaging data coming from every day of every subject. The graphs in the left column represent data from daytime at rest, while the graphs in the right column represent data coming from nighttime acquisitions. Data is mean \pm standard deviation.	59
Figure 6.7: Comparison of time and volume respiratory parameters between the baseline (Pre-Ex) and the end of the exercise program (Post-Ex). Daytime at rest and nighttime were analyzed separately. Statistically significant differences between Pre- and Post-Ex were found for inspiratory time, inspiratory to expiratory time ratio and minute ventilation during nighttime. The asterisk is set as statistical significance ($p < 0.05$).	62
Figure 6.8: Comparison of sigh rate and sigh amplitude relative to surrounding breaths between the baseline (Pre-Ex) and the end of the exercise program (Post-Ex). Daytime at rest and nighttime were analyzed separately. Statistically significant differences between Pre- and Post-Ex were found for relative sigh amplitude during daytime at rest. The asterisk is set as statistical significance ($p < 0.05$).	63
Figure 6.9: Comparison of variability in time elapsed between sighs and sigh amplitude relative to surrounding breaths between the baseline (Pre-Ex) and the end of the exercise program (Post-Ex). Daytime at rest and nighttime were analyzed separately. Statistically significant differences between Pre- and Post-Ex were found for variability in relative sigh amplitude during daytime at rest. The asterisk is set as statistical significance ($p < 0.05$).	67

Abstract

Aim of the study

The aim of this work was to investigate the effects of a twelve-week moderate intensity aerobic exercise program on respiratory health of previously sedentary adults.

Moreover, the hypothesis that sigh breath variability in terms of both rate and amplitude could be an indicator of lung health was tested for the first time.

The work will be presented in six chapters, the content of which is briefly summarized below.

Chapter 1: The Respiratory System

The first chapter of this thesis provides a general description of the respiratory system. Firstly, anatomy and physiology are illustrated. Then, ventilation mechanics are described. Lastly, the physiological mechanisms associated with the control of breathing are discussed.

Chapter 2: Monitoring Respiratory Health

The second chapter provides a review of the measurements performed to assess the health status of the respiratory system. Both time parameters such as respiratory rate and lung volumes and capacities such as tidal volume are described, and their meaning is explained.

Moreover, the standard tests performed to measure both relative and absolute lung volumes and capacities are described.

Chapter 3: Respiratory Variability

The third chapter introduces the concept of respiratory variability. Both random and nonrandom respiratory variability are discussed, explaining how the respiratory system adapts and responds to external stimuli in order to maintain homeostasis. Similarly to heart rate variability, nonrandom respiratory variability appears to be functional and healthy.

Furthermore, this chapter discusses the theme of sigh breaths. A definition of sighing is provided, along with the description of central and peripheral physiological factors that influence sighing.

Lastly, the hypothesis that sighs serve as a physiological resetters of optimal respiratory regulation is covered. Among other things, according to this hypothesis randomness in respiratory variability should increase while approaching the next sigh, and, following a spontaneous sigh, autocorrelation in breathing parameters should be reset. This hypothesis has been investigated in this work, and significant results have been obtained.

Chapter 4: Airgo™

Chapter four describes Airgo™, the device through which all data used in the present work was acquired. The recorded signal is a measure of resistance of the belt which is placed around the subject's chest in a patented position: the resistance of the belt changes accordingly to the expansion and contraction of the subject's chest, capturing movements of both the rib cage and the diaphragm. Starting from the raw Airgo™ signal both time parameters, such as respiratory rate and inhalation time, and relative lung volumes, such as tidal volume, can be derived.

Moreover, a description of Airgo™ software and current device applications is provided. Nowadays, the Airgo™ device is mainly used for sleep analysis.

Chapter 5: Study Description

The fifth chapter describes the participants, methods and results of the study *Brain Age and Exercise: A Trial of Aerobic Exercise to Improve Brain Health in Older Adults*, conducted by An Ouyang and his collaborators in Boston, MA.

The aim of the study was to investigate the effects of a twelve-week aerobic exercise program on previously sedentary adults. Cardiovascular fitness, cognitive performance and sleep quality were considered.

The Airgo™ device was worn continuously by the participants: the data acquired was stored and left for future analysis, which was the focus of this thesis.

Chapter 6: Airgo™ Data Analysis

The last chapter provides a detailed description of the procedures followed to analyze Airgo™ data coming from the study conducted by An Ouyang and his collaborators in Boston, MA.

Starting from the raw Airgo™ belt signal, breaths were identified and represented as vectors (CQBV) using Airgo™ patented algorithms. From CQBV, time and volume breathing parameters were calculated.

Daytime and nighttime were analyzed separately. For daytime analysis, resting state was isolated using an automated algorithm. Moreover, sighs were identified in the signal using another automated algorithm.

Changes in time and volume parameters were sought comparing data acquired at the beginning of the program, taken as baseline, with data acquired at the end. The hypothesis that sighs may serve as respiratory variability resetters was investigated using data acquired throughout the exercise program.

Chapter 1 The Respiratory System

The respiratory system begins at the nose and ends at the alveoli. As shown in Figure 1.1, it is divided into the upper and lower respiratory tracts. The upper respiratory tract consists of nose (or nostrils), nasal cavity, pharynx, and larynx; the lower respiratory tract consists of trachea and, inside the lungs, bronchi, bronchioles, and alveoli.

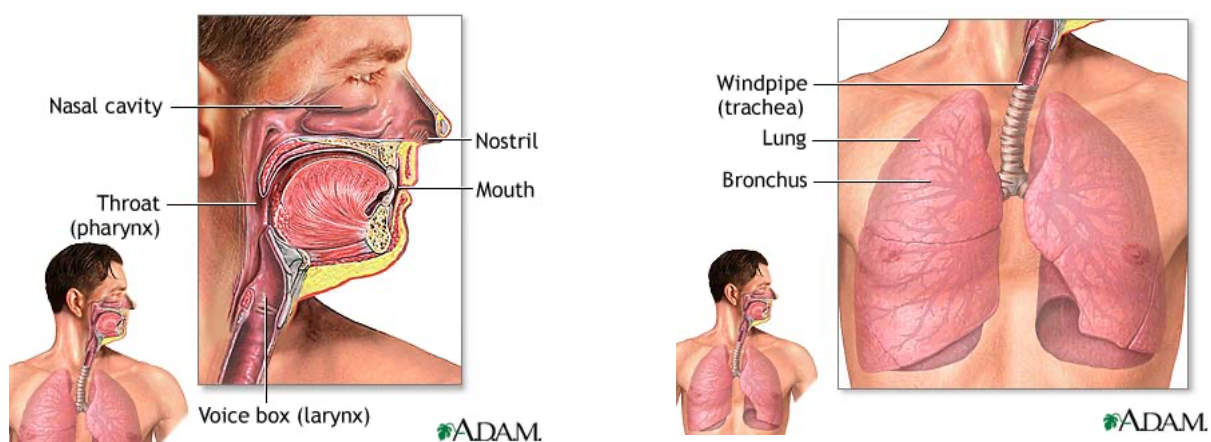


Figure 1.1: The upper respiratory tract (left) consists of nose (or nostrils), nasal cavity, mouth, pharynx, and larynx. The lower respiratory tract (right) consists of trachea and, inside the lungs, bronchi, bronchioles, and alveoli. Source: [137] and [138].

The role of the respiratory system is to provide gas exchange between the body and the atmosphere; to achieve this purpose, it works in synergy with the cardiovascular system. The exchange process occurs at the alveoli: here, oxygen flows from the external air into the blood carried by pulmonary capillaries and carbon dioxide goes the opposite way, thus exiting the body.

1.1 Anatomy and Physiology

1.1.1 Airways

The airways start from the nose and the mouth, where the inhaled air is warmed and moistened [1], continue into the pharynx, which is in common with the digestive system, and proceed into the larynx.

The epiglottis, a cartilaginous structure present at the entrance of the larynx prevents liquids or food from proceeding further in the airways as it closes during swallowing, thus

forcing food and liquids to go along the esophagus instead.

The larynx, which is also called *voice box*, is the first tract of the trachea and hosts the vocal cords. Air proceeds along the trachea and, at its end, divides in the two primary bronchi, one for each lung.

As shown in Figure 1.2, each of the two main bronchi divides in two secondary bronchi, each of which further divides in smaller and smaller branches. The smallest structures are the bronchioles, which terminate in the alveoli.

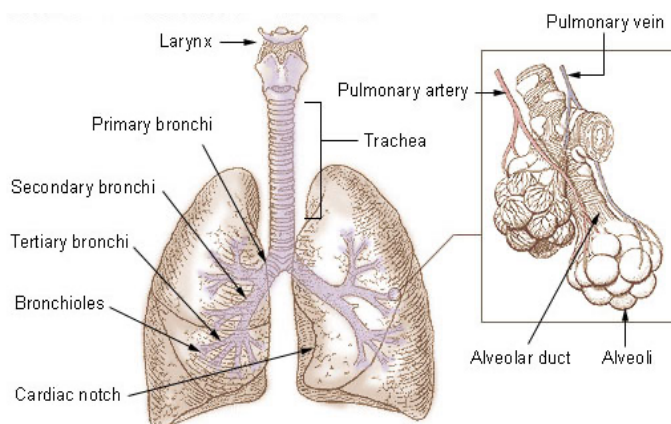


Figure 1.2: Lungs, bronchial tree and alveoli. Source: [135].

The alveoli are the small air sacs where the gas exchange takes place. As shown in Figure 1.3, they are made of simple squamous epithelium, which consists of a single layer of polygonal cells (Type I), and cuboidal cells (Type II) which secrete surfactant. The aim of the surfactant is to maintain the alveolus fluid balanced.

In a human adult, the estimated number of alveoli is of the order of hundreds of millions per lung: the actual number increases with the lung size [2]. The large number of alveoli provides an enormous surface to be used for gas exchanging. The mean size of the single alveolus is around $4.2 \times 10^6 \mu\text{m}^3$ (range: $3.3 - 4.8 \times 10^6 \mu\text{m}^3$; coefficient of variation: 10%), independently on the lung size [2].

External air, which enters the airways at ambient temperature, is warmed up to body temperature before reaching the alveoli. Moreover, since the walls of the bronchi and of the following structures are rich with blood vessels and mucus, which is 97% water [3], the air is moistened until water saturation. Thus, the air that reaches the alveoli is referred to as BTPS (Body Temperature and Pressure, Saturated).

Figure 1.3: Schematic illustration of the anatomy of an alveolus and a surrounding pulmonary capillary. Source: [134].

Each alveolus is in close contact with the surrounding pulmonary

capillaries. External air enters the alveolus as the person inhales: at this point, only two single-cell layers separate air and blood; these two layers (the endothelium of the capillary and the epithelium of the alveolus) form the respiratory membrane. Due to the very low thickness of the respiratory membrane, which varies from 0.2 to 0.6 μm [4], gases can diffuse very quickly between air and blood; the speed of diffusion must be adequate for achieving the proper gas exchange. O_2 diffuses from air to blood, while CO_2 flows in the opposite direction: after the gas exchange at the alveoli, the oxygenated blood in the pulmonary capillaries is ready to return to the heart and enter the systemic circulation.

As the person exhales, the CO_2 -rich air in the lungs is expelled from the body; the expired air differs from the BTPS condition as its temperature decreases from body temperature to ambient temperature. The exhaled air, which remains fully saturated with water vapor, is referred to as ATPS (Ambient Temperature and Pressure, Saturated).

1.1.2 Pulmonary pleurae

The pulmonary pleurae are serous membranes that allow the adhesion of the lungs to the inside of the chest walls. As shown in Figure 1.4, the inner pleura, called *visceral pleura*, covers the surface of the lungs; the outer one, the *parietal pleura*, wraps the inside of the thorax. Each pleura is composed of three layers: a single layer of mesothelial cells, a membrane and a layer of connective tissue containing lymphatics and blood vessels [5].

The space between the pleurae is referred to as *pleural cavity*, *pleural space* or *interpleural space*; it is filled with pleural fluid, which is a serous fluid produced by the pleurae.

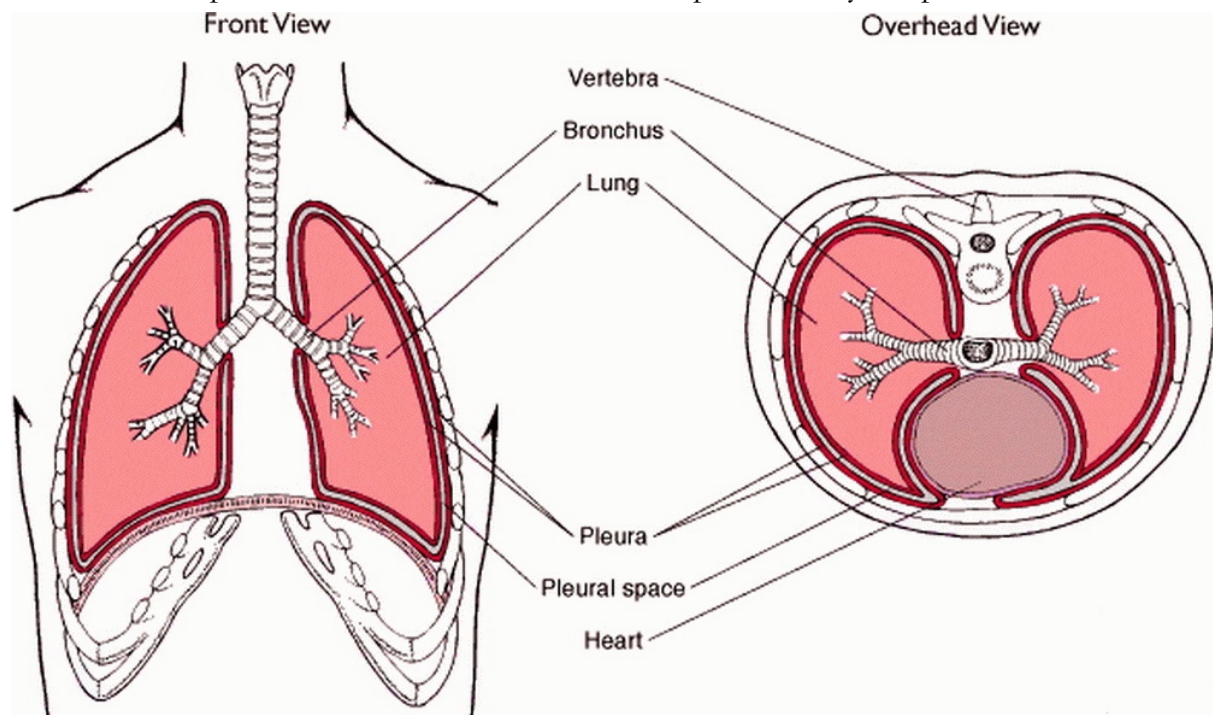


Figure 1.4: Frontal (left) and transversal (right) view of the lower respiratory tract, with particular attention to pulmonary pleurae and pleural space. Source: [136].

The layer of pleural fluid is very thin and has excellent lubricating properties.

The pleural fluid is produced continuously, and its excess is removed by the lymphatic system: this allows to maintain a slight suction, which creates a pressure gradient between the intrapleural space and the atmospheric pressure. The pressure gradient keeps the lungs attached to the thoracic cavity and links their movement to it, thus preventing them from collapsing.

1.2 Ventilation Mechanics

The ventilation consists of the alternance of a phase of inspiration, in which air flows into the lungs, and a phase of expiration, during which air flows out. The air movement is caused by pressure gradients created by the contraction of specific thoracic muscles; thus, the ventilation mechanics are strictly related to the anatomy of the chest.

1.2.1 Gas pressure and Boyle's law

In a gas, molecules are in constant random motion. While moving, the molecules frequently collide with each other and with the walls of the container. As the molecules collide with the walls of the container, they produce a force perpendicular to its wall. The pressure of a gas is defined as the sum of all the forces produced by the impact of the molecules on the walls divided by the wall area.

Boyle's law describes the relationship between the volume and the pressure of a gas: as volume increases, pressure decreases and vice-versa [6]. The law is mathematically stated as:

$$P \propto \frac{1}{V} \quad (1)$$

1.2.2 Inspiration

Inspiration is obtained as a result of increasing the volume of the thoracic cavity.

The pressures involved in pulmonary ventilation are atmospheric pressure, intrapulmonary (intra-alveolar) pressure and intrapleural pressure [7]. As the volume of the thoracic cavity increases, so does the volume of the lungs due to the intrapleural pressure. As the volume of the lungs increases the intrapulmonary pressure decreases, as stated by Boyle's law. This produces a negative pressure gradient between the air inside the lungs and the air in the atmosphere, which causes external air to flow into the lungs.

The muscles belonging to the thoracic wall act primarily during breathing [8]; the most important of these muscles are the diaphragm and the external and internal intercostals.

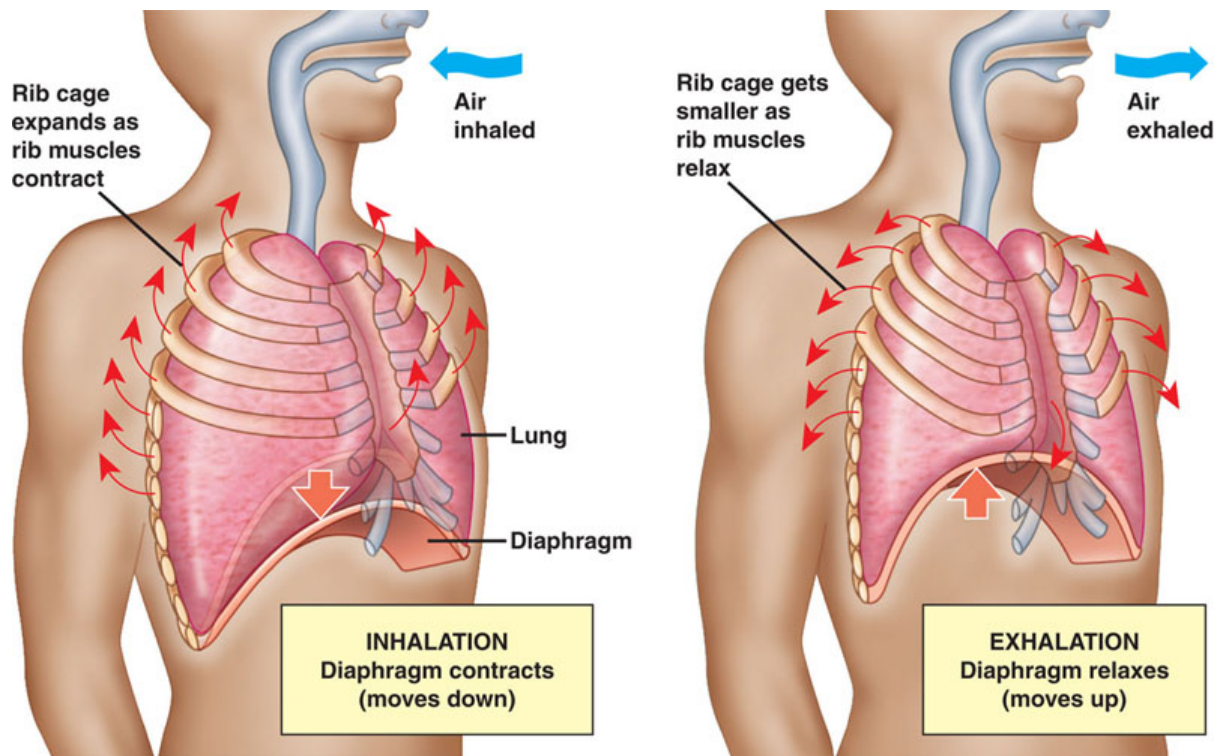


Figure 1.5: During inspiration (left), the diaphragm contracts and the external intercostal muscles contract, expanding the rib cage and causing air to flow into the lungs; during expiration (right), the diaphragm and the intercostal muscles relax, reducing the volume of the thoracic cavity and causing air to exit the lungs. Source: [139].

As shown in Figure 1.5, the muscles involved in the inspiration phase of tidal breathing are the diaphragm and the intercostal muscles.

During demanding physical activity, the respiratory system adapts to the oxygen demands of the body: the rib cage moves faster with respect to resting states to allow the increase of respiratory rate. In this case, other muscles add to the normally recruited ones: the pectoralis minor, the scalene, and the sternocleidomastoid [9].

1.2.2.1 Diaphragm

The diaphragm is the skeletal muscle that separates the thoracic and abdominal cavities.

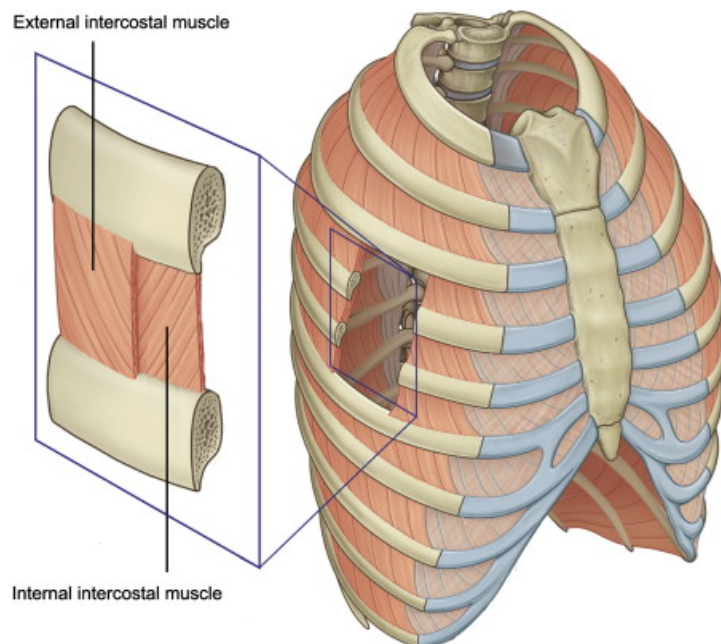
As shown in Figure 1.5, when relaxed the diaphragm assumes a dome-like shape; its contraction makes it flatten and move down towards the abdomen, thus increasing the volume of the thoracic cavity. During tidal breathing, the diaphragm is responsible for 75% of the air movement [9].

Using MRI techniques, the average inferior-superior excursion of the diaphragm during tidal breathing was evaluated to be of the order of a few tens of millimeters [10].

1.2.2.2 Intercostal muscles

The expansion of the thoracic cavity is also obtained contracting the external intercostal muscles and relaxing the internal ones (Figure 1.6).

The synergic contraction of the external intercostal muscles and the serratus posterior superior pulls the ribs and the sternum upwards and outwards.



1.2.3 Expiration

During normal breathing, the expiration phase occurs passively; as shown in Figure 1.5, the exhalation of air is obtained relaxing the diaphragm and the external intercostal muscles, which reduces the volume of the thoracic cavity; the elastic recoil of the lung tissue also contributes to the volume reduction. The reduction of the intrathoracic volume increases its pressure, as stated by Boyle's law; this produces a positive pressure gradient between the air inside the lungs and the air in the atmosphere, which causes external air to exit the lungs.

Figure 1.6: Rib cage and intercostal muscles; intercostal muscles are located between the ribs. Source: [140].

During forced expiration, in addition to the relaxation of the diaphragm and the external intercostal muscles, the innermost intercostal muscles contract, applying force to the bottom and sides of the lungs. Abdominal muscles can also be recruited to assist the inner intercostal muscles and force the diaphragm upwards [9].

Although forced expiration reduces the thoracic volume to a smaller value with respect to the resting volume, it is not possible to completely empty the lungs.

1.2.4 Dead space

When a person breathes in, not all the inhaled air reaches the gas-exchanging areas of the airways. The last air to enter the body remains far from the terminal bronchioles and can't even reach them via diffusion in the short time between the inspiration and the following expiration. Dead space represents the volume of ventilated air that does not take part in gas exchange.

Two types of dead space can be identified:

- anatomical dead space: volume of airways which does not provide any means of gas exchange, which includes nose and mouth, trachea and bronchi. Therefore, anatomical dead space only has the function of conducting air to and from the gas-exchanging sites.
- physiologic (or *total*) dead space: anatomical dead space plus alveolar dead space. Alveolar dead space is the volume of air that reaches the alveoli but does not take part in gas exchange. In healthy individuals, alveolar dead space is considered negligible; thus, physiologic dead space assumes the same value as the anatomical dead space.

The value of dead space in adult men is evaluated as 30% of normal tidal volume, which is 500 mL (see section 2.2), thus resulting in 150 mL [11].

1.3 Control of Ventilation

Breathing is essential to supply oxygen to the body and remove the excess of carbon dioxide. Through ventilation control, which refers to the physiological mechanisms

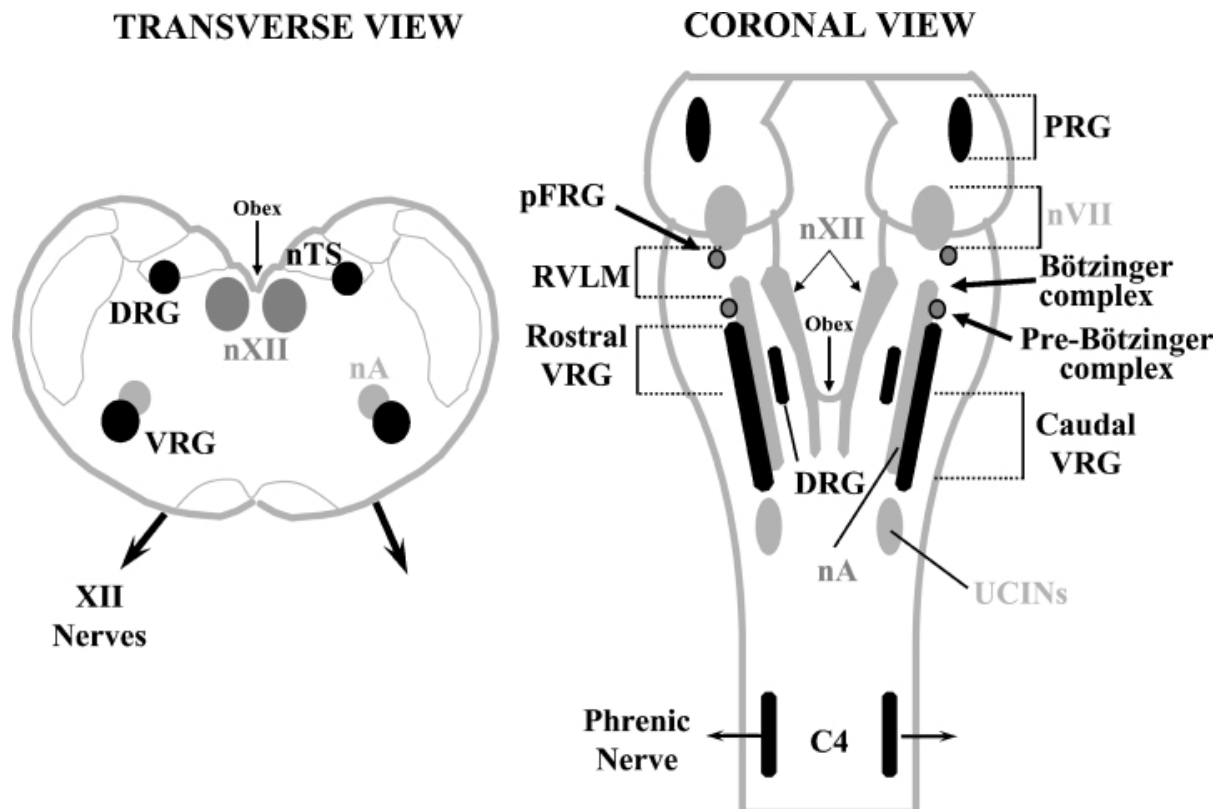


Figure 1.7: Schematic representation of the respiratory areas in the brain stem and spinal cord. Abbreviations: nA, nucleus ambiguus; nVII, facial nucleus; nXII, hypoglossal nucleus; nTS, nucleus of the solitary tract; DRG, dorsal respiratory group; PRG, pontine respiratory group; RVLM, rostral ventrolateral medulla; pFRG, para-facial respiratory group; VRG, ventral respiratory group; and C4, corresponding segment of the spinal cord. Source: [141].

associated with the control of breathing, the respiratory system adapts its activity to match the needs of the body.

Ventilation is controlled by the central nervous system; both voluntary and involuntary control of ventilation are possible. Voluntary control arises from the cerebral cortex, while involuntary control comes from the brain stem, in particular from pons and medulla [12].

Through experiments on animals that involved the transection of the brain stem at different levels, the existence of the following structures was discovered:

- Pontine respiratory group (PRG): it switches off inspiration.
- Apneustic center in the middle pons: it prevents the switch off of inspiration.
- Dorsal respiratory group (DRG), located in the dorsal medial medulla.
- Ventral respiratory group (VRG), located in the ventrolateral region of the medulla.

A schematic representation of the respiratory areas in the brain stem is shown in Figure 1.7.

1.3.1 Dorsal respiratory group

The DRG receives sensory information from the peripheral chemoreceptors in the aortic and carotid body (see subsection 1.3.3) and from pulmonary stretch receptors (see subsection 1.3.5). This afferent information reaches the DRG via the vagus and glossopharyngeal nerves.

The DRG is mainly composed of neurons called *I neurons*, which stands for neurons that drive inspiration. I neurons excite motor neurons whose axons form the phrenic nerve, which activates the diaphragm.

Consistently with the other structures in the central nervous system, the DRG is divided in a left and a right half; efferent fibers from the two halves cross the midline at the medulla, thus heading to the contralateral side.

1.3.2 Ventral respiratory group

In addition to containing I neurons, which fire action potentials during inspiration, the VRG also contains E neurons. E neurons, where E stands for Expiratory, fire action potentials during the expiratory phase of the respiratory cycle.

As it happens for the DRG, the VRG is divided in a left and a right half; the axons of both I and E neurons cross the midline and project to the contralateral side of the body.

Another bilateral and symmetrical structure is located in the VRG: the pre-Bötzinger complex (preBötC). The preBötC was identified as the region of the brain where

respiratory rhythm is generated [13]. Each of the two regions of the preBötC shows an independent pacemaker activity; the two sides synchronize their rhythmic activity by communicating with each other via synaptic connections [14]. In addition to generating respiratory rhythm, the preBötC shows respiratory pattern-generating mechanisms [15].

1.3.3 Peripheral chemoreceptors

Thanks to peripheral chemosensors, the respiratory system adapts its activity in response to changes in blood pH and arterial gas partial pressures. In particular, receptors for pH and partial pressure of oxygen (P_{O_2}) and carbon dioxide (P_{CO_2}) are located in the carotid and aortic bodies, as shown in Figure 1.8.

The chemosensors located in the aortic bodies are of secondary importance with respect to the ones located in the carotid bodies. Besides that, the carotid bodies are the only sensors in the human body which sense P_{O_2} : the hyperventilation due to low P_{O_2} is entirely induced from afferent signals coming from these sites [12].

Sensory information coming from the aortic bodies reaches the central nervous system via the glossopharyngeal nerve (cranial nerve IX), while the one from the carotid bodies travels through the vagus nerve (cranial nerve X).

Afferent information carried via the glossopharyngeal and vagus nerves reaches the brain stem; in particular, the cranial nerves make synaptic contact with I neurons in the DRG. Thus, an increasing firing rate of the chemosensors results in an increased inspiratory activity.

The conditions that produce an increased firing rate of the chemoreceptors are hypercapnia, which means an excess of CO_2 level in blood, and acidemia, that is a decrease in blood pH. The body responds to these stimuli increasing ventilation, which tends to remove the excess of CO_2 in blood, thus lowering P_{CO_2} and increasing blood pH.

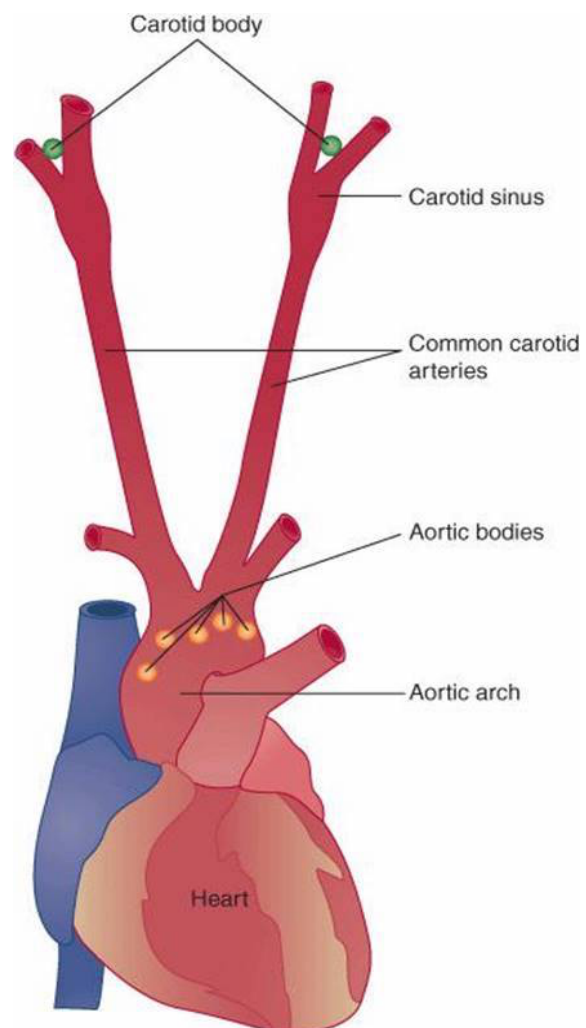


Figure 1.8: The aortic bodies are located near the aortic arch; the carotid bodies are located close to the carotid bifurcation on each side. Source: [26].

This response, schematized in Figure 1.9, represents an example of negative feedback loop.

Another condition that stimulates the increase of ventilation is hypoxia: when P_{O_2} decreases below about 60 mmHg [12], the peripheral chemosensors increase their firing rate, thus sending the command to increase ventilation. The increased respiratory activity causes P_{CO_2} to decrease, which eventually causes blood pH to increase (alkalemia). The reduced P_{CO_2} also alkalinizes the cerebrospinal fluid, which reduces the firing rate of the central chemoreceptors (see subsection 1.3.4). The ultimate result is a decrease of the respiratory rate.

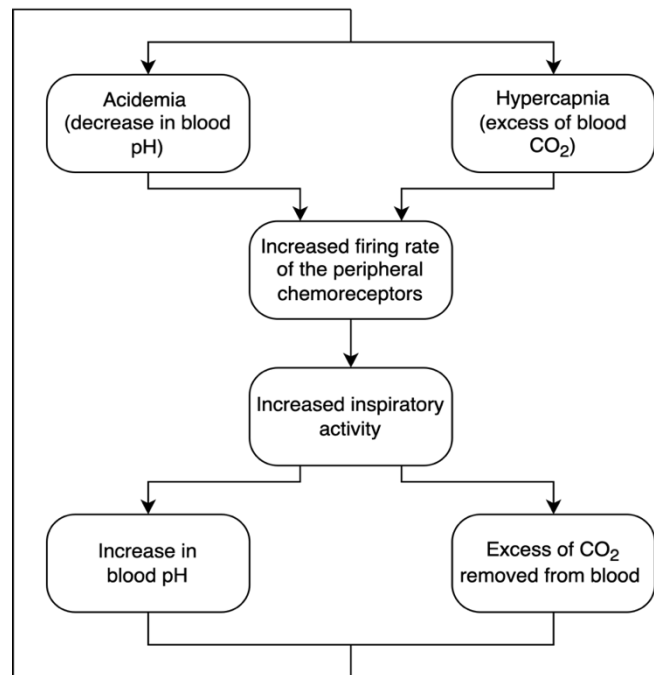


Figure 1.9: Negative feedback loop induced by the effect of acidemia or hypercapnia on peripheral chemoreceptors in the control of ventilation.

1.3.4 Central chemoreceptors

Through surgical removal of peripheral chemoreceptors, it was observed that 90% of the response to acidemia and hypercapnia was preserved. Thus, it was proven that there are chemosensitive areas in the brain stem as well. The exact location of the central chemoreceptors was identified through several experiments, which included focal application of chemicals, electric stimulation and lesioning: as shown in Figure 1.10, they reside in the ventral medulla [12].

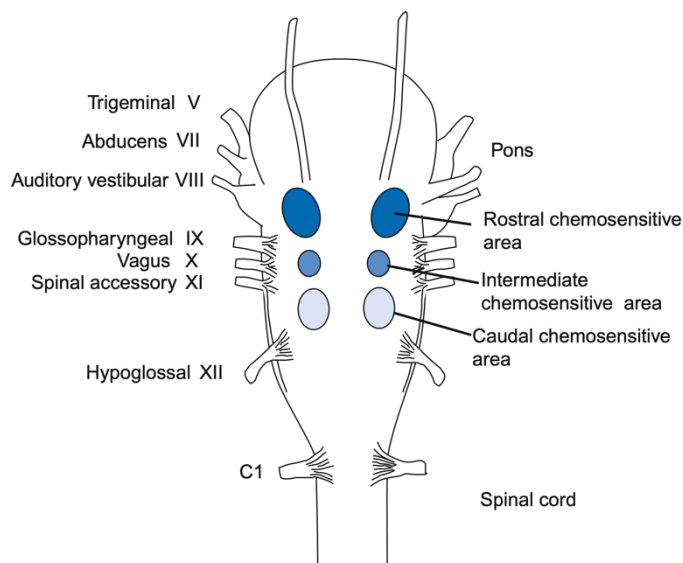


Figure 1.10: Ventral view of the brain stem in which the three chemosensitive areas on each side of the ventral medulla are highlighted. Source: [12].

The response induced by the central chemoreceptors treats acidemia and hypercapnia as independent stimuli: thus, pH and P_{CO_2} are measured independently from each other.

Unlike the peripheral chemoreceptors, the central chemosensitive areas are not in direct contact with blood: the

Unlike the peripheral chemoreceptors, the central chemosensitive areas are not in direct contact with blood: the

blood-brain barrier (BBB), a highly selective semipermeable barrier composed of astrocytes and endothelial cells, separates central chemosensors from blood.

Ions such as H^+ and HCO_3^- cannot cross BBB easily while CO_2 can, due to its lipophilic nature. Thus, the concentration of CO_2 in the cerebrospinal fluid (CSF) is in equilibrium with the one in blood: in case of an excess of CO_2 in blood, also P_{CO_2} in CSF raises; this leads to a decrease of pH in CSF. The central chemoreceptors react to acidosis in the CSF, eventually increasing ventilation, which tends to bring CO_2 concentration and pH back to normal levels.

The mechanism applied is a negative feedback loop similar to the one which occurs for peripheral chemosensors, schematized in Figure 1.9.

1.3.5 Lung receptors

A variety of sensory receptors in the lungs are responsible for the following involuntary behaviors:

- Hering-Breuer inflation reflex, which is due to mechanical stimuli
- Pulmonary chemoreflex, which is caused by chemical substances

1.3.5.1 Hering-Breuer inflation reflex

Pulmonary stretch receptors are located on the walls of the bronchi and bronchioles; their function is to prevent excessive stretching of the lung tissue during large inspirations.

When an excessively large inspiration is performed, these sensors activate and the afferent sensory input travels to the brain stem via the vagus nerve. The stimulus reaches the pontine respiratory group, thus inhibiting further inflation of the lungs [12]. This mechanism is known as Hering-Breuer inflation reflex.

1.3.5.2 Pulmonary chemoreflex

Bronchopulmonary C fibers (PCFs) are unmyelinated nerves located in the bronchi; they represent around 80% of the vagal bronchopulmonary afferents innervating the airways and the lungs [16].

The activation of PCFs evokes the pulmonary chemoreflex, which is a critical reflex that modulates both respiratory and cardiological responses: the symptoms include apnea, hypotension and bradycardia [17]. The reflex is then immediately followed by tachypnea, which is rapid shallow breathing.

The PCFs that appear to be more sensitive to chemicals are the ones located near the capillaries, while the ones located in the bronchi respond mainly to stretch [12].

Chapter 2 Monitoring Respiratory Health

To assess the health status of the respiratory system, quantitative measurements on standard parameters must be performed. Respiration can be analyzed through both time parameters and volumetric measurements.

2.1 Time Parameters

The respiratory signal can be analyzed through parameters in both time and frequency domain. In this section, a brief description of these parameters is provided.

2.1.1 Respiratory rate

The main temporal parameter that should be considered when monitoring respiratory health is respiratory rate, also known as *respiratory frequency*, which counts the number of times the person breathes in a minute.

Although it is often neglected, respiratory rate is considered to be one of the most informative vital signs ([18], [19]). Respiratory frequency is sensitive to environmental, psychological and physiological stressors ([20], [21], [22]); it was also proven to be an early indicator of physiological deterioration ([23], [24]) and a predictor of cardiac arrest and intensive care unit admission [18]. Moreover, respiratory frequency provides a simple and inexpensive variable for the risk assessment after myocardial infarction [25].

The normal respiratory rate for adults during tidal breathing is between twelve to sixteen breaths per minute [26]. It is much higher in children and decreases with age: newborns and infants show a respiratory rate around thirty to sixty breaths per minute, while children from six to twelve years old breathe eighteen to thirty times per minute [27].

Measuring respiratory rate can be challenging since drawing the patient's attention to their respiration may induce conscious control of breathing, thus resulting in inaccurate measurements [28]. Moreover, some problems may arise from the fact that it is possible to measure respiratory rate by reducing the assessment time to fifteen or thirty seconds and multiplying by four or two, respectively, to obtain the number of breaths in one full minute. There is evidence that this procedure results in an underestimation of one or two breaths per minute [29].

2.1.2 Inspiratory and expiratory time

As described in section 1.2, during tidal breathing inspiration is the only active phase of respiration. Therefore, since muscle contraction is faster than elastic recoil of tissues, inspiratory time is significantly lower than expiratory time.

Typically, inspiratory to expiratory time ratio is studied: this parameter, also referred to as *Inspiratory:Expiratory ratio* or *I:E ratio*, describes how the total time required to perform each breath is distributed between inhalation and exhalation. A lower I:E ratio implies a shorter inhalation time and/or a longer exhalation time.

A typical I:E ratio for healthy adults at rest is 1:2 [30]. Certain pathologies can lead to a variation of this parameter; for example, asthmatics might have I:E ratios up to 1:3 or even 1:4 [31].

Knowing both I:E ratio and respiratory rate, it is possible to calculate the mean inspiratory and expiratory time within one minute.

2.1.3 Minute ventilation

Minute ventilation, also known as *respiratory minute volume* or *minute volume*, represents the volume of air inhaled or exhaled from the lungs in one minute. The parameter is defined regardless of the type of inflation: ventilation can be either spontaneous or assisted by a mechanical ventilator [32].

Respiratory minute volume can be measured directly using specific devices. The other option to obtain the value of minute ventilation is to derive it as:

$$\text{minute ventilation} = \text{tidal volume} \times \text{respiratory rate} \quad (2)$$

Thus, an increase in tidal volume (see section 2.2) or respiratory rate will result in an increase in minute ventilation.

The average minute ventilation for adult men, considering a tidal volume of 500 mL and a respiratory rate of 12 breaths per minute, results around 6000 mL per minute [33].

2.2 Lung Volumes and Capacities

Lung volume measurements are very useful in lung disease assessment and quantification [34]. In some cases, accurate measurements of lung volumes may be of great help in order to make a correct diagnosis [35].

Both lung volumes, which are also known as respiratory volumes, and lung capacities are, in fact, volume measurements. The difference between the two is that lung capacities are

derived as sum of two or more respiratory volumes [36]. Figure 2.1 shows the standard lung volumes and capacities on a schematic volume-time spirogram.

The whole volume of air within the lungs is referred to as *lung volume* [34]. Lung volume is subdivided in four standard respiratory volumes:

- Tidal volume (V_T or TV) represents the amount of air inhaled or exhaled during a normal resting respiratory cycle. For healthy human adults, V_T measures around 500 mL in males and 400 mL females [37].
- Inspiratory reserve volume (IRV) refers to the volume of air that can be breathed in starting from the end of a tidal inspiration.
- Expiratory reserve volume (ERV) is the volume of air that can be breathed out starting from the end of a tidal expiration.
- Residual volume (RV) is the volume of air which is still in the lungs after a maximal expiration. Remember from Chapter 1, subsection 1.2.3: lungs cannot be emptied completely.

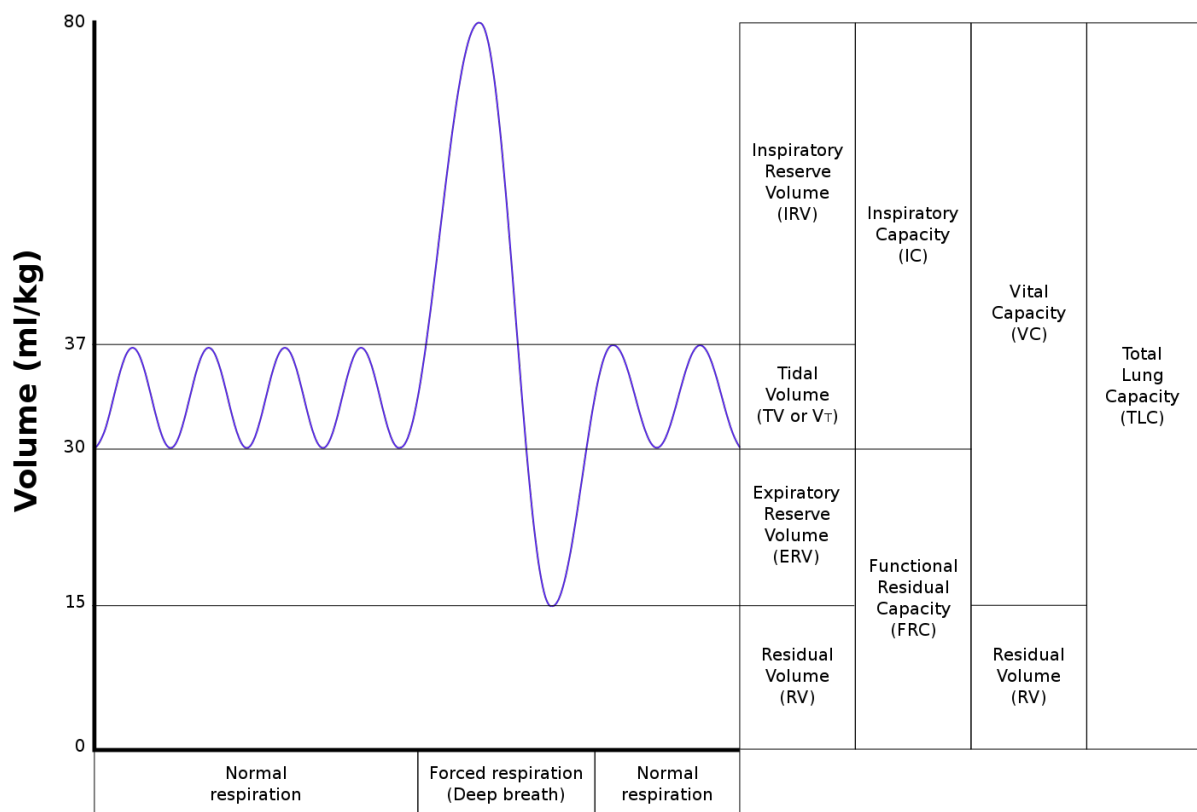


Figure 2.1: Schematic representation of standard lung volumes and capacities on a volume-time spirogram. The four standard lung volumes are tidal (TV or V_T), inspiratory reserve (IRV), expiratory reserve (ERV) and residual (RV) volumes. The four standard lung capacities are inspiratory (IC), functional residual (FRC), vital (VC) and total lung (TLC) capacities [144]. Source: [143].

The four standard lung capacities are:

- Functional residual capacity (FRC) refers to the volume of air still within the lungs at the end of a tidal expiration. It is derived as the sum of expiratory reserve volume and residual volume.
- Inspiratory capacity (IC) is the volume of air that can be breathed in starting from the end of a tidal expiration. It can be obtained as the sum of tidal volume and inspiratory reserve volume.
- Vital capacity (VC) represents the volume of air that can be breathed in starting from the end of a forced expiration. It can be obtained as the sum of tidal volume, inspiratory reserve volume and expiratory reserve volume.
- Total lung capacity (TLC) represents the total volume of air within the lungs after a maximal inspiration. It can be evaluated as the sum of all four lung volumes.

Several factors influence respiratory volumes in adults:

- Height. Taller people have higher lung volumes and capacities [38].
- Body fat content. Increased body weight in obese subjects leads to lower lung volumes and capacities [39], while in athletes an increase in muscle mass (and consequently an increase in body weight) is associated to bigger lung volumes and capacities ([40], [41], [42]). Thus, body fat content is considered to be a better predictor, compared to BMI, for decreased lung volumes and capacities [43].
- Age. A human adult reaches full pulmonary development at around 20-25 years; after that, no relevant changes occur for around ten years [44]. Starting at the age of 35, lung volumes and capacities start diminishing as age grows [45]. This is mainly due to stiffening of the rib cage and decreased elastic recoil of the alveoli ([46], [47]).
- Gender. Males have more bronchioles, wider airway diameter and larger lung size compared to females of the same height and age ([48], [49]).
- Ethnicity. Variations in lung volumes and capacities between subjects of different ethnicity have been largely attributed to the difference in anthropometric measurements between people coming from different ethnic groups ([50], [51], [52]).
- Level of physical activity is well correlated with lung volumes [53]. Swimming and endurance training in particular, but in general also regular exercise, tend to increase lung volumes [40].

Inspired and expired lung volume measurements (i.e. IRV, V_T , IC, ERV and VC) can be performed using a spirometer, while absolute lung volume measurements (i.e. RV, FRC and TLC) need more complex exams such as body plethysmography, radiographic imaging, inert gas dilution or nitrogen washout methods ([34], [54]).

2.2.1 Spirometry

Spirometry, which literally means *measuring of breath*, is the most widespread test among the pulmonary function tests (PFTs).

Spirometry is a very rapid and completely painless test, which requires only a little collaboration from the patient. To conduct the test, the patient is asked to breathe through a mouthpiece linked to an instrument called spirometer. A clip is used to seal the patient's nose in order to avoid air leakage. At the beginning of the test, the patient is instructed to breathe normally through the mouthpiece. After a few breaths, the patient is asked to perform a maximal inspiration, which means inspiring as deeply as possible. When the maximal inspiration is reached, the patient should blast air out of their lungs until a maximal expiration is reached; the indicator of maximal expiration is either a plateau in the spirometer graph, or a total of fifteen seconds of forced expiratory time. After reaching a full expiration, the patient can be asked to perform another maximal inspiration, which will provide a measure of forced inspiratory vital capacity [55].

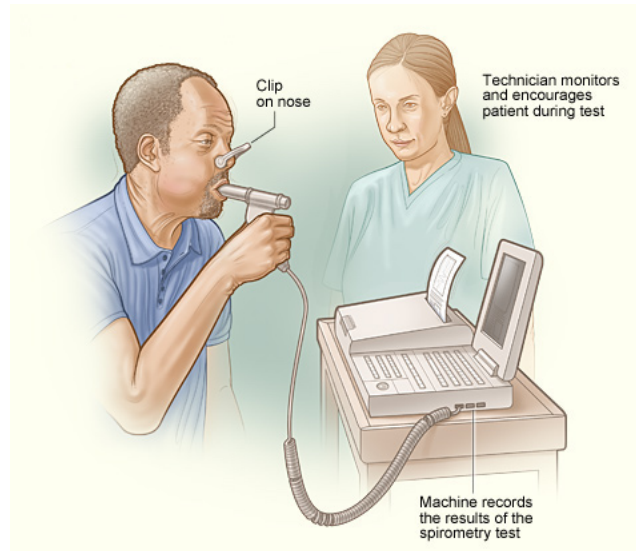


Figure 2.2: Patient undergoing a spirometry test, assisted by a technician. Modified from [145].

Common spirometers can generate two graphs as output, called *spirograms*:

- A volume-time curve, shown in Figure 2.1, which has volume along the y-axis and time along the x-axis.
- A flow-volume curve, which shows the speed of the air flow (y-axis) as a function of total inspired or expired volume (x-axis).

2.2.2 Gas dilution

Gas dilution techniques are widely used to provide measurements of absolute lung volumes such as functional residual capacity (FRC). They are simple, non-invasive techniques based on the principle of conservation of mass of an inert gas [56].

The most used gas dilution methods are:

- Closed-circuit helium dilution
- Open-circuit nitrogen washout

2.2.2.1 Helium dilution

Helium (He) is an inert gas, which is natively not found in lungs and is insoluble in blood.

In this closed-circuit technique, the patient breathes through a spirometer containing a known concentration of helium (C_i). Initially, as said above, the concentration of helium in the lungs is equal to zero; after several minutes of breathing through the spirometer, the concentration of helium reaches equilibrium between the instrument and the patient's lungs (C_f). Knowing the initial volume of helium (V_i), it is possible to calculate the unknown volume of the patient's lungs (V_f) as follows [54]:

$$C_i \times V_i = C_f (V_i + V_f) \quad (3)$$

And solving equation 3 for V_f :

$$V_f = V_i \left(\frac{C_i}{C_f} - 1 \right) \quad (4)$$

2.2.2.2 Nitrogen washout

As nitrogen (N_2) is the major component of air, precisely dry air is 78 vol% nitrogen [57], N_2 is naturally present in the lungs.

In this open-circuit technique, the patient inhales through a mouthpiece connected to a source of 100% oxygen (O_2); the exhaled air is collected in a container. The entrance of the container is sealed by one-way valves, so that the air exhaled from the patient cannot flow out of it. Moreover, prior to the exam, the container is flushed with oxygen to remove all the nitrogen from its inside. The patient keeps inhaling from the mouthpiece and exhaling in the container until the concentration of nitrogen in the exhaled air falls below 2 vol%. At this point, the volume of N_2 in the container is measured [56].

Knowing that at the beginning of the test the nitrogen concentration in the lungs is around 80 vol%, FRC can be calculated as shown for helium dilution (equations 3 and 4) [58].

Gas washout takes three to four minutes for healthy patients but can require more than fifteen minutes for patients affected by severe obstructive airway diseases [56].

2.2.3 Plethysmography

The term *plethysmography* refers to a test which allows to measure volume changes of a portion of the body. Within the human body, volume changes occur mainly due to blood or air flows.

In respiratory applications, plethysmography is used to obtain lung volume measurements. Two main typologies of plethysmography tests can be performed:

- Body plethysmography
- Respiratory inductive plethysmography
- Optoelectronic plethysmography

2.2.3.1 Body plethysmography

Total body plethysmography represents the gold standard of plethysmography methods in clinical practice. It is based on Boyle's law, described in subsection 1.2.1.

Body plethysmography allows the measurement of absolute lung volumes; in particular, functional residual capacity (FRC) is assessed. If the patient is instructed to breathe deeply, residual volume (RV) and total lung capacity (TLC) can be calculated as well [59].

To perform this test, the patient sits in an airtight cabin and is instructed to breathe through a mouthpiece which is connected to a flow sensor, as shown in Figure 2.3.

During exhaling phases of respiration, the gas in the patient's lungs becomes compressed, the lung volume decreases and the pressure inside the cabin changes due to the increase of gas volume. Since the volume of the chamber is known, measuring the changes in pressure of the cabin at the mouth it is possible to calculate the change in volume in the lungs.

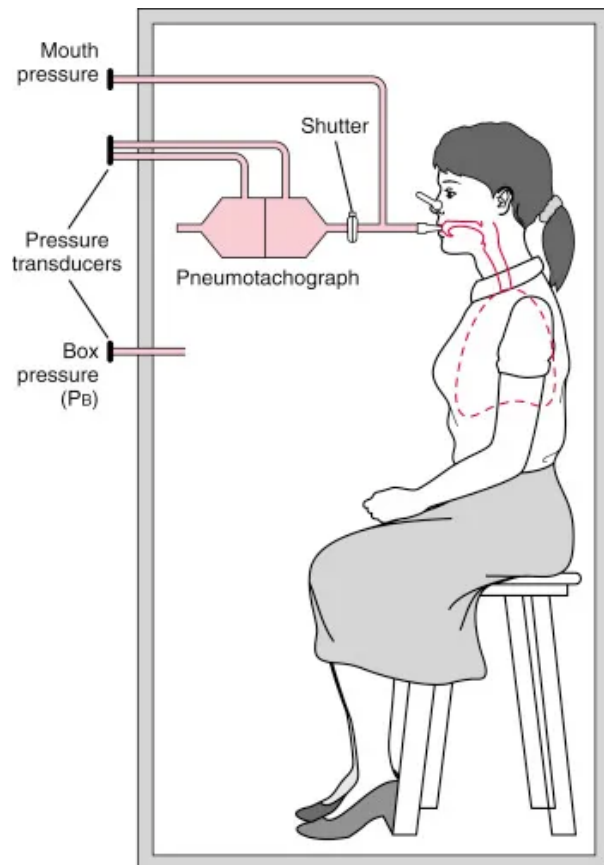


Figure 2.3: Patient sitting in a body plethysmography chamber. Modified from:

2.2.3.2 Respiratory inductive plethysmography

Respiratory inductive plethysmography (RIP), also known as *respiratory inductance plethysmography*, is a diffuse non-invasive method to assess pulmonary ventilation. In particular, the movement of the chest and of the abdominal wall is measured in order to track the movement of the rib cage and diaphragm, respectively.

At first, when RIP was invented, the respiratory inductance plethysmograph consisted in a vest made of elastic material in which insulated wires were stitched. Nowadays, two adhesive elastic bands are used; each band is around 2.5 cm wide and contains an insulated wire coil. Plethysmography bands can be purchased from several manufacturers, or they can be custom-made in case of special needs.

To perform the test, the first band is placed at the level of the nipples to measure the expansion of the rib cage, while the second band is placed at the umbilicus to record the movements of the diaphragm [60]. A schematic representation of the band placement is shown in Figure 2.4.

The two sensors evaluate the contraction and expansion of the volume they enclose by measuring the variations of their circumference; thus, it is not necessary to align specific portions of the bands to anatomical reference points.

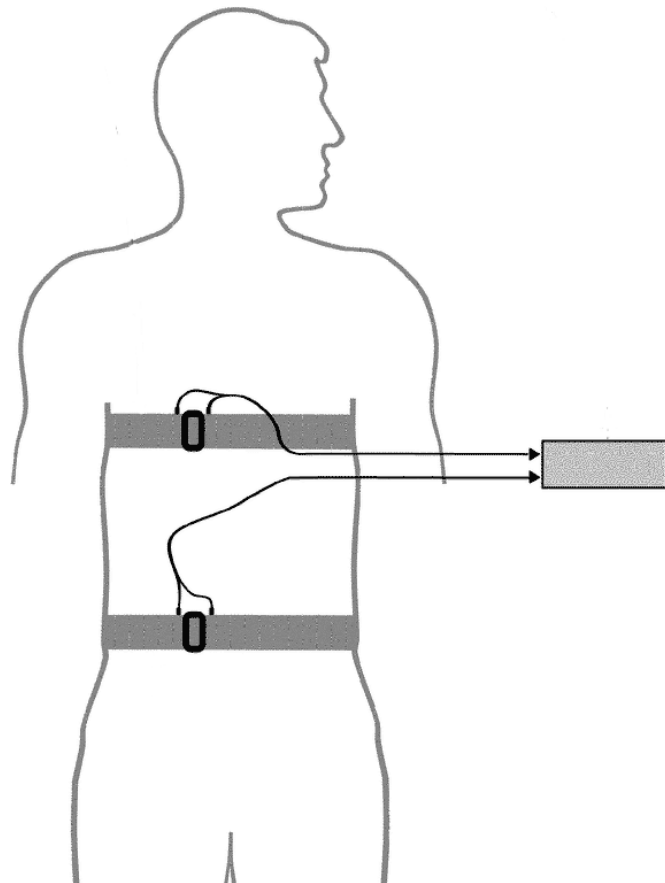


Figure 2.4: Elastic band placement for respiratory inductive plethysmography: the first band is placed at the level of the nipples, while the second one is placed at the umbilicus. Modified from: [148].

2.2.3.3 Optoelectronic plethysmography

Optoelectronic plethysmography (OEP) was developed at the Bioengineering Department of the Politecnico di Milano. This typology of plethysmography measures lung volumes through external measurements of movements of the chest wall.

Optoelectronic methods measure movement of body parts using passive or active markers placed on the patient's body, which movements are monitored continuously by multiple cameras. Through a careful initial calibration of the system and an appropriate choice of body model, very accurate three-dimensional measurements can be obtained.

OEP is a versatile technique as it can be performed in standing, sitting, prone or supine positions [61], during both rest and exercise [62]. The protocol designed for standing and sitting positions involves the use of eighty-nine markers placed in standard positions on the thoraco-abdominal surface [63]. An example of marker placement is shown in Figure 2.5.

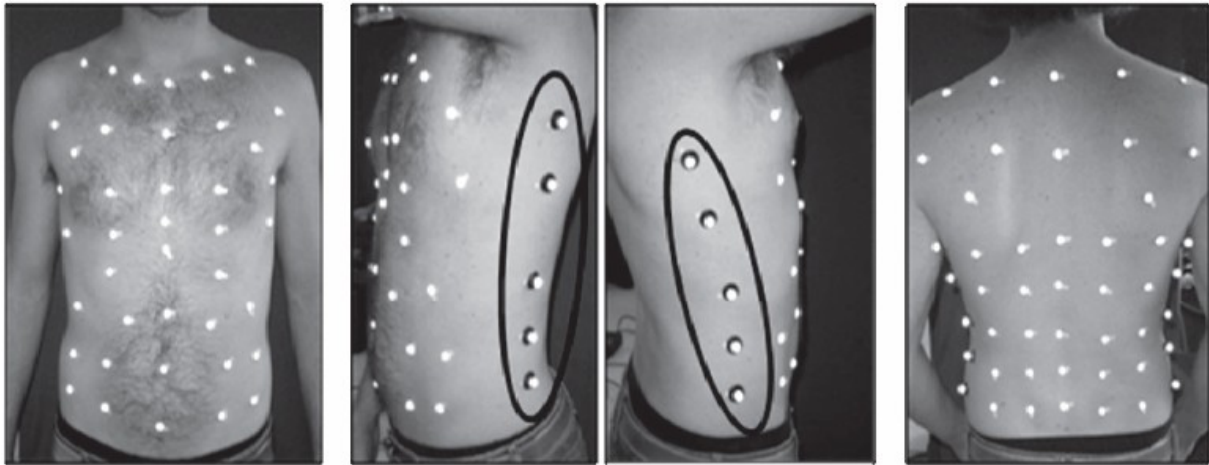


Figure 2.5: Example of marker placement for optoelectronic plethysmography. Source: [146].

Chapter 3 Respiratory Variability

As explained in Chapter 1, the goal of the respiratory system is to deliver oxygen where it is needed and ensure that carbon dioxide is removed where there is an excess. The respiratory system must adapt to environmental fluctuations in order to maintain homeostasis; thus, homeostatic regulation cannot be a static process.

The respiratory system is defined to be stable if, in response to a transient disturbance, it reverts to its original steady state breath-to-breath variability and level of ventilation. Since the average level of ventilation during spontaneous tidal breathing remains fairly steady over a long period of time, this condition is generally considered as a representative output of a stable respiratory system. Nevertheless, a relevant amount of breath-to-breath variability can be observed even during spontaneous tidal breathing [64].

A healthy respiratory system, which is able to maintain homeostasis despite being constantly subjected to the change of internal and external demands, is therefore characterized by complex variability. It is important to notice that this kind of innate variability is not just random uncontrolled fluctuation, but it is there by design [65].

It has been proven that under stressful conditions, respiratory variability tends to decrease. In particular, both mechanical (resistive [66] and elastic [67] loading) and chemical (hyperoxic hypercapnia [68] and isocapnic hypoxia [69]) stress were studied. Moreover, certain pathologic conditions have been proven to decrease respiratory variability as well: restrictive lung disease [70], endotoxemia [71] and unconsciousness [72].

Total respiratory variability consists of both random and nonrandom components [73]:

- Random, non-deterministic variations are caused by behavioral inputs. External perturbations appear as noise in the respiratory signal, but they are thought to improve the responsiveness of the system [74]. Thus, random variability reflects system sensitivity to stimuli.
- Nonrandom variations are induced by homeostatic processes (see section 3.1). This kind of variability is characterized by deterministic, time-dependent, structured and correlated breath-to-breath variations; oscillatory variability is included in this category.

An imbalance between random and nonrandom variability may contribute to system irregularities: an excess of random components can lead to system dysregulation because

of not allowing it to return to its dynamic steady state; on the other hand, an excess or a lack in system sensitivity may lead to regulation deficits [75].

Several studies on respiratory variability in human adults and infants have been conducted over the years, focusing on both waking and sleeping states (e.g. [76], [77], [78], [79]). As shown in Figure 3.1, attention to this topic is growing in the last few years.

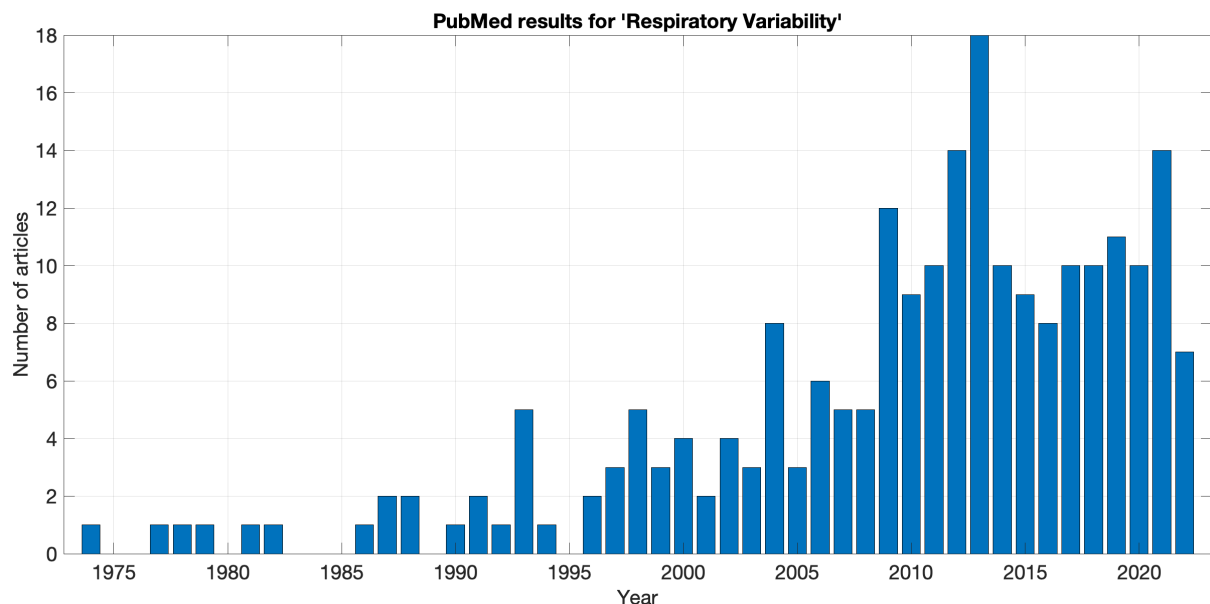


Figure 3.1: Graph showing the growth of interest by the scientific community to respiratory variability over the last fifty years. Data source: [142].

3.1 Nonrandom Variability

Nonrandom variability appears as breath-to-breath variations induced by the respiratory system in order to return to its dynamic steady-state conditions after an external perturbation has occurred [80]. Since the return to steady-state conditions is not instantaneous, small adjustments to breath parameters are applied between each breath.

This kind of variability characterizes resting-state respiration primarily during wakefulness; it persists during sleep as well, although with lower intensity ([81], [82]).

Spontaneous tidal breathing during both wakefulness and sleep in adults seems to be characterized by nonrandom variability with an autoregressive structure in minute ventilation, inspiratory time and inspiratory volume [82]. Since successive breaths are correlated with previous ones, nonrandom variability can be studied using measures of autocorrelation on the respiratory signal. In particular, the mean autocorrelation coefficient at one breath lag for tidal volume, inspiratory and expiratory time, calculated during tidal breathing over a representative time window, should be significantly different from zero [83]. Moreover, the same autocorrelation coefficients should remain significant if calculated at up to three breath lags, thus indicating the presence of short-term memory, which is

defined as the number of breath lags with for which the autocorrelation coefficient remains significantly different from zero [83].

Thus, in analogy with other forms of short-term variability (e.g., heart rate variability), nonrandom respiratory variability appears to be functional and healthy. For example, a study has proven that spontaneous nonrandom variability and respiratory short-term memory are significantly higher for patients who successfully separated from mechanical ventilation compared to patients who failed the separation process [84]. Moreover, the beneficial effect of introducing variability in mechanical ventilation has been assessed through mathematical modelling [85] and studies on anaesthetized pigs [86].

Oscillations should be considered when studying the behavior of the respiratory system. These are fluctuations, or rather, repetitive patterns of respiratory volume and time within a time period; thus, oscillations produce systematic respiratory rhythms [74].

Oscillatory variability of the respiratory system arises from the fact that regulatory negative feedback loops (see subsections 1.3.3 and 1.3.4) are not instantaneous: some delay occurs between when the conditions deviate from the standards and when the respiratory system actually activates in order to respond to internal demands [64]. Thus, respiratory oscillations show how homeostasis is a dynamic process rather than a static one.

The result of the intrinsic delays of the regulatory negative feedback loops is an overcorrection of the original perturbation, which leads to the generation of a new perturbation in the other direction [64]. For example, in case of hyperpnea, which lowers arterial P_{CO_2} , after some delay a decrease of ventilation would be triggered. Since at the moment of intervention much of the original hyperpnea has already occurred, the decrease of ventilation would not only neutralize its effects, but it would also cause a slight hypopnea. The ultimate result is an oscillatory response of the respiratory system.

3.2 Sighs

Sighs are defined as long, audible exhalations; they appear as occasional deep breaths.

Sighs can be identified in the respiratory signal as breaths with a tidal volume at least double (or triple) in amplitude with respect to the mean tidal volume in a surrounding representative interval [87]. Due to their marked difference from the surrounding breaths, sighs are often considered disturbances of normal respiration and removed from the respiratory data during signal processing.

The pattern of generation of sighs is not fully clear; several hypotheses have been explored. Physiologically, the cause appears to be a double burst of the pre-Bötzinger complex: each preBötC burst causes a contraction of the inspiratory muscles, a second burst, immediately following the first one, leads to a bigger inspiration which results in a sigh ([88], [89], [90]).

Spontaneous sighing occurs several times per hour in humans [91]; in resting conditions, sigh rate in young male and female adults is around 10 sighs per hour. Moreover, no relation was found between respiratory and sigh rates [92].

3.2.1 Physiological factors influencing sighs

To provide a possible explanation to the role of sighs, it is important to highlight the mechanisms that influence sigh rate. Both central and peripheral factors have been proven to influence sigh generation directly.

3.2.1.1 Central factors

First, it was found that in vivo stimulation of the pre-Bötzinger complex generates sighs in cats [93] and rats [94]. Second, sigh rate increases in rats following the disinhibition of the dorsomedial hypothalamus [95].

Moreover, some limbic brain areas show a modulation in their activity concurrent to sighs:

- The medial paraventricular hypothalamus shows decreased activity during a sigh ([96], [97]).
- The dorsal hippocampus shows increased activity before a sigh, a peak at sigh inspiration onset, then a decrease followed by another increase to eventually return to a baseline [96].

3.2.1.2 Peripheral factors

Chemoreceptor feedback influences sigh rate: in rats, hypocapnic hypoxia increases sigh frequency [98], while exposure to acetazolamide, which offsets respiratory alkalosis during hypoxia, reduces the frequency of sighs induced by hypocapnic hypoxia [99]. Furthermore, still referring to rats, peripheral chemoreceptors ablation suppresses sighs completely [100].

Sigh rate is influenced by feedback coming from mechanoreceptors as well. As said above, sighs are fundamental to reinflate atelectatic airspaces: as atelectasis is detected by the mechanoreceptors, the feedback provided evokes a sigh ([101], [92]).

Lastly, sighs are completely suppressed with vagotomy in various animal species: rabbits [102], rats ([100], [103]) and cats ([104], [105]).

3.2.2 Sighs as resetters

From a physiological point of view, sighs are starting to be seen as functional elements for the respiratory system: in particular, they may play the role of supporters of the homeostatic control of respiration. A valuable hypothesis is that sighs may serve as physiological resetters of optimal respiratory regulation [80].

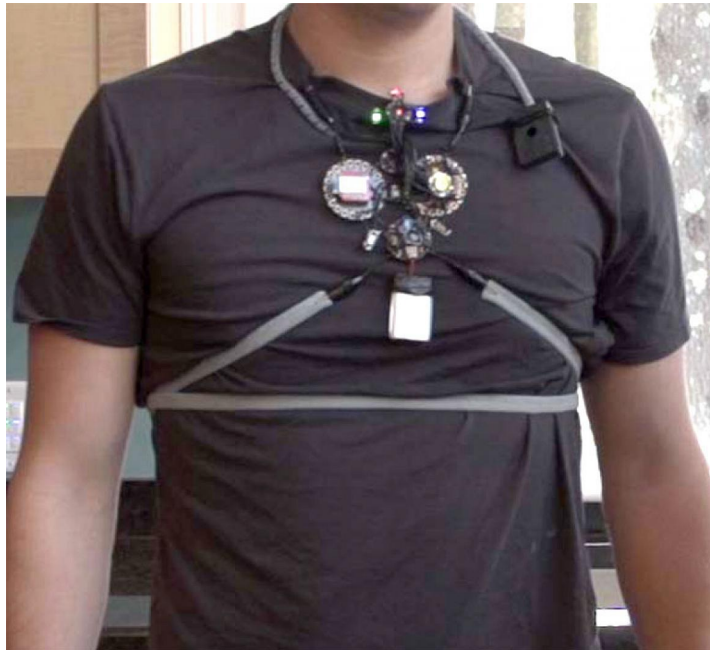
Several studies suggest that sighs are evoked whenever the body is in a state of:

- Lack of respiratory variability. In particular, there is evidence of the ability of sighs to restore a healthy lung state, which can be compromised by nonvariable respiratory activity ([92], [100], [106], [107]).
- Imbalance between random and nonrandom respiratory variability. In particular, it was proven that the randomness in breathing variability increases while approaching the next sigh, and, following a spontaneous sigh, autocorrelation of minute ventilation is reset ([75], [108], [109], [110], [111]).
- Physiological stress, such as hypoxia and hypercapnia: there is evidence of the ability of sighs to reduce both of these conditions. This suggests that sighs enhance gas exchange [100].

Furthermore, the results of several studies suggest that sighs are not only fundamental to reinflate atelectatic airspaces, including collapsed alveoli ([92], [106], [112]), but they also prevent the atelectatic condition and help restoring lung compliance in both adults and infants ([103], [106], [107], [113]).

Chapter 4 Airgo™

Airgo™ was created by David T. Kuller and collaborators for the 2013 US HHS / EPA *My Air, My Health Sensor Challenge*. The aim of the challenge was “to create a new sensor integrating air quality information with human health conditions” [114]. Airgo™, which name used to be *Conscious Clothing*, won the first prize at the contest, beating multinational companies like Philips Respironics and renowned universities such as Carnegie Mellon University. A picture of the first prototype of the Conscious Clothing system is shown in Figure 4.1.



MyAir Inc. was found in 2015 in Boston, Massachusetts, to continue the development of Airgo™.

Nowadays, the aim of the device is to satisfy the need to monitor respiration directly and continuously in a non-invasive and non-intrusive way. Thanks to its versatility, Airgo™ allows for such measurements in any environment and under any condition: both sleeping and waking states can be monitored, as well as rest and exercise.

Figure 4.1: The first prototype of the Conscious Clothing system, which won the 2013 US HHS / EPA “My Air, My Health Sensor Challenge”, and eventually evolved to become Airgo™. Source: [149].

The device can be worn by a person continuously for several days, thus leading them to forget they are wearing it. This is a key point, considering that it is well known that drawing a person’s attention to their breathing may induce conscious control of breathing to replace the spontaneous autonomic one, thus leading to inaccurate measurements [28].

Nowadays, especially due to the wide diffusion of smartphones and smartwatches, the market is teeming with mobile applications for health and fitness. Despite the convenience and ease of use of such applications and devices, almost none of them is CE nor FDA approved; thus, they cannot be referred to as *medical devices*, and the data they provide cannot be considered reliable and cannot be used for medical purposes.

Moreover, accurate real-time monitoring of respiration in terms of lung volumes and ventilation is quite complex; thus, many biomedical wearable sensors only provide real-time feedback of simple parameters, such as respiratory rate.

4.1 Device Description

Airgo™ is a patented [115], CE Class IIa wearable medical device which received CE mark in 2020 [116]. Many things about the device changed since when its name used to be Conscious Clothing, including its aspect, which is shown in Figure 4.2.



Figure 4.2: Current (2022) external appearance of Airgo™. The wearable device consists of two parts: Airgo™ Recorder and a Ware strap belt.

The device is capable of measuring both lung volumes and time parameters. In particular, the measured respiratory parameters are:

- Respiratory rate (RR)
- Relative tidal volume (TV or V_T)
- Relative minute ventilation (M_V)
- Inhalation time (T_i)
- Exhalation time (T_e)

For an accurate description of the parameters mentioned above, refer to Chapter 2. Moreover, body posture and activity level are monitored using accelerometers.

As shown in Figure 4.2, the wearable device consists of two separate parts:

- Airgo™ Recorder
- aWare strap belt

4.1.1 Airgo™ Recorder

Airgo™ Recorder is the core of the device. It contains a microprocessor and a motion detection circuit, which consists of three accelerometers, one for each axis of the Cartesian coordinates.

The microprocessor samples data at a frequency of 10 Hz. It includes an analog to digital converter, which is used to convert the resistance signal acquired from the belt into a 10-bit number. The microprocessor uses Bluetooth technology (BLE) to exchange data with the app (see subsection 4.2.1); data exchange can occur in both real time and a posteriori.

Airgo™ Recorder is battery powered; its battery capacity allows the device to record continuously for up to three weeks. Moreover, the onboard memory can store up to 50 days of recorded data. These two factors allow for the clinical use of the device in a longitudinal study.

A LED has been placed in the anterior part of the device, under the translucent power button. LED alarms have been set up in order to indicate if some error has been detected, for example if the belt hasn't been put on correctly, to prevent factors that may invalidate the whole exam if not spotted in time.

4.1.2 aWare strap belt

Airgo™ bases all its measurements on the variations of length of the aWare strap belt. The belt consists of a knitted matrix of nylon and spandex with which a silver coated yarn is interweaved. A close-up picture of the belt is shown in Figure 4.3.



Figure 4.3: A close-up picture of the aWare strap belt. A silver coated yarn is interweaved in the nylon and spandex matrix.

The belt comes in five sizes (extra-small, small, medium, large and extra-large) in order to fit the circumference of the patient's thorax as well as possible. The lifespan of aWare is several months of continuous use.

The silver coated wire, as it is electrically conductive and therefore has electrical properties, allows for belt resistance measurements: the elastic band changes its electrical resistance according to the expansion and contraction of the volume of the chest it encloses, thus allowing to track each and every breath directly. The relationship between the length of the belt and its resistance is covered in details below.

Comparing the resistance signal acquired using Airgo™ to traditional spirometry, it was proven that the changes in resistance directly map to the amount of air the person inhales and exhales [117]. Figure 4.4 shows the comparison between Airgo™ and a traditional spirometer (SensorMedics) breath signal.

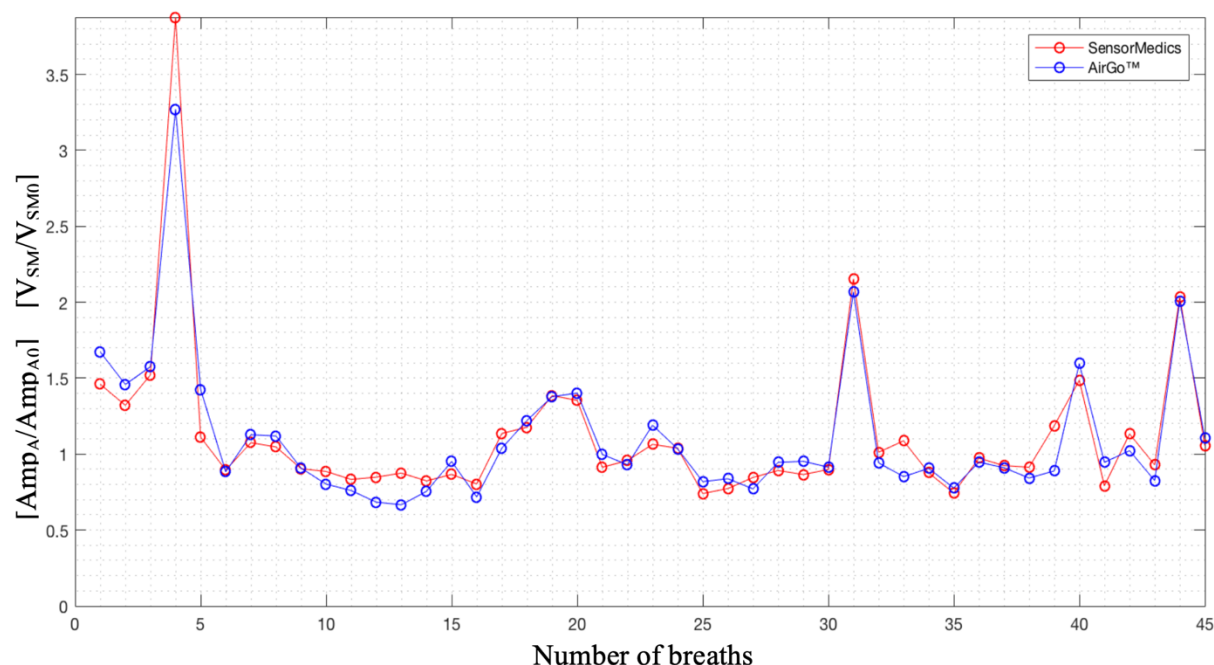


Figure 4.4: SensorMedics' normalized volumes and AirGo™'s normalized amplitudes in standing position for one of the subjects enrolled for the validation study. Source: [117].

As shown in Figure 4.5, the relationship between the length of aWare belt and its electric resistance is non-linear. The curve can be subdivided into four regions: chaotic, linear dynamic, flat and reverse.

In the chaotic region, delimited by the stretch percentages L0 (0%) and L1 (3%), the resistance increases rapidly with the length of the belt. After L1, the linear dynamic region starts: in this region, there is a linear increase in resistance with respect to belt length. The size of the belt should be chosen so that the device working region is the linear dynamic one. After L2 (30%), the flat region begins: in this region, the resistance of the belt continues to increase with length but with smaller and smaller increments, until it reaches

a plateau. Once LT (50%) is reached, the reverse region begins. LT is the length threshold beyond which measurements would be inaccurate and misleading as the resistance decreases with increasing length: the belt should never work in the reverse region. The maximum stretch that the belt can reach without damaging, indicated in Figure 4.5 as LM, is 80%.

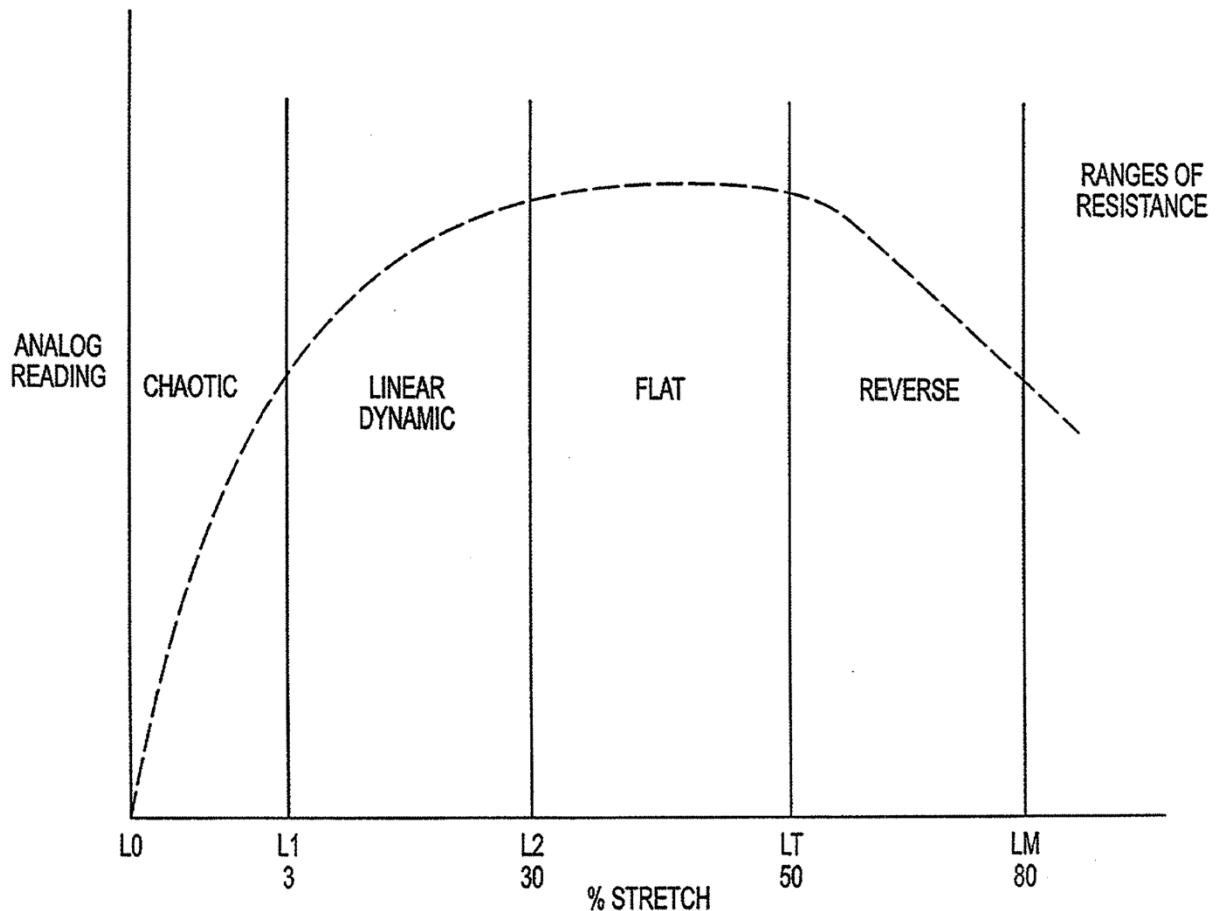


Figure 4.5: Exemplary graph showing the non-linear relationship between the stretch of a Ware belt and its electric resistance. The range of work should be in the “linear dynamic” region, between L1 and L2. LT is the length threshold and LM is the maximum length. Source: [115].

4.1.3 Device positioning

To allow the proper recording of all the respiratory features, the device must be placed correctly around the torso of the patient. The correct position of the belt is of vital importance for Airgo, to such a point that MyAir Inc. decided to patent it [115].

First of all, the Airgo™ Recorder must be placed ventrally, right on top of the xiphoid process, which is a cartilaginous extension of the most inferior part of the sternum. Furthermore, in order to allow the motion circuit mentioned above to detect the patient’s posture correctly, it is important to orient the Airgo™ Recorder properly to distinguish between left and right and between top and bottom: the logo has to be placed outward so

that it is readable and the side on which the small orange spot is located should be placed upwards.

The belt has to be positioned in such a way that it passes over the floating ribs, i.e. the two lowermost (eleventh and twelfth) rib pairs, which are not attached to the sternum. In the back, the belt should pass over the junction point between the floating ribs and the spinal column.

The Airgo™ meridian obtained, shown in Figure 4.6, is an inclined plane that starts higher ventrally and ends lower dorsally: in such way, making use of just one belt Airgo™ is able to capture both intercostal and diaphragmatic breathing. This particular belt placement distinguishes Airgo™ from many other systems commercially available, which make use of multiple belts in order to record all the possible movements of the thorax.

Last but not least, the belt should be positioned so that the silver coated yarn points out, away from the skin, and it should not be tightened excessively around the body, but just tightened enough to avoid any undesired movement of the device during daily activities and nighttime.

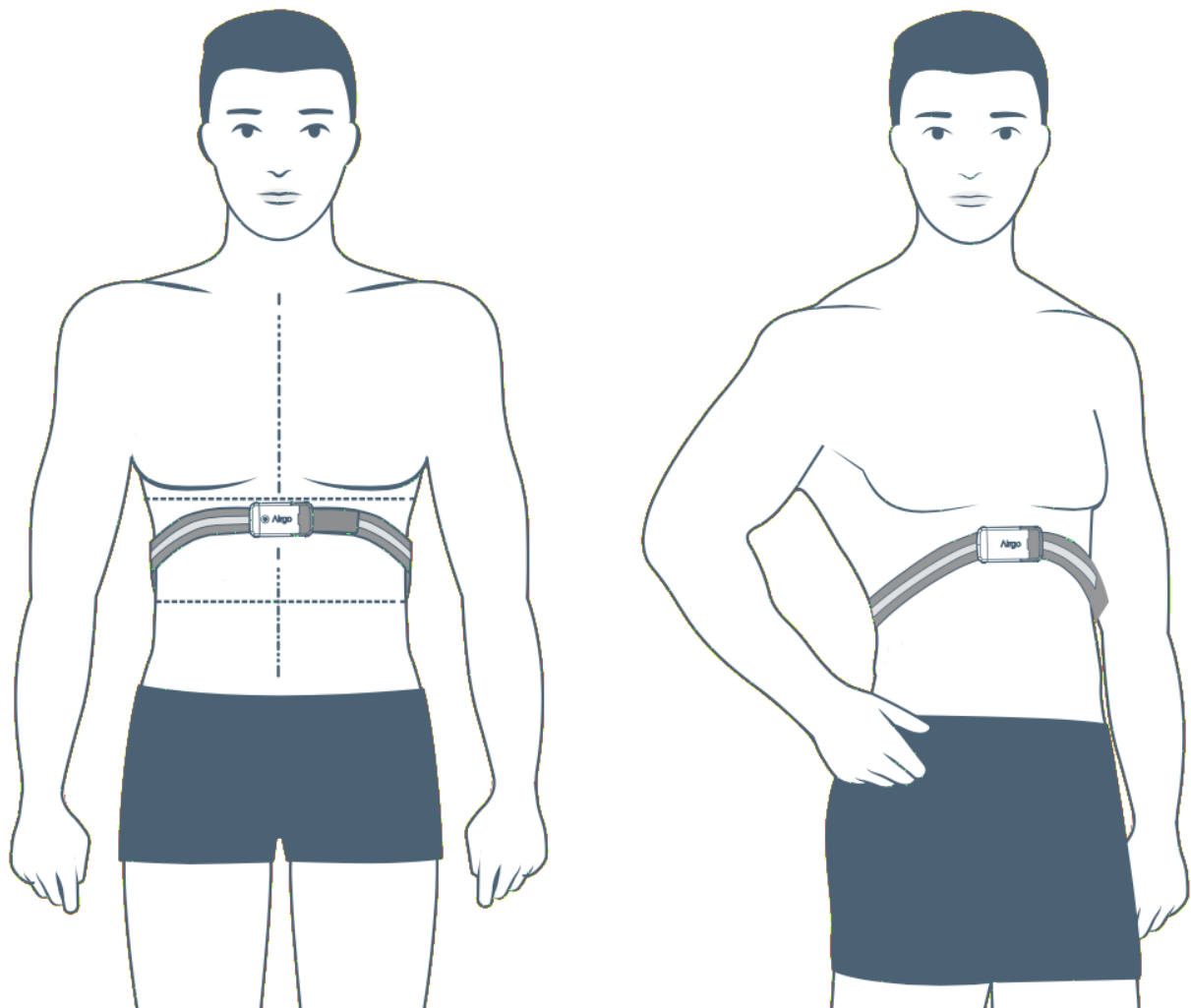


Figure 4.6: Schematic representation of the patented [115] belt placement of the Airgo™ device.

4.2 Software Description

The Airgo™ system highly relies on the power of its patented algorithms [115] and on artificial intelligence assisted pattern recognition. The two main software components of Airgo™ are the mobile application and the Semantic Engine: the app allows for data exchange between the Airgo™ devices and the Semantic Engine.

4.2.1 Airgo™ app

The Airgo™ app has been designed to run on any portable device: it is available for both iOS and Android.

The app allows for both real-time and a posteriori data exchange with the microprocessor inside the Airgo™ Recorder. In fact, first of all it is possible to manage the recorded sessions onboard and forward them via internet to a doctor for analysis. Moreover, it is possible to monitor the patient in real time using telemedicine: this allows for real-time breath to breath analytics at a distance to cover patients that are in critical care without the doctor's need to get close to them. This feature has been of great help during COVID-19 pandemic lockdowns.

Moreover, as shown in Figure 4.7, as an Airgo™ device is connected the app provides the patient with step-by-step instructions for the correct onboarding of the device.

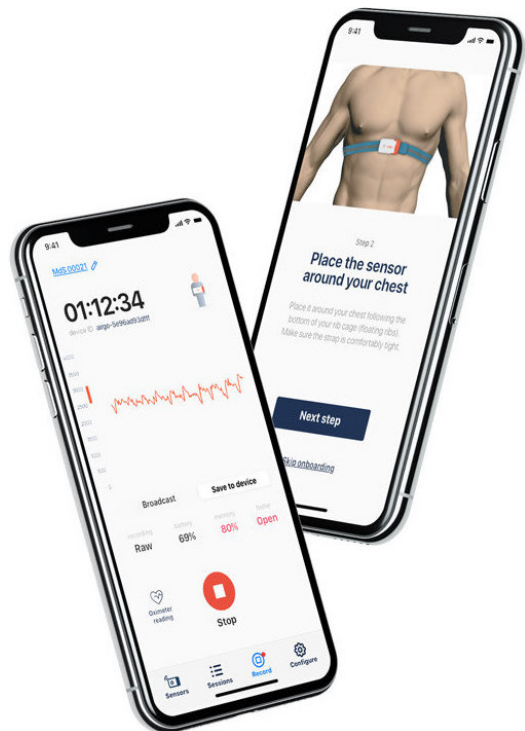


Figure 4.7: iOS version of the Airgo™ app for mobile devices. Source: [116].

4.2.2 Airgo™ Semantic Engine

Airgo™ Semantic Engine is the core of the Airgo™ software. After receiving the raw data from the Airgo™ devices via the app, the Semantic Engine processes it and extracts all the useful information and parameters. Predictive analysis occurs in the proprietary patented algorithms using a physiological model of respiratory dynamics and employing AI analysis and machine learning.

First of all, the Engine provides an accurate real-time reading of respiratory rate (RR). This goes in contrast with many other devices, since nowadays it is common to derive RR from hearth rate monitoring. Although, the algorithms that derive RR from heart rate are not very precise and tend to make errors: in particular, they work well when the patient is

healthy and breathes normally, whereas in case of respiratory pathologies like COVID-19 the RR estimations derived from these algorithms are often misleading and almost always underestimated. Underestimation of RR tends to happen also when breaths are counted looking at a clock (remember from subsection 2.1.1).

Moreover, Airgo™ Semantic Engine provides an indication of the patient's type of breathing: smooth compliant breathing comes out looking like a very smooth Airgo™ signal, but when the patient is not compliant (for example if they have obstruction or if they fight with the respiratory machine), the signal becomes irregular and chaotic.

With respect to sleep analysis, MyAir Inc. has devised the Respiratory Instability Curves™ (RICs™). Four RICs™ are computed, one for each posture in which the patient may sleep: supine, prone, right side and left side; in case of detection of a sleep disorder, this allows to detect whether it has a postural nature or not.

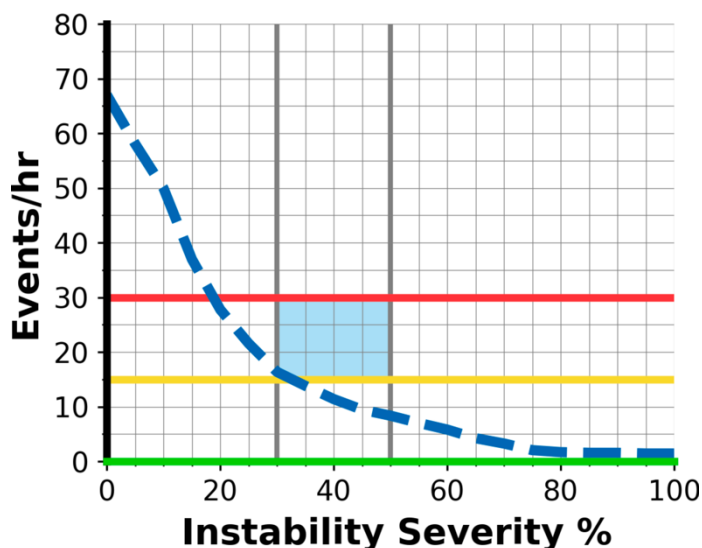


Figure 4.8: Example of Respiratory Instability Curve™. As shown in Figure 4.8, on the y-axis is the number of respiratory instability events per hour while on the x-axis is the percentage of event severity. To detect respiratory instability events, Airgo™ makes use of minute ventilation. In particular, for each moment the average minute ventilation over the last sixty seconds (Mv60) and over the last ten seconds (Mv10) are calculated; Mv60 is then used as a reference compared to Mv10: a reduction in ventilation is observed every time the Mv10/Mv60 ratio drops below 1. When the Mv10/Mv60 ratio remains below 1 for at least ten seconds, a respiratory instability event is detected and considered to calculate the RICs™. Instability severity is calculated considering the depth of the reduction of ventilation for that specific event. Considering both the number of events and their severity allows to consider all kinds of respiratory instabilities at once, ranging from mild hypopneas to apneas.

The rectangular area colored in light blue in the graph (Figure 4.8), identified as *Target*, can help physicians to read RICs™ more easily. In fact, the Target serves the purpose to give an idea at first glance of the quality of the subject's sleep.

The external limits of the Target area, 15-30 events per hour on the y-axis and 30-50% instability severity on the x-axis, have been established based on extensive clinical validation based on over 1200 patients. During clinical validation Airgo™ was compared with

polysomnography (PSG), the gold standard for sleep analysis, and it was found that a 30% drop in ventilation for at least ten seconds corresponds to the 3% drop in oxygen saturation used in Apnea-Hypopnea Index (AHI) classification following the American Academy of Sleep Medicine (AASM) guidelines, while at least 35% drop in ventilation is required to induce a 4% drop in oxygen saturation.

As shown in Figure 4.9, the position of the curve with respect to the Target area determines the severity of the patient's sleep disorders: if the blue dashed line passes below the square sleep quality is high, while the more the line goes up towards more events per hour and/or higher instability severity, the worst the quality of the subject's sleep gets.

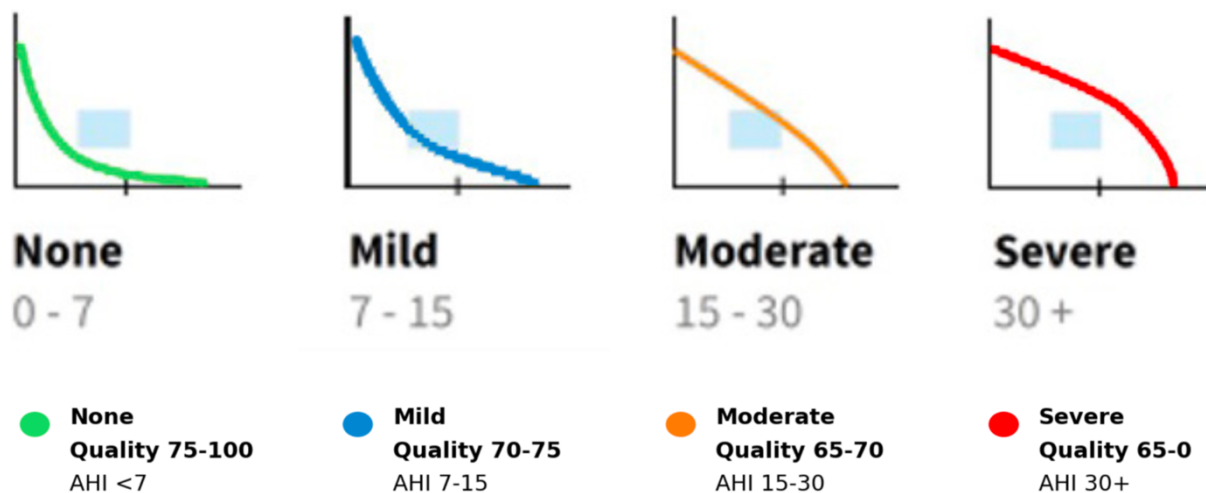


Figure 4.9: How the RIC™ is oriented with respect to the light blue Target area indicates the severity of the patient's sleep disorders. The green curve represents a Risk Category of "None", which in traditional PSG corresponds to AHI < 7; the blue curve represents a Risk Category "Mild", which corresponds to AHI between 7 and 15; the orange curve represents a Risk Category "Moderate", which corresponds to AHI between 15 and 30; the red curve represents a Risk Category "Severe", which corresponds to AHI > 30.

4.3 Device Applications

Airgo™ is the first non-invasive and non-intrusive device which is able to provide precise measurements of breath dynamics 24/7 in all possible conditions. In this section, a brief description of the current applications of the device is provided.

4.3.1 Sleep quality assessment

Nowadays, the most widespread application is the assessment of a person's sleep quality from a respiratory point of view, with particular attention to sleep disorders, such as obstructive sleep apnea (OSA) and central sleep apnea (CSA), and abnormal breathing patterns like Cheyne-Stokes respiration and Kussmaul breathing. Airgo™ has been proven to identify patients affected by OSA with 94% positive predictive value (PPV) and 89%

negative predictive value (NPV) [118]. Moreover, Airgo™ sleep scoring showed 97.5% correlation to polysomnography (PSG), the gold standard for sleep analysis, during clinical trials on more than four hundred patients at Massachusetts General Hospital, more than sixty patients at Minnesota Lung Center and more than one hundred and fifty patients at Fondazione Maugeri IRCCS in Veruno, Italy. ([119], [120]).

Thanks to Airgo™ Semantic Engine, sleep disorder screening is fully automated. The software analyzes the data acquired from a night of sleep and calculates indexes such as Respiratory Disturbance Index (RDI) and Apnea-Hypopnea Index (AHI) and derives a sleep quality score that ranges from 0 to 100. Thanks to the presence of the motion detection circuit, all the scores provided are classified according to the posture in which the subject was sleeping. In this way, it is possible to obtain an indication of the possible postural nature of any disorders.

Moreover, analyzing the movement of both the rib cage and the diaphragm, Airgo™ Semantic Engine performs automated sleep staging. Lastly, through the analysis of the fragmentation of the breath vectors identified by the software, snoring recognition is performed without the need of using microphones; this is a key point nowadays, considering how big of a concern privacy is.

Sleep reports can be generated for each night of sleep of the patient. The report cover provides an overview of the patient's sleep quality, showing the sleep quality index and the four Respiratory Instability Curves™ on top of the page (Figure 4.10).

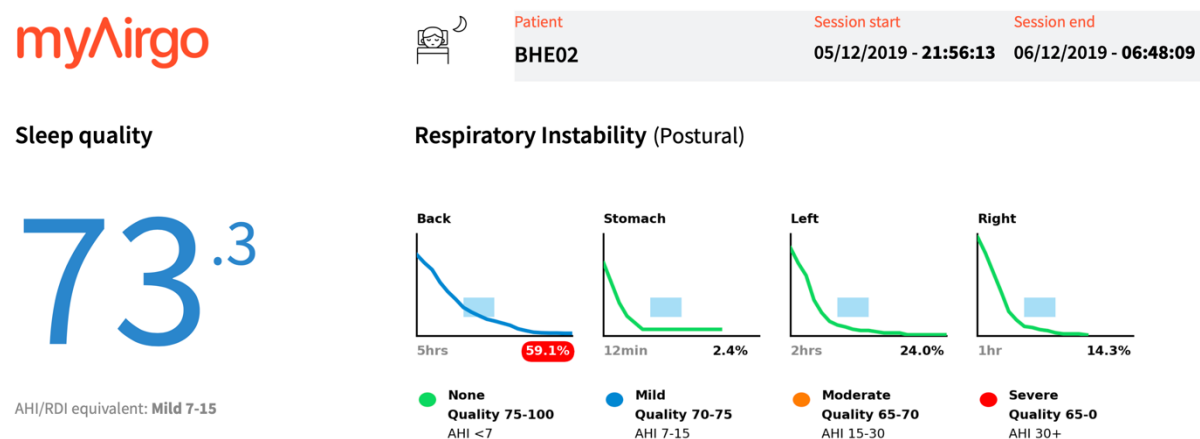


Figure 4.10: The cover of the sleep report provides an overview of the patient's sleep quality, showing the sleep quality index and the Respiratory Instability Curves™.

4.3.2 Other applications

Thanks to the versatility of the device, respiratory health can be monitored analyzing respiration throughout the whole day. Airgo™ lends itself well to promotion of health in terms of measuring respiratory activity as part of the quest for personal fitness and a healthy lifestyle.

Moreover, since it is well known that controlled breathing is crucial for elite athletes, Airgo™ can be used to track respiration during athletic performances. In this way, athletes can gain awareness of their respiration patterns, and coaches can instruct them on where some improvements have to be achieved.

Furthermore, Airgo™ can provide real-time feedback to other medical devices to improve their performance: for example, Airgo™ data may be used to activate or modify the pressure of a continuous positive airway pressure device (CPAP), which is used to treat sleep apneas, according to the current breathing patterns of the patient [115].

Lans but not least, Airgo™ is used for a wide range of clinical applications [121]:

- Post operative care
- Hospital discharge and readmission control
- Physiotherapy and rehabilitation (continuity of care)
- Intensive care unit (ICU) and COVID-19 respiratory monitoring
- General care floors
- Remote patient monitoring and telehealth
- Emergency department, to triage faster and with more confidence.

Chapter 5 Study Description

It is well known that physical activity is of great help in terms of preserving and enhancing overall health of human beings. A group of researchers, An Ouyang et al., from Massachusetts General Hospital (MGH) in Boston, MA, decided to conduct this study, namely *Brain Age and Exercise: A Trial of Aerobic Exercise to Improve Brain Health in Older Adults*, to investigate whether a twelve-week aerobic training program would improve brain health, sleep quality and cardiovascular fitness in middle-aged sedentary adults.

5.1 Participants

To be eligible to participate in the study, the subjects had to meet the following characteristics:

- Be aged between fifty and seventy-five years old
- Have spent an average of less than sixty minutes per week exercising in the past six months
- Be cleared by primary care physician to participate to the twelve-week exercise program

Eligible participants were selected also considering the following exclusion criteria:

- Diagnosed with moderate or severe sleep apnea (AHI > 15) or using a continuous positive airway pressure (CPAP) device
- History of neuropsychiatric illness
- History of falling in the past six months
- Development of cardiac symptoms or failure to complete cardiopulmonary exercise testing (CPET) during the enrollment testing phase.

Out of the 185 people who showed to the eligibility screening, thirty participants were enrolled from the greater Boston area between November 2019 and June 2021. Subsequently, two participants withdrawn because of personal reasons related to the COVID-19 pandemic, and other two quit the program because of difficulties in accessing exercise resources during COVID-19 lockdowns. The characteristics of the twenty-six remaining participants are shown in Table 5.1.

	Pre-Exercise	Post-Exercise
Age	60.11 ± 7.37	-
Sex	20 Females 6 Males	-
Race	1 American Indian 3 Asian 1 Black or African 23 White	-
Body Mass Index (BMI)	25.86 ± 4.16	25.83 ± 3.97

Table 5.1: Participants characteristics. Two participants selected more than one race. Data is mean ± standard deviation. The difference in the average BMI between Pre- and Post-Exercise is not statistically significant.

5.2 Methods

5.2.1 Study design

On the enrollment day, participants underwent cardiopulmonary exercise testing (CPET), cognitive testing and blood draw. One week later, they went to the American Academy of Sleep Medicine (AASM)-Accredited MGH Sleep Disorders Unit to undergo a diagnostic polysomnography exam (PSG), which was then repeated at the end of the twelve-week exercise program. During PSG, a minimum of six hours of overnight sleep was monitored using a conventional in-lab polysomnograph (Compumedics, NC).

After completing the initial testing phase, participants started a 12-week aerobic training program that prescribed maintaining heart rate between 50% and 75% of maximal heart rate (calculated as 220 minus person's age in years) for thirty minutes per day, five days per week. Since all participants were fully sedentary, they were prescribed to exercise fifteen minutes a day for three times over the first week, twenty minutes a day for four times over the second week and then proceeded to train at full regimen from the third week on. In case of failure to complete thirty minutes of continuous workout, participants were allowed to split training time into sets of ten-fifteen minutes of continuous work followed by five minutes of rest interval. To ensure that the subjects' training sessions met the prescribed criteria in terms of both duration and intensity, they were instructed to wear a physical activity tracker (Fitbit, USA).

Last but not least, as described in subsection 5.2.2, during the 12-week program several kinds of data were collected from the participants to monitor their progress. A summary of the study design is shown in Figure 5.1.

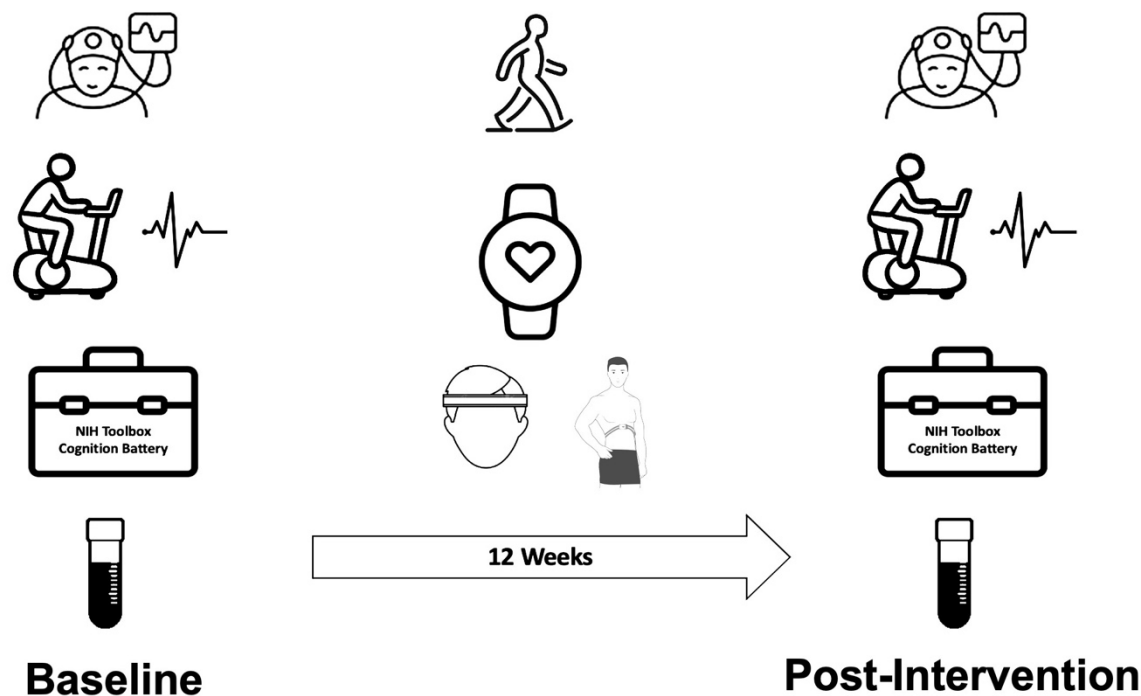


Figure 5.1: Summary of the study design. PSG, CPET, cognitive testing and blood draw were repeated before and after the twelve-week exercise program during which the participants were continuously monitored using screening devices at home.

5.2.2 Home data collection

Participants were constantly monitored from home thanks to the continuous use of two devices:

- Fitbit watch was used to monitor the subjects' heart rate. The participants were instructed to upload the data stored on device on the cloud every five days, so that the study team could check if they were following the exercise program correctly.
- Airgo™ was worn by the participants 24/7. Every fourteen days, each subject's device was replaced with another one so that the data stored in it could be uploaded on the cloud by the study team. Airgo™ data was not analyzed by An Ouyang and its team, but it was left out for future analysis, which I took care of. Airgo™ data analysis will be discussed in Chapter 6.

Moreover, sleep EEG was recorded twice a week using a home sleep headband (Prodigy, Canada; Dreem 2, France). EEG data was examined weekly by the study team and sleep staging was performed using an automated algorithm based on deep neural networks [122].

5.3 Results

In this section, all data is expressed in form of Mean \pm Standard Deviation (SD). The statistical analysis performed is based on paired t-tests between data acquired prior to the twelve-week exercise program, taken as baseline, and data acquired at the end of the study. Statistical significance was defined as p-value < 0.05 .

Based on heart rate data and exercise logs, participants exercised for 47 ± 13 days over the twelve-week program; training sessions lasted 55 ± 9.8 minutes.

5.3.1 Physicality

Starting from the physicality of the participants, the average BMI at the end of the program (25.83 ± 3.97) was slightly lower, but not statistically different from the baseline BMI (25.86 ± 4.16).

5.3.2 Cardiovascular fitness

Speaking of cardiovascular fitness, statistically significant results were obtained (Figure 5.2): increased $VO_2\max$ (Pre-Ex: 21.11 ± 1.03 mL/kg/min, Post-Ex: 22.39 ± 1.12 mL/kg/min; $p = 0.0413$), which means *Volume of O₂ Maximum* and is a measurement of how much oxygen a person's body can use at maximal sustained output ($VO_2\max$ was calculated during CPET), decreased daytime resting heart rate (Pre-Ex: 66.66 ± 0.83 bpm, Post-Ex: 65.13 ± 0.61 bpm, $p = 0.011$) and decreased sleeping heart rate (Pre-Ex: 64.55 ± 1.28 bpm, Post-Ex: 62.93 ± 1.03 bpm; $p = 0.028$).

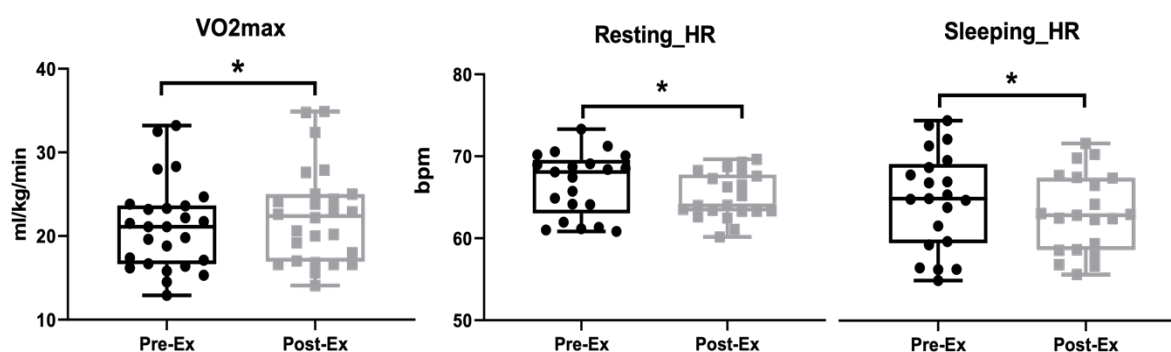


Figure 5.2: Comparison of cardiovascular fitness indicators ($VO_2\max$, resting heart rate and sleeping heart rate) between the baseline (Pre-Ex) and the end of the twelve-week exercise program (Post-Ex). The asterisk is set as statistical significance ($p < 0.05$).

5.3.3 Cognitive performance

Cognitive performance of the participants significantly improved in multiple domains during the twelve-week program, including the composite domains of crystallized

intelligence (Pre-Ex: 115.1 ± 1.4 , Post-Ex: 117.4 ± 1.38 ; $p = 0.0008$), fluid intelligence (Pre-Ex: 104.8 ± 2.35 , Post-Ex: 109.3 ± 2.23 ; $p = 0.0058$) and total cognition (Pre-Ex: 111.1 ± 1.70 , Post-Ex: 115.2 ± 1.60 ; $p = 0.0001$). Moreover, improvements in Pattern Comparison Processing Speed (Pre-Ex: 100.7 ± 3.92 , Post-Ex: 107.6 ± 3.52 ; $p = 0.036$) and Oral Reading Recognition (Pre-Ex: 113 ± 1.19 , Post-Ex: 116.5 ± 1.13 ; $p < 0.0001$) were observed.

5.3.4 Sleep analysis

As previously mentioned, sleep was analyzed using both in-lab traditional PSG and a home headband which recorded sleep EEG.

As shown in Figure 5.3, in terms of sleep staging neither of the two techniques found significant differences in stage percentages:

- Wake (W):
 - PSG: Pre-Ex: $16.63 \pm 2.46\%$, Post-Ex: $17.83 \pm 2.12\%$; $p = 0.6498$
 - Home EEG: Pre-Ex: $21.27 \pm 2.3\%$, Post-Ex: $21.18 \pm 2.57\%$; $p = 0.9659$
- Rapid eye movement (REM):
 - PSG: Pre-Ex: $16.63 \pm 2.46\%$, Post-Ex: $21.31 \pm 2.80\%$; $p = 0.8107$
 - Home: Pre-Ex: $19.95 \pm 1.45\%$, Post-Ex: $19.94 \pm 1.14\%$; $p = 0.9932$
- Non-rapid eye movement (NREM):
 - PSG: Pre-Ex: $62.49 \pm 3.39\%$, Post-Ex: $60.86 \pm 3.06\%$; $p = 0.5982$
 - Home: Pre-Ex: $57.99 \pm 2.15\%$, Post-Ex: $58.53 \pm 2.15\%$; $p = 0.7493$

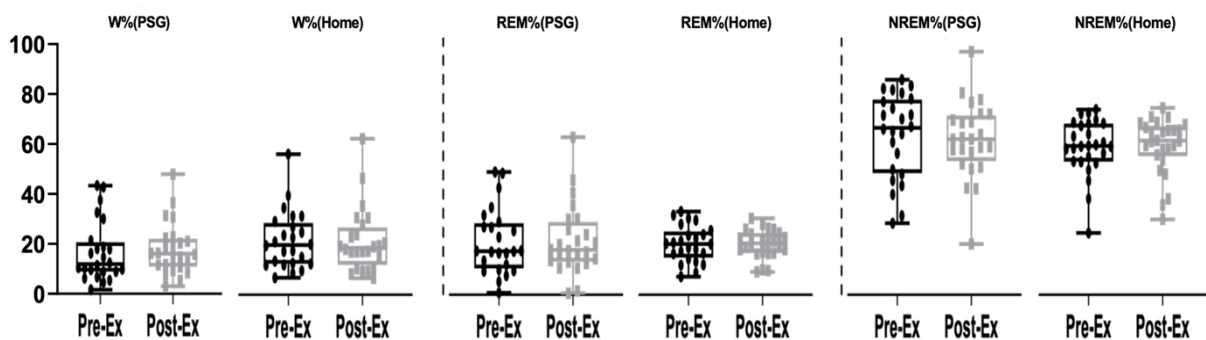


Figure 5.3: Comparison of sleep stage percentages between the baseline (Pre-Ex) and the end of the twelve-week exercise program (Post-Ex). W is for Wake, REM is for rapid eye movement and NREM is for non-rapid eye movement. Neither technique (PSG nor Home EEG) found statistically significant differences between Pre- and Post-Ex.

Moreover, recalling that being diagnosed with moderate or severe sleep apnea (AHI > 15) was one of the exclusion criteria for the study participants, a difference was found in

average AHI values between the baseline (4.05 ± 3.92) and the end of the training program (3.06 ± 3.94).

Last but not least, as shown in Figure 5.4 neither of the two techniques found statistically significant differences between traditional sleep quality measures derived from sleep macro-architecture:

- Sleep efficiency:
 - PSG: Pre-Ex: $83.37 \pm 2.46\%$, Post-Ex: $82.17 \pm 2.12\%$; $p = 0.6498$
 - Home EEG: Pre-Ex: $76.8 \pm 2.99\%$, Post-Ex: $78.27 \pm 2.72\%$; $p = 0.3697$
- Awakening index:
 - PSG: Pre-Ex: 3.58 ± 0.58 , Post-Ex: 2.91 ± 0.36 ; $p = 0.2592$
 - Home EEG: Pre-Ex: 5.96 ± 0.86 , Post-Ex: 5.26 ± 0.72 ; $p = 0.2160$
- Wake after sleep onset (WASO):
 - PSG: Pre-Ex: 61.52 ± 11.11 min, Post-Ex: 66.58 ± 10.77 min; $p = 0.7250$
 - Home EEG: Pre-Ex: 67.27 ± 10.39 min, Post-Ex: 71.5 ± 14.21 min; $p = 0.5903$

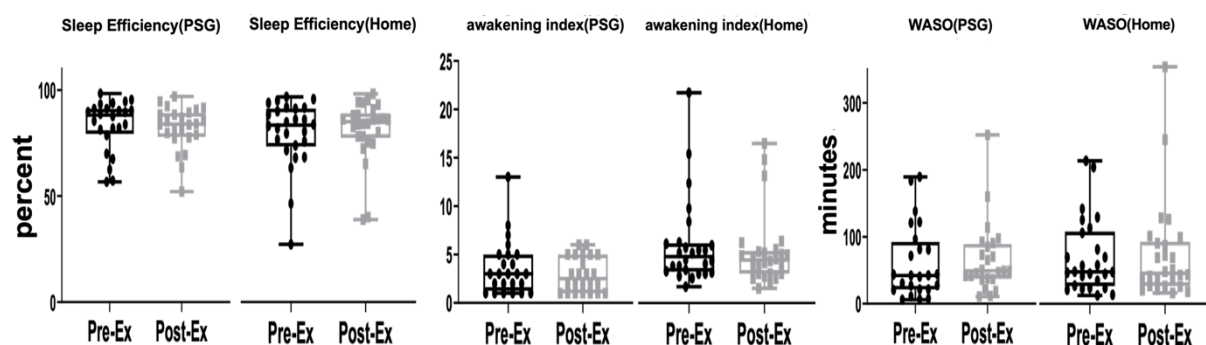


Figure 5.4: Comparison of traditional sleep quality measures between the baseline (Pre-Ex) and the end of the twelve-week exercise program (Post-Ex). WASO is for wake after sleep onset. Neither technique (PSG nor Home EEG) found statistically significant differences between Pre- and Post-Ex.

Chapter 6 Airgo™ Data Analysis

6.1 Airgo™ Data

As mentioned in Chapter 5, Airgo™ data was not analyzed by An Ouyang and his team. All participants were required to wear the Airgo™ device continuously over the twelve-week training program; during that period of time, the study team took care of uploading data collected from the Airgo™ devices to the cloud.

Since the data was not analyzed during the program, any device malfunctions or misplacements on the subjects' bodies was not detected in time to be fixed. This led to missing data for a few subjects, which had to be excluded from the analysis.

Out of the original twenty-six participants, data was missing or insufficient for nine: thus, all further considerations are made upon data coming from seventeen subjects.

6.2 Methods

6.2.1 Breath vectors (CQBV)

Starting from the raw resistance signal acquired by the aWare strap belt, Airgo™ patented algorithms [115] identify each breath and represent it as a vector, which is called *Cluster Qualified Breath Vector* (CQBV), as follows:

- Relative minimum and maximum points are identified in the raw signal

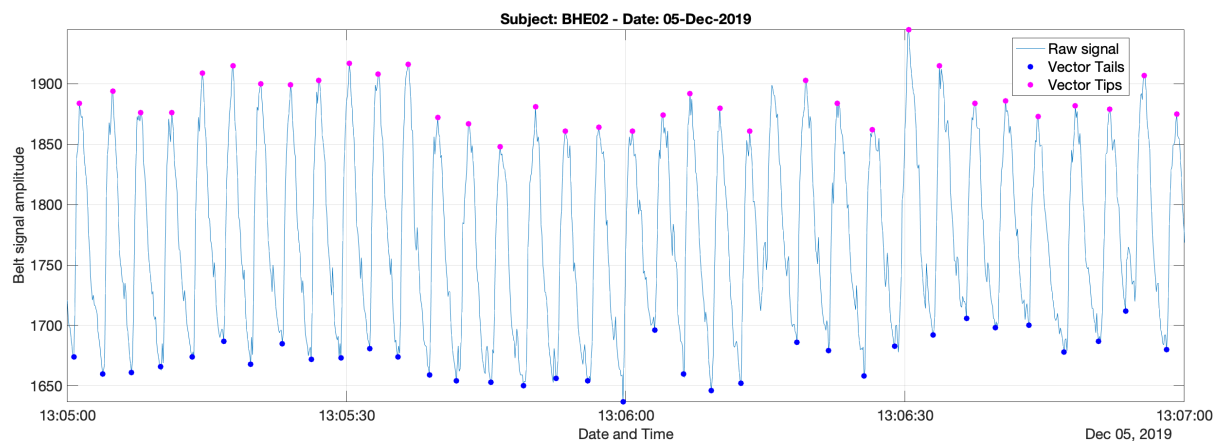


Figure 6.1: Two minutes of raw belt signal with superimposed tail and tip points of the computed CQBV for a subject (BHE02).

- Each relative minimum marks the tail of a breath vector, which tip is marked by the following relative maximum point
- Breath vectors obtained are processed by an algorithm based on artificial intelligence, which through clustering methods merges any vectors that represent only a fraction of breaths instead of full ones into single larger vectors

An example of comparison between the raw signal acquired from the belt and the computed CQBV is shown in Figure 6.1.

6.2.2 Calculation of parameters

Starting from CQBV vectors computed by Airgo™ software, the following breath-to-breath time and volume parameters were calculated:

- Inspiratory Time (seconds), calculated as the elapsed time between the tail and the tip points of each vector:

$$\text{Inspiratory Time} = \text{timestep}_{tip} - \text{timestep}_{tail} \quad (5)$$

- Respiratory Rate (RR, breaths/minute), calculated as the reciprocal of the time (in minutes) elapsed between the start of each vector and the start of the following one:

$$RR_i = (\text{timestep}_{tail,i+1} - \text{timestep}_{tail,i})^{-1} \quad (6)$$

- Inspiratory to Expiratory Time Ratio (IE_ratio, dimensionless), calculated as the ratio between the inspiratory time (see Equation 5) and the time elapsed between the tip of the current vector and the tail of the following one (expiratory time):

$$IE_ratio_i = \frac{\text{Inspiratory Time}}{\text{timestep}_{tail,i+1} - \text{timestep}_{tip,i}} \quad (7)$$

- Tidal Volume (TV, relative), calculated as the difference in amplitude of the signal at the tip and tail of each vector:

$$TV = \text{amplitude}_{tip} - \text{amplitude}_{tail} \quad (8)$$

- Minute Ventilation (MV, relative), calculated as the product of Respiratory Rate and Tidal Volume of each breath:

$$MV = RR \times TV \quad (9)$$

Moreover, in order to distinguish between rest and activity states during daytime, it was necessary to calculate the mean activity level over each breath. To do so, data collected by the accelerometers inside the Airgo™ device was used. For each breath, the Euclidean norm of the mean acceleration vector was computed as follows:

$$\|\vec{a}\| = \sqrt{a_x^2 + a_y^2 + a_z^2} \quad (10)$$

In Equation 10, a_i is the mean acceleration data collected by the accelerometer in direction i (where $i = x, y, z$) between the timestep of the tail of the current vector and the timestep of the tail of the following one. Starting from the Euclidean norms of the acceleration vectors, the mean activity level over each breath was calculated as the absolute value of the difference between the Euclidean norm of the vector over the current breath and the following one:

$$ACT_i = | \|\vec{a}\|_{i+1} - \|\vec{a}\|_i | \quad (11)$$

An example of the calculated parameters for a subject is shown in Figure 6.2.

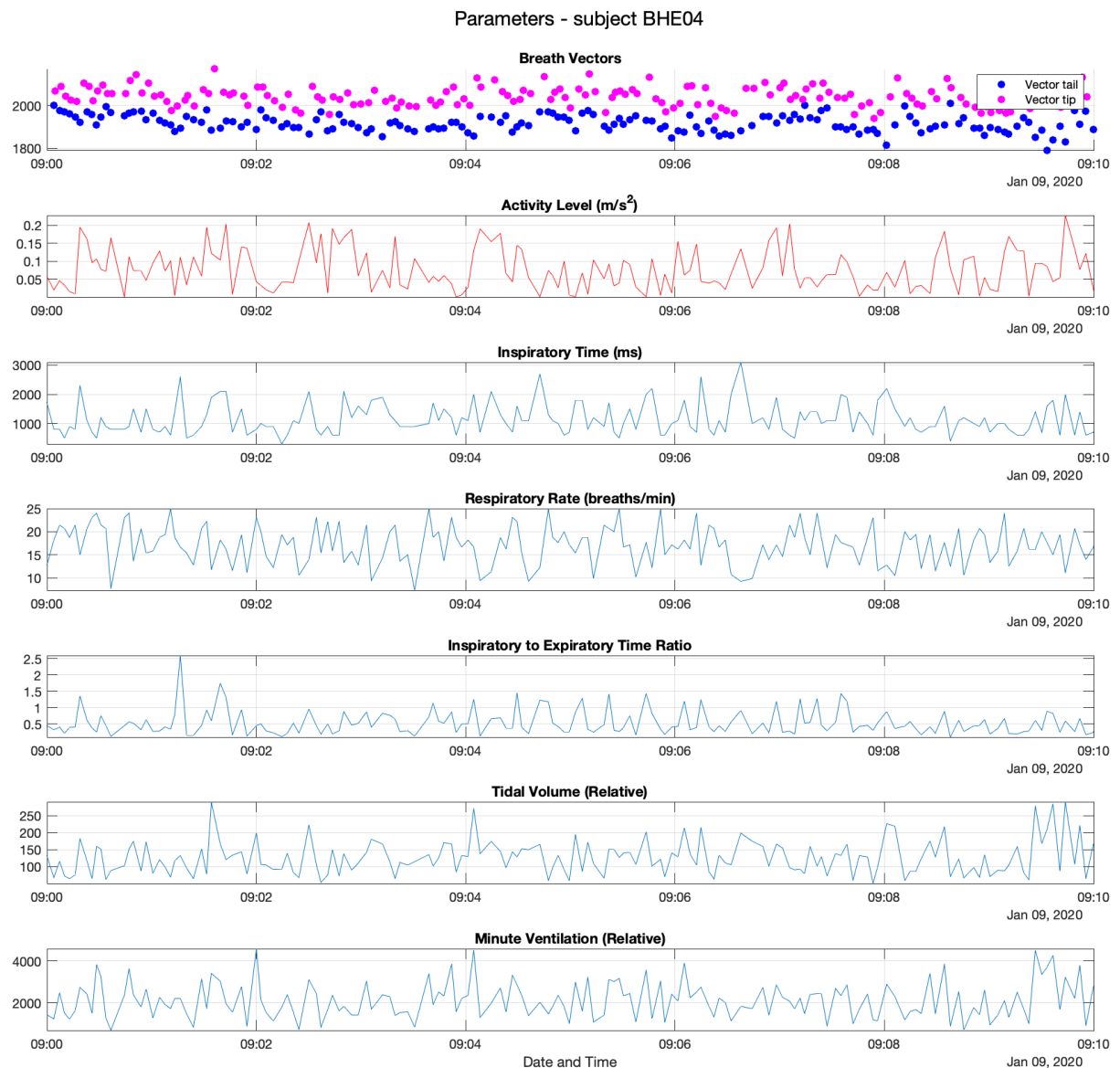


Figure 6.2: Ten minutes of breath vectors, activity level, time and volume parameters calculated for a subject (BHE04).

6.2.3 Daytime and Nighttime isolation

Since breathing-related parameters can be very different if analyzed during waking or sleeping state, the first step of this analysis consisted in isolating daytime and nighttime data.

To ensure that all seventeen subjects would be awake during the hours picked as daytime and asleep during the ones picked as nighttime, time slots with safely wide margins were selected:

- Daytime from 9:00 a.m. to 9:00 p.m.
- Nighttime from 12:00 a.m. to 6:00 a.m.

After choosing the time slots, the whole data from each subject was analyzed separately day by day and night by night. Days and nights for which less than two hours of data was available were excluded to avoid considering non-representative time intervals. The final number of available days and nights for each subject is shown in Table 6.1.

	Available Days	Available Nights	Start Date	End Date	Days Elapsed
BHE02	25	27	05 Dec 2019	02 Feb 2020	59
BHE04	24	25	08 Jan 2020	25 Mar 2020	76
BHE05	65	60	10 Feb 2020	11 May 2020	91
BHE06	23	19	12 Feb 2020	21 Apr 2020	69
BHE10	59	56	09 Mar 2020	18 May 2020	70
BHE15	25	22	15 Sep 2020	03 Nov 2020	48
BHE16	30	27	24 Sep 2020	11 Dec 2020	78
BHE17	20	19	24 Sep 2020	13 Dec 2020	80
BHE18	18	15	13 Oct 2020	18 Nov 2020	36
BHE19	28	26	15 Oct 2020	19 Nov 2020	33
BHE20	29	28	15 Oct 2020	20 Jan 2021	96
BHE21	33	27	27 Oct 2020	21 Jan 2021	84
BHE22	53	49	16 Dec 2020	09 Mar 2021	82
BHE26	37	36	14 Jan 2021	11 Mar 2021	55
BHE28	33	29	24 Feb 2021	14 May 2021	79
BHE29	27	27	24 Feb 2021	22 May 2021	87
BHE31	30	28	19 Mar 2021	16 Jun 2021	89

Table 6.1: Available days and nights of data for each subject. The column “Days Elapsed” represents the number of days between the first and the last available Airgo™ data acquisition.

6.2.4 Resting state detection

Activity level, calculated as mentioned in subsection 6.2.2, was used to differentiate between resting and active states during daytime. The reason behind this is that breathing parameters are deeply influenced by the person's activity level, thus it is important to isolate resting state before making any considerations.

To detect resting state during daytime, each day was analyzed separately as follows:

- The mean activity level throughout the day was calculated
- The day was divided into five-minute epochs
- If the mean activity level calculated over the i -th epoch was smaller than the mean activity level calculated over the full day, that epoch was considered as resting state

Figure 6.3 shows the result of the resting state detection algorithm for one day of a subject. All further analysis on daytime has been conducted on resting-state epochs only.

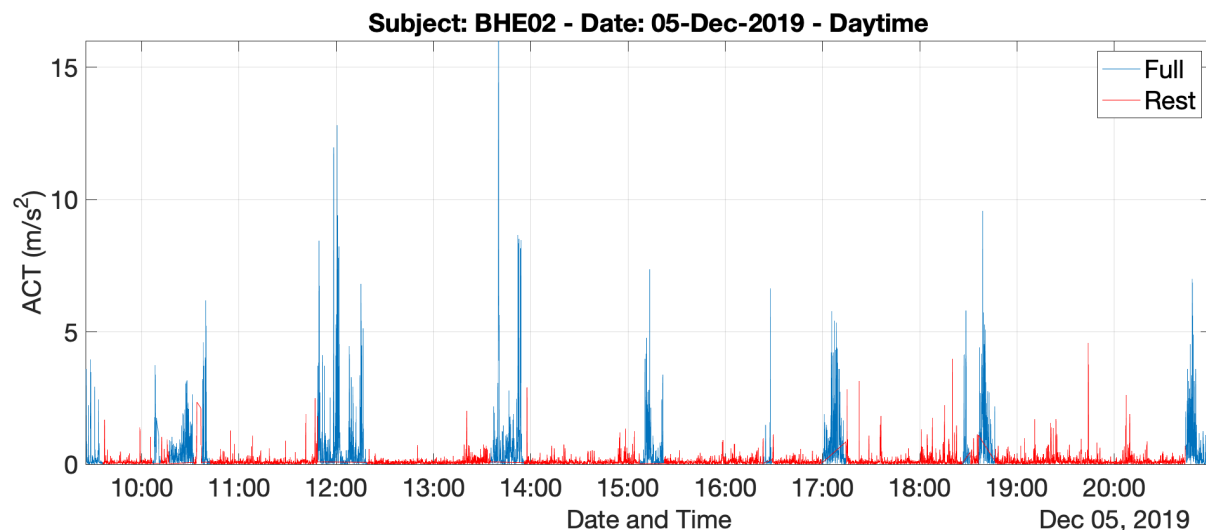


Figure 6.3: Result of the resting state detection algorithm on the first day of a subject (BHE02). Blue represents the full activity level signal; superimposed in red is the activity level of the epochs detected by the algorithm as resting state.

6.2.5 Sigh identification

As described in section 3.2, sighs can be identified in the respiratory signal as breaths with a tidal volume at least double (or triple) in amplitude with respect to the mean tidal volume in a surrounding representative interval [87].

The representative interval was chosen on the basis of the expected sigh rate, which is around ten sighs per hour [91], thus corresponding to 0.1667 sighs per minute. Choosing a control interval of six minutes ($1 \div 0.1667 \approx 6$) and considering an average sigh rate of twelve breaths per minute on the worst case (recalling from subsection 2.1.1, the normal

respiratory rate for adults during tidal breathing is between twelve to sixteen breaths per minute [26]), this corresponds to seventy-two breaths ($6 \times 12 = 72$). Following this logic, each breath should have been compared to a surrounding interval composed of the previous and the following thirty-six breaths. To account for any variability in sigh rate and to keep safety margins, an interval of forty breaths was chosen; thus, each breath was compared to an interval composed of the previous and the following twenty breaths.

Following the definition of sigh that can be found in literature, each breath was analyzed singularly. Sighs were identified as follows:

- The mean tidal volume over the surrounding interval of the current breath was calculated
- If the tidal volume of the current breath was greater than 2.5 times the mean tidal volume calculated over the surrounding interval, such breath was identified as a sigh

6.2.6 Respiratory variability analysis

Variability analysis on breathing signal focused mainly on respiratory rate, tidal volume and inspiratory time, as suggested by the literature ([82], [83]).

Since correlation between adjacent breaths is being sought, autocorrelation was chosen as measure of nonrandom variability. The autocorrelation sequences (ACSs) described below were calculated using the function *autocorr*, which is part of the Econometrics Toolbox in MATLAB R2022a, MathWorks® [123].

Moreover, as data has been organized in such a way that each breath corresponds to only one element in the vectors, the lags on which ACSs is computed correspond exactly to breath numbers.

To further clarify the procedure followed for the ACS analysis, which is described below, a recapitulatory scheme is shown in Figure 6.4.

Nonrandom respiratory variability was investigated following these steps:

- Around each sigh, identified as described in subsection 6.2.5, two distinct intervals were considered: the first interval was composed by the fifty breaths preceding the sigh, while the second interval included the initial fifteen post-sigh breaths [108]
- Over each pre- and post-sigh interval, autocorrelation sequences on respiratory rate, tidal volume and inspiratory time were calculated
- The mean pre-sigh and post-sigh ACSs for each day and night were calculated averaging the ACSs calculated over all the pre-sigh and post-sigh intervals belonging to each day and night respectively.

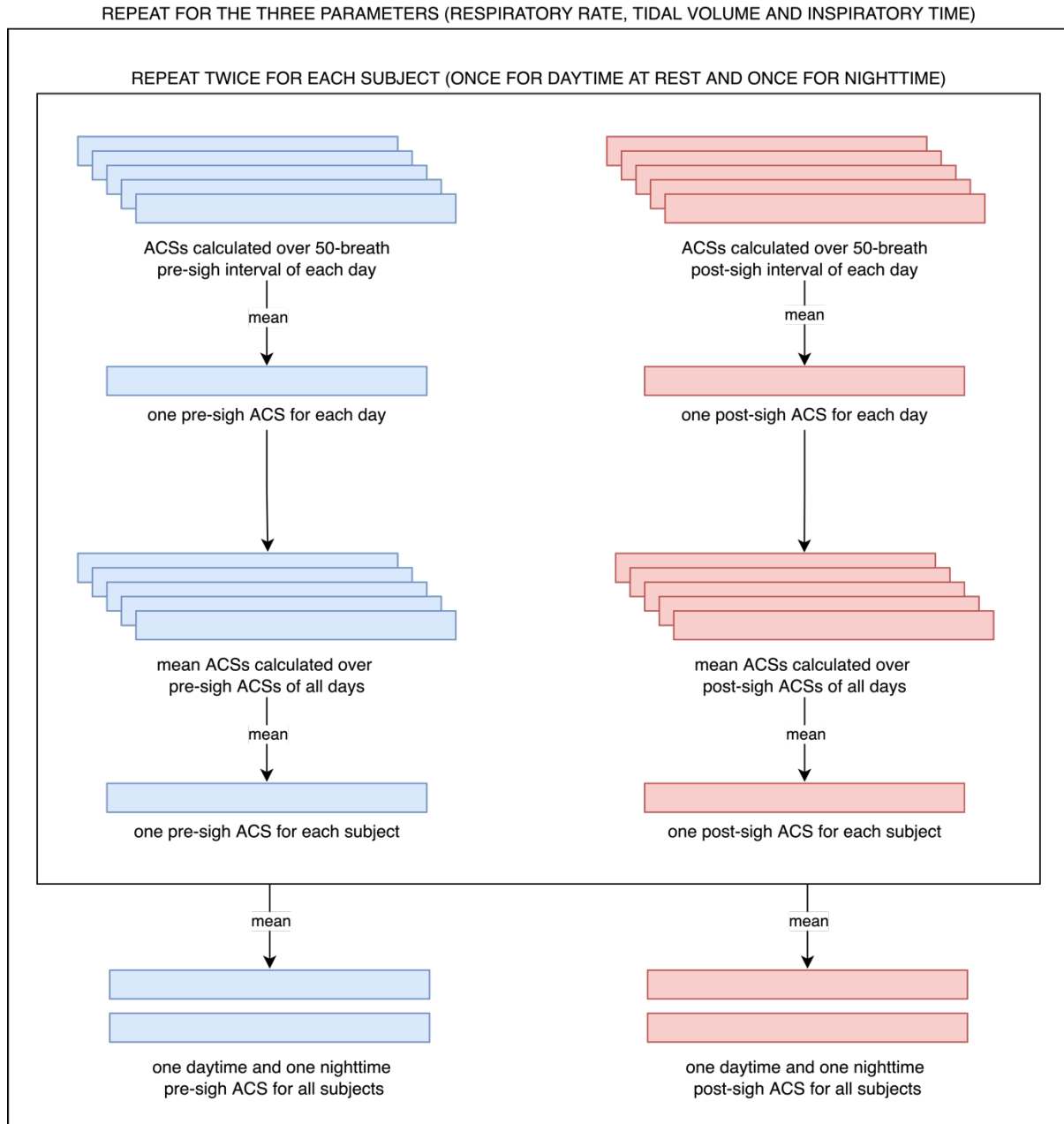


Figure 6.4: Recapitulatory scheme about the procedures followed in the analysis of the autocorrelation sequences, described in subsection 6.2.6.

An example of autocorrelation sequence calculated on respiratory rate, tidal volume and inspiratory time for a subject is shown in Figure 6.5.

Subsequently, the mean autocorrelation sequences for pre- and post-sigh intervals were calculated for each subject averaging the ACSs calculated for each day and night, thus obtaining only two ACSs for daytime (one for pre- and one for post-sigh intervals) and two for nighttime for each subject.

Lastly, the daytime and nighttime ACSs of all subjects were averaged to obtain two ACSs (one for pre- and one for post-sigh intervals) for all subjects. The final ACSs obtained are shown in Figure 6.6.

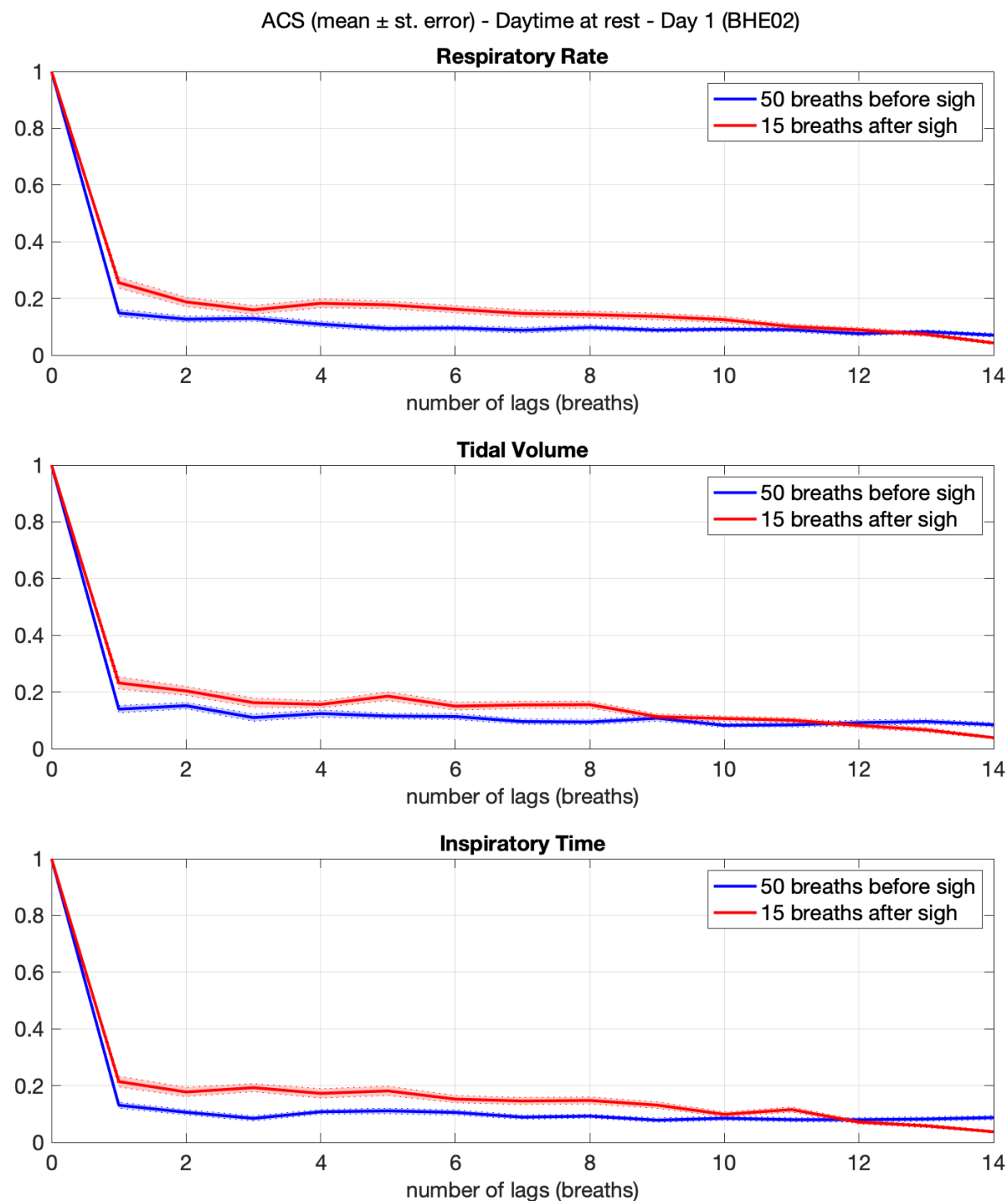


Figure 6.5: Autocorrelation sequences calculated on respiratory rate, tidal volume and inspiratory time for a subject (BHE02) over the resting epochs of the first day of acquisition (5th December 2019). Data is mean \pm standard error.

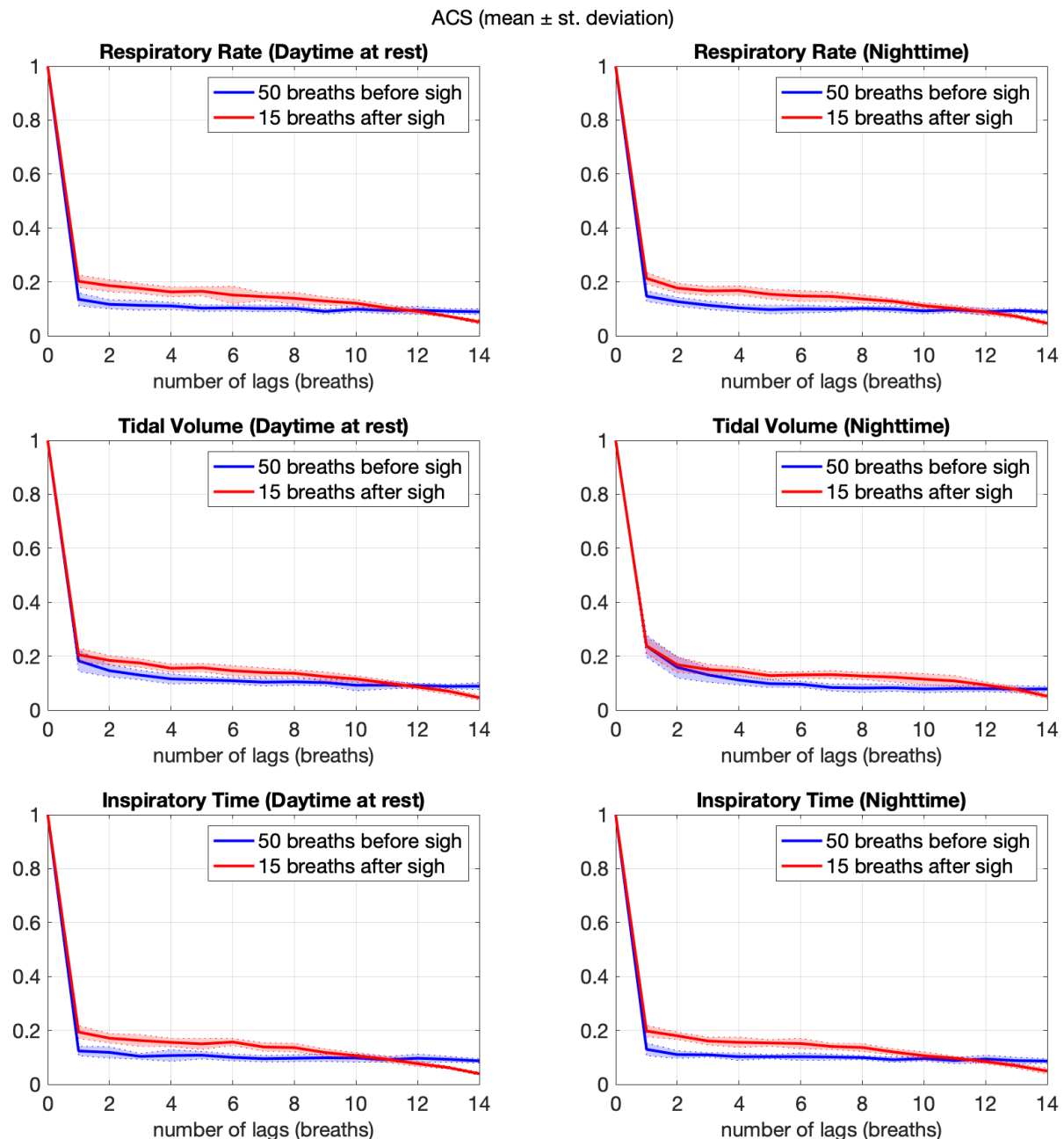


Figure 6.6: Autocorrelation sequences (ACSs) obtained averaging data coming from every day of every subject. The graphs in the left column represent data from daytime at rest, while the graphs in the right column represent data coming from nighttime acquisitions. Data is mean \pm standard deviation.

6.2.7 Sigh breath variability

Following the idea of Professor Riccardo Pellegrino, luminary in the field of diseases of the respiratory system and currently employed at Koelliker Hospital in Turin, variability in sigh breaths was investigated.

In particular, his idea claims that variability in sigh breaths in terms of both rate and amplitude relative to surrounding breaths could be evidence of lung elasticity and lung

health. Since the benefits of exercise to human health in general are well known, changes in such variability over the exercise program were investigated.

For this analysis, sigh rate was considered in terms of time (in seconds) elapsed between each sigh and the following one, instead of being considered as a proper rate expressed in sighs/hour as it is done in all other sections of this work. Sighs were identified as explained in subsection 6.2.5.

Daytime at rest and nighttime were investigated separately, and each subject was considered on his own. Variability was investigated for each day and night calculating the standard deviation of each of the two parameters considered.

6.3 Results

In this section, all data is expressed in form of Mean \pm Standard Deviation (SD). The statistical analysis performed is based on paired t-tests between data acquired prior to the twelve-week exercise program, taken as baseline, and data acquired at the end of the study. Statistical significance was defined as p-value < 0.05 .

T-tests were performed using the function *ttest*, which is part of the Statistics and Machine Learning Toolbox in MATLAB R2022a, MathWorks® [124].

6.3.1 Time and Volume parameters

Time and volume parameters, calculated as described in subsection 6.2.2, were compared between the baseline (Pre-Ex) and after completing the exercise program (Post-Ex). Daytime at rest and nighttime were analyzed separately; all results are shown in Figure 6.7.

The results obtained for each parameter are the following:

- Inspiratory time:
 - Daytime at rest: Pre-Ex: 1229.40 ± 140.18 ms, Post-Ex: 1270.60 ± 207.15 ms; $p = 0.4226$
 - Nighttime: Pre-Ex: 1437.80 ± 183.94 ms, Post-Ex: 1579.20 ± 176.77 ms; $p = 0.0008$ (statistically significant)
- Respiratory rate:
 - Daytime at rest: Pre-Ex: 16.76 ± 1.18 breaths/min, Post-Ex: 17.02 ± 1.71 breaths/min; $p = 0.4564$
 - Nighttime: Pre-Ex: 15.16 ± 1.22 breaths/min, Post-Ex: 14.99 ± 1.14 breaths/min; $p = 0.3623$
- Inspiratory to Expiratory time ratio:
 - Daytime at rest: Pre-Ex: 0.6266 ± 0.1212 , Post-Ex: 0.6800 ± 0.1853 ; $p = 0.3295$
 - Nighttime: Pre-Ex: 0.6542 ± 0.1606 , Post-Ex: 0.7707 ± 0.1444 ; $p = 0.0138$ (statistically significant)
- Tidal Volume:
 - Daytime at rest: Pre-Ex: 148.44 ± 71.32 , Post-Ex: 122.88 ± 84.23 ; $p = 0.1937$
 - Nighttime: Pre-Ex: 82.12 ± 57.92 , Post-Ex: 54.62 ± 25.51 ; $p = 0.0569$

○ Minute Ventilation:

- Daytime at rest: Pre-Ex: 2525.10 ± 1334.80 , Post-Ex: 2270.70 ± 2053.20 ; $p = 0.5508$
- Nighttime: Pre-Ex: 1226.60 ± 798.75 , Post-Ex: 812.10 ± 402.56 ; $p = 0.0451$ (statistically significant)

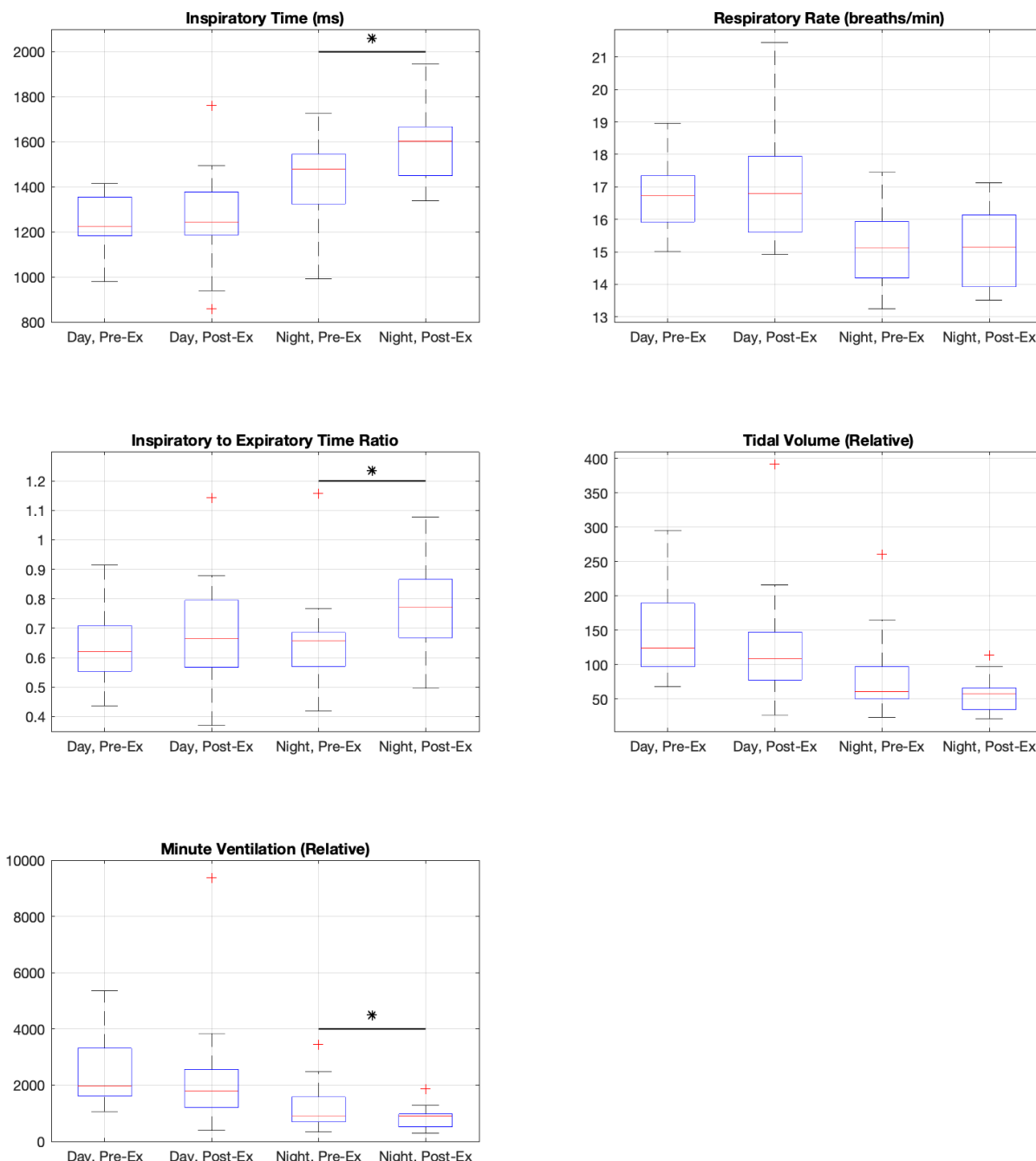


Figure 6.7: Comparison of time and volume respiratory parameters between the baseline (Pre-Ex) and the end of the exercise program (Post-Ex). Daytime at rest and nighttime were analyzed separately. Statistically significant differences between Pre- and Post-Ex were found for inspiratory time, inspiratory to expiratory time ratio and minute ventilation during nighttime. The asterisk is set as statistical significance ($p < 0.05$).

6.3.2 Sigh rate and amplitude

Changes in sigh rate and sigh amplitude relative to surrounding breaths (calculated as described in subsection 6.2.5) over the exercise program were investigated. In particular, the parameters calculated for all subjects were compared between the baseline (Pre-Ex) and after completing the exercise program (Post-Ex). Daytime at rest and nighttime were analyzed separately; all results are shown in Figure 6.8.

The results obtained for each parameter are the following:

- Sigh rate:
 - Daytime at rest: Pre-Ex: 21.80 ± 7.40 , Post-Ex: 25.27 ± 9.28 ; $p = 0.1887$
 - Nighttime: Pre-Ex: 27.93 ± 10.57 , Post-Ex: 28.50 ± 9.86 ; $p = 0.8546$
- Sigh amplitude relative to surrounding breaths:
 - Daytime at rest: Pre-Ex: 3.172 ± 0.270 , Post-Ex: 3.540 ± 0.654 ; $p = 0.0357$ (statistically significant)
 - Nighttime: Pre-Ex: 4.875 ± 1.206 , Post-Ex: 4.958 ± 1.149 ; $p = 0.7884$

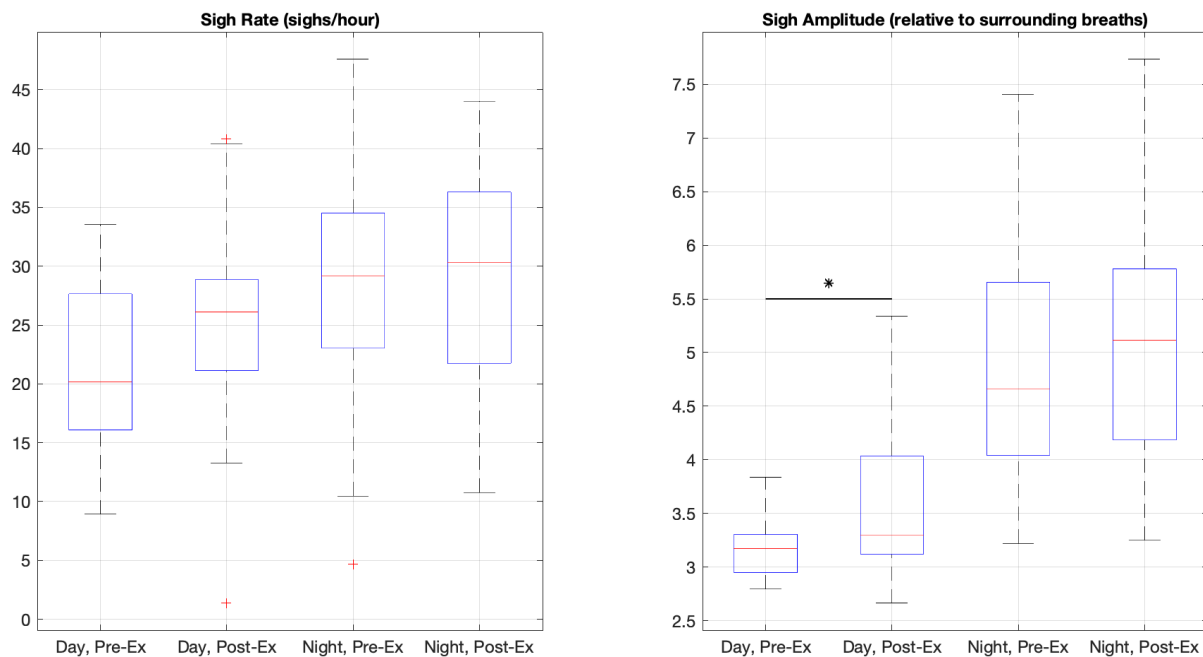


Figure 6.8: Comparison of sigh rate and sigh amplitude relative to surrounding breaths between the baseline (Pre-Ex) and the end of the exercise program (Post-Ex). Daytime at rest and nighttime were analyzed separately. Statistically significant differences between Pre- and Post-Ex were found for relative sigh amplitude during daytime at rest. The asterisk is set as statistical significance ($p < 0.05$).

6.3.3 Respiratory variability

Starting from the autocorrelation sequences calculated as described in subsection 6.2.6, the following statistically significant differences were found:

- Respiratory rate:
 - Daytime at rest: T-test rejected the null hypothesis with $p = 0.0036$. Table 6.2 contains pre- and post-sigh ACSs averaged between all subjects.

Autocorrelation sequence (Daytime at rest)

Lags	0	1	2	3	4	5	6	7
Pre-Sigh	1	0.1355	0.1168	0.1131	0.1109	0.1027	0.1035	0.1011
Post-Sigh	1	0.2023	0.1859	0.1756	0.1628	0.1654	0.1513	0.1454
Lags	8	9	10	11	12	13	14	-
Pre-Sigh	0.1015	0.0905	0.0988	0.0939	0.0948	0.0914	0.0894	-
Post-Sigh	0.1391	0.1288	0.1211	0.1033	0.0910	0.0724	0.1391	-

Table 6.2: Autocorrelation sequences calculated on respiratory rate over pre- and post-sigh intervals during daytime at rest.

- Nighttime: T-test rejected the null hypothesis with $p = 0.0062$. Table 6.3 contains pre- and post-sigh ACSs averaged between all subjects.

Autocorrelation sequence (Nighttime)

Lags	0	1	2	3	4	5	6	7
Pre-Sigh	1	0.1472	0.1268	0.1134	0.1034	0.0971	0.0996	0.0987
Post-Sigh	1	0.2134	0.1769	0.1665	0.1682	0.1542	0.1477	0.1462
Lags	8	9	10	11	12	13	14	-
Pre-Sigh	0.1017	0.0989	0.0923	0.0965	0.0897	0.0939	0.0884	-
Post-Sigh	0.1366	0.1279	0.1119	0.1014	0.0883	0.0724	0.0465	-

Table 6.3: Autocorrelation sequences calculated on respiratory rate over pre- and post-sigh intervals during nighttime.

○ Tidal Volume:

- Daytime at rest: T-test rejected the null hypothesis with $p = 0.0130$. Table 6.4 contains pre- and post-sigh ACSs averaged between all subjects.

Autocorrelation sequence (Daytime at rest)

Lags	0	1	2	3	4	5	6	7
Pre-Sigh	1	0.1826	0.1460	0.1296	0.1156	0.1120	0.1086	0.1034
Post-Sigh	1	0.2053	0.1842	0.1744	0.1551	0.1571	0.1459	0.1393
Lags	8	9	10	11	12	13	14	-
Pre-Sigh	0.1049	0.1020	0.0922	0.0923	0.0910	0.0878	0.0886	-
Post-Sigh	0.1364	0.1240	0.1154	0.1005	0.0852	0.0700	0.0460	-

Table 6.4: Autocorrelation sequences calculated on tidal volume over pre- and post-sigh intervals during daytime at rest.

- Nighttime: T-test rejected the null hypothesis with $p = 0.0018$. Table 6.5 contains pre- and post-sigh ACSs averaged between all subjects.

Autocorrelation sequence (Nighttime)

Lags	0	1	2	3	4	5	6	7
Pre-Sigh	1	0.2374	0.1583	0.1304	0.1112	0.0979	0.0960	0.0836
Post-Sigh	1	0.2384	0.1682	0.1505	0.1434	0.1277	0.1304	0.1314
Lags	8	9	10	11	12	13	14	-
Pre-Sigh	0.0816	0.0826	0.0783	0.0802	0.0796	0.0776	0.0781	-
Post-Sigh	0.1263	0.1222	0.1146	0.1079	0.0931	0.0766	0.0515	-

Table 6.5: Autocorrelation sequences calculated on tidal volume over pre- and post-sigh intervals during nighttime.

 ○ Inspiratory time:

- Daytime at rest: T-test rejected the null hypothesis with $p = 0.0277$. Table 6.6 contains pre- and post-sigh ACSs averaged between all subjects.

Autocorrelation sequence (Daytime at rest)

Lags	0	1	2	3	4	5	6	7
Pre-Sigh	1	0.1234	0.1184	0.1035	0.1066	0.1078	0.0998	0.0950
Post-Sigh	1	0.1938	0.1710	0.1624	0.1554	0.1499	0.1567	0.1386
Lags	8	9	10	11	12	13	14	-
Pre-Sigh	0.0966	0.0983	0.0975	0.0916	0.0966	0.0927	0.0869	-
Post-Sigh	0.1360	0.1179	0.1061	0.0929	0.0764	0.0619	0.0392	-

Table 6.6: Autocorrelation sequences calculated on inspiratory time over pre- and post-sigh intervals during daytime at rest.

- Nighttime: T-test rejected the null hypothesis with $p = 0.0068$. Table 6.7 contains pre- and post-sigh ACSs averaged between all subjects.

Autocorrelation sequence (Nighttime)

Lags	0	1	2	3	4	5	6	7
Pre-Sigh	1	0.1297	0.1102	0.1093	0.1022	0.1025	0.1024	0.1010
Post-Sigh	1	0.1975	0.1798	0.1604	0.1556	0.1533	0.1512	0.1403
Lags	8	9	10	11	12	13	14	-
Pre-Sigh	0.0990	0.0912	0.0952	0.0880	0.0937	0.0878	0.0862	-
Post-Sigh	0.1365	0.1201	0.1060	0.0969	0.0840	0.0689	0.0491	-

Table 6.7: Autocorrelation sequences calculated on inspiratory time over pre- and post-sigh intervals during nighttime.

6.3.4 Sigh breath variability

Changes in sigh breath variability were investigated over two parameters: time elapsed between each sigh and the following one and sigh amplitude relative to surrounding breaths, calculated as described in subsection 6.2.7. In particular, the variability of the two parameters calculated for all subjects were compared between the baseline (Pre-Ex) and after completing the exercise program (Post-Ex). Daytime at rest and nighttime were analyzed separately; all results are shown in Figure 6.9.

The results obtained for each parameter are the following:

- Variability in time elapsed between sighs:
 - Daytime at rest: Pre-Ex: 0.376 ± 0.067 , Post-Ex: 0.414 ± 0.074 ; $p = 0.1507$
 - Nighttime: Pre-Ex: 0.457 ± 0.055 , Post-Ex: 0.482 ± 0.026 ; $p = 0.0916$
- Variability in sigh amplitude relative to surrounding breaths:
 - Daytime at rest: Pre-Ex: 0.771 ± 0.407 , Post-Ex: 1.332 ± 1.051 ; $p = 0.0207$ (statistically significant)
 - Nighttime: Pre-Ex: 2.982 ± 1.590 , Post-Ex: 3.428 ± 2.589 ; $p = 0.5077$

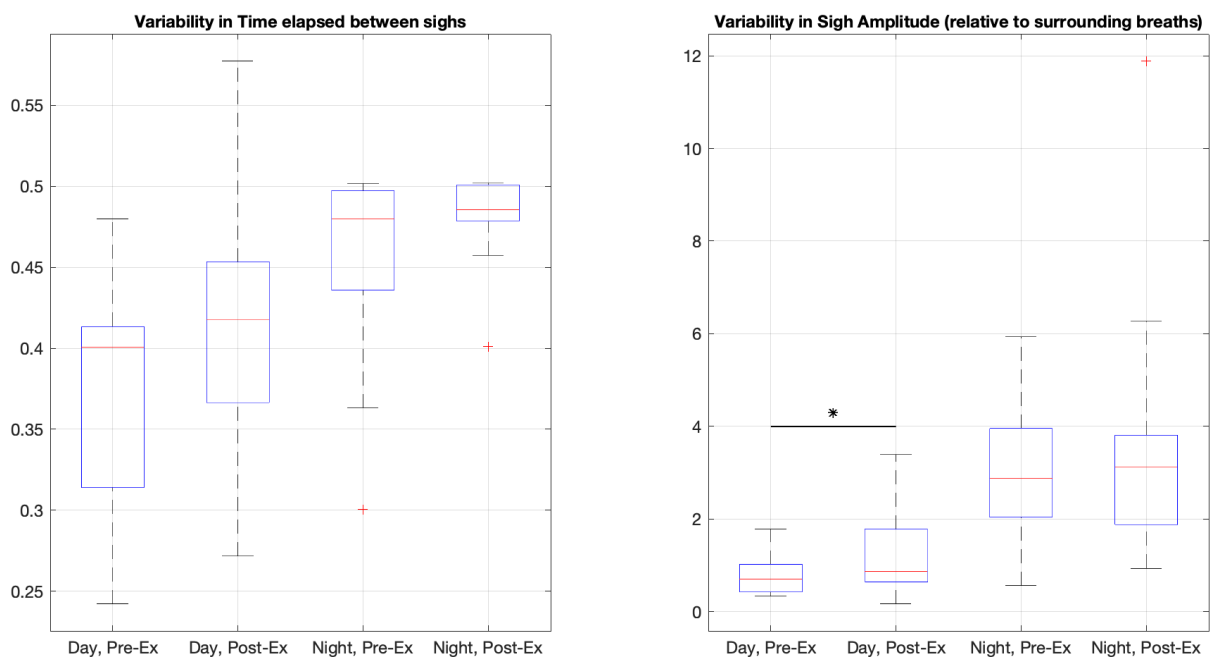


Figure 6.9: Comparison of variability in time elapsed between sighs and sigh amplitude relative to surrounding breaths between the baseline (Pre-Ex) and the end of the exercise program (Post-Ex). Daytime at rest and nighttime were analyzed separately. Statistically significant differences between Pre- and Post-Ex were found for variability in relative sigh amplitude during daytime at rest. The asterisk is set as statistical significance ($p < 0.05$).

6.4 Discussion

The aim of this work was to investigate whether a twelve-week aerobic exercise program would induce changes in respiratory parameters and sigh variability in sedentary adults. In this section, the significant results obtained will be discussed.

6.4.1 Respiratory parameters

In terms of respiratory parameters, statistically significant differences were found in inspiratory time, inspiratory to expiratory time ratio and minute ventilation during nighttime. In particular, an increase was seen in the first two parameters, while a decrease in the last one occurred.

A potential explanation for the increase in inspiratory time and inspiratory to expiratory time ratio could be that exercise, promoting lung health and thus increasing lung elasticity and decreasing bronchopulmonary obstruction, caused the elastic recoil of the pulmonary tissue during expiration to encounter less resistance. As a consequence, since no significant change was observed in respiratory rate and inspiratory time was proven to be increased, expiratory time decreased.

As concerns minute ventilation, since both respiratory rate and tidal volume remained unchanged, its decrease could be explained by the same reason just mentioned: assuming a decreased bronchopulmonary obstruction would agree with the fact that the subjects need to inhale less volume of air in the time unit in order to provide the needed gas exchange to their bodies.

These changes seem to occur during daytime as well, but none of them is statistically significant. The reason behind this might be the fact that during sleep expiration is mainly passive, thus it is the condition in which the elastic recoil of the pulmonary tissue mostly influences breathing mechanics.

6.4.2 Sigh rate and amplitude

During daytime at rest the mean sigh rate increased, but its changes were not proven to be statistically significant. Still regarding daytime at rest, a significant increase in sigh amplitude has occurred. This could be explained by the same reason cited in subsection 6.4.1 when discussing about respiratory parameters: a promoted lung health and consequently an increase in lung elasticity and a decrease in bronchopulmonary obstruction would explain a bigger sigh amplitude since encountering less resistance would produce a sigh with greater amplitude in response to an inspiratory muscle contraction of the same magnitude.

As concerns sigh rate and amplitude during nighttime, these two parameters remained almost unchanged with respect to the baseline. An explanation could be that sighs during nighttime are primarily associated with sleep arousals and, since none of the subjects suffered from sleep disturbances (see criteria of exclusion in section 5.1), overall sleep quality did not change.

6.4.3 Sigh breath variability

The mean variability in time elapsed between sighs slightly increased during both daytime at rest and nighttime, although neither case proved to be statistically significant.

Variability in sigh amplitude remained almost unchanged during nighttime, while a significant increase was seen during daytime at rest. Such increase provides evidence to Professor Pellegrino's assumptions about sigh breath variability as an indicator of lung health, since much other evidence provided by both this work and the study conducted by An Ouyang and his collaborators (Chapter 5) suggest that the exercise program has improved the general health conditions of the participants.

6.4.4 Sighs as nonrandom respiratory variability resetters

The increase in the autocorrelation sequences calculated over post-sigh intervals with respect to pre-sigh was proven to be statistically significant for all three parameters considered: respiratory rate, tidal volume and inspiratory time. Statistical significance was found during both daytime and nighttime.

Recalling that the parameters calculated have been organized in such way as to have correspondence between samples and breaths (only one sample for each breath, see subsection 6.2.6), these findings provide more evidence to support the hypothesis described in subsection 3.2.2, which claims that the randomness in breathing variability increases while approaching a sigh, after which autocorrelation of breathing parameters is reset.

6.5 Limitations

As discussed in sections 5.1 and 6.1, the sample size of this study is limited to seventeen subjects out of the expected thirty. The two main reasons for this are:

- The COVID-19 pandemic, which stopped the enrollment of new participants and caused four subjects to withdraw from the training program
- The poor quality and/or quantity of the Airgo™ signals acquired for nine subjects, since no checks on the signals were carried out during the program

Moreover, the COVID-19 pandemic itself might have caused some bias in the results, since it is well known that lockdowns were strongly associated with significant lifestyle changes (increase in daily sedentary time) [125], increases in depression and anxiety levels ([126], [127], [128]) and decreased sleep quality ([129], [130], [131]).

6.6 Conclusion

This work along with the study conducted by An Ouyang and his collaborators (Chapter 5) provide evidence that an aerobic training program improves overall health conditions in previously sedentary adults.

In particular, the following improvements have occurred:

- Increased aerobic and cardiovascular fitness (subsection 5.3.2)
- Increased brain cognitive health (subsection 5.3.3)
- Increased lung health (section 6.4)

Therefore, further evidence is provided to support how important physical activity is for overall physical and mental wellbeing in humans.

References

- [1] E. McLafferty, C. Johnstone, C. Hendry and A. Farley, "Respiratory system part 1: pulmonary ventilation," *Nursing Standard*, vol. 27, no. 22, pp. 40-47, 2013.
- [2] M. Ochs, J. R. Nyengaard, A. Jung, L. Knudsen, M. Voigt, T. Wahlers, J. Richter and H. J. G. Gundersen, "The number of alveoli in the human lung," *American Journal of Respiratory and Critical Care Medicine*, vol. 169, no. 1, pp. 120-124, January 2004.
- [3] J. V. Fahy and B. F. Dickey, "Airway Mucus Function and Dysfunction," *New England Journal of Medicine*, vol. 363, no. 23, pp. 2233-2247, 2010.
- [4] J. E. Hall, Guyton and Hall Textbook of Medical Physiology, Saunders, 2010, p. 489–491.
- [5] "Pleural effusion," in *Murray and Nadel's textbook of respiratory medicine*, WB Saunders, 2016, pp. 1396-1424.
- [6] N. Hall, "Boyle's Law," NASA, [Online]. Available: <https://www.grc.nasa.gov/www/k-12/airplane/boyle.html>. [Accessed 17 March 2022].
- [7] "Mechanics of Ventilation," SEER Training, [Online]. Available: <https://training.seer.cancer.gov/anatomy/respiratory/mechanics.html>. [Accessed 16 March 2022].
- [8] P. Wilson, "Anatomy of Muscle," in *Reference Module in Biomedical Sciences*, Elsevier, 2014.
- [9] D. A. Rubenstein, W. Yin and M. D. Frame, "Flow in the lungs," in *Biofluid Mechanics*, Third ed., Elsevier, 2022.
- [10] P. Kolář, J. Neuwirth, J. Šanda, V. Suchánek, Z. Svatá, J. Volejník and M. Pivec, "Analysis of diaphragm movement, during tidal breathing and during its activation while breath holding, using MRI synchronized with spirometry," *Physiological Research*, pp. 383-392, 2009.
- [11] S. Intagliata, A. Rizzo and W. Gossman, Physiology, Lung Dead Space, StatPearls, 2021.

-
- [12] J. Feher, "Control of Ventilation," in *Quantitative Human Physiology (Second Edition)*, Elsevier, 2017, pp. 602-610.
- [13] J. C. Smith, H. H. Ellenberger, K. Ballanyi, D. W. Richter and J. L. Feldman, "Pre-Bötzinger Complex: a Brainstem Region that May Generate Respiratory Rhythm in Mammals," *Science*, vol. 254, no. 5032, pp. 726-729, 1991.
- [14] N. Koshiya and J. C. Smith, "Neuronal pacemaker for breathing visualized in vitro," *Nature*, vol. 400, no. 6742, pp. 360-363, 1999.
- [15] K. Kam, J. W. Worrell, W. A. Janczewski, Y. Cui and J. L. Feldman, "Distinct Inspiratory Rhythm and Pattern Generating Mechanisms in the preBotzinger Complex," *Journal of Neuroscience*, vol. 33, no. 22, pp. 9235-9245, 2013.
- [16] Z. Yang, J. Zhuang, L. Zhao, X. Gao, Z. Luo, E. Liu, F. Xu and Z. Fu, "Roles of Bronchopulmonary C-fibers in airway Hyperresponsiveness and airway remodeling induced by house dust mite," *Respiratory Research*, vol. 18, no. 1, 2017.
- [17] I.-L. Tsai and K.-Z. Lee, "Attenuation of the pulmonary chemoreflex following acute cervical spinal cord injury," *Journal of Applied Physiology*, vol. 116, no. 7, pp. 757-766, 2014.
- [18] M. A. Cretikos, R. Bellomo, K. Hillman, J. Chen, S. Finfer and A. Flabouris, "Respiratory rate: the neglected vital sign," *Medical Journal of Australia*, vol. 188, no. 11, pp. 657-659, 2008.
- [19] P. B. Lovett, J. M. Buchwald, K. Stürmann and P. Bijur, "The vexatious vital: neither clinical measurements by nurses nor an electronic monitor provides accurate measurements of respiratory rate in triage," *Annals of Emergency Medicine*, vol. 45, no. 1, pp. 68-76, 2005.
- [20] A. Nicolò, M. Girardi and M. Sacchetti, "Control of the depth and rate of breathing: metabolic vs. non-metabolic inputs," *The Journal of Physiology*, vol. 595, no. 19, pp. 6363-6364, 2017.
- [21] A. Nicolò, M. Girardi, I. Bazzucchi, F. Felici and M. Sacchetti, "Respiratory frequency and tidal volume during exercise: Differential control and unbalanced interdependence," *Physiological Reports*, vol. 6, no. 21, 2018.
- [22] M. J. Tipton, A. Harper, J. F. R. Paton and J. T. Costello, "The human ventilatory response to stress: Rate or depth?," *The Journal of Physiology*, vol. 595, no. 17, pp. 5729-5752, 2017.
- [23] R. Parkes, "Rate of respiration: the forgotten vital sign," *Emergency Nurse*, vol. 19, no. 2, pp. 12-17, 2011.
-

-
- [24] I. Smith, J. Mackay, N. Fahrid and D. Kruckeck, "Respiratory rate measurement: a comparison of methods," *British Journal of Healthcare Assistants*, vol. 5, no. 1, pp. 18-23, 2011.
- [25] P. Barthel, R. Wensel, A. Bauer, A. Müller, P. Wolf, K. Ulm, K. .. Huster, D. P. Francis, M. Malik and G. Schmidt, "Respiratory rate predicts outcome after acute myocardial infarction: A prospective cohort study," *European Heart Journal*, vol. 34, no. 22, pp. 1644-1650, 2012.
- [26] K. E. Barrett, S. M. Barman, S. Boitano and H. L. Brooks, "Regulation of Respiration," in *Ganong's Review of Medical Physiology*, New York, McGraw-Hill Medical, 2012.
- [27] A. Herbert, J. Pearn and S. Wilson, "Normal Percentiles for Respiratory Rate in Children — Reference Ranges Determined from an Optical Sensor," *Children*, vol. 7, no. 10, 2020.
- [28] A. Hill, E. Kelly, M. S. Horswill and M. O. Watson, "The effects of awareness and count duration on adult respiratory rate measurements: An experimental study," *Journal of Clinical Nursing*, vol. 27, no. 3-4, pp. 546-554, 2017.
- [29] M. W. Semler, D. G. Stover, A. P. Copland, G. Hong, M. J. Johnson, M. S. Kriss, H. Otepka, L. Wang, B. W. Christman and T. W. Rice, "Flash mob research: a single-day, multicenter, resident-directed study of respiratory rate," *Chest*, vol. 143, no. 6, pp. 1740-1744, 2013.
- [30] E. Sembroski, D. Sanghavi and A. Bhardwaj, "Inverse Ratio Ventilation," StatPearls [Internet], 2 August 2021. [Online]. Available: <https://www.ncbi.nlm.nih.gov/books/NBK535395/>. [Accessed 12 April 2022].
- [31] "I:E ratio," SICS: Scottish Intensive Care Society, [Online]. Available: <https://www.scottishintensivecare.org.uk/training-education/sics-induction-modules/ventilation-i-e-ratio/>. [Accessed 12 April 2022].
- [32] J. P. Goldsmith, E. H. Karotkin, M. Keszler and G. K. Suresh, *Assisted Ventilation of the Neonate*, Elsevier, 2017.
- [33] R. G. Carroll, *Elsevier's Integrated Physiology*, Elsevier, 2007.
- [34] J. Wanger, J. L. Clausen, A. Coates, O. F. Pedersen, V. Busasco, F. Burgos, R. Casaburi, R. Crapo, P. Enright, C. P. M. Van der Grinten, P. Gustafsson, J. Hankinson, R. Jensen, D. Johnson, N. MacIntyre, McKayR., M. R. Miller and D. Navajas, "Standardisation of the measurement of lung volumes," *European Respiratory Journal*, vol. 26, no. 3, pp. 511-512, 2005.
-

-
- [35] R. Pellegrino, G. Viegi, V. Brusasco, R. O. Crapo, F. Burgos, R. Casaburi, A. Coates, C. P. M. Van der Grinten, P. Gustafsson, J. Hankinson, R. Jensen, D. C. Johnson, N. MacIntyre, R. McKay, M. R. Miller, D. Navajas and O. F. Pedersen, "Interpretative strategies for lung function tests," *European Respiratory Journal*, vol. 26, no. 5, pp. 948-968, 2005.
- [36] S. Ajeyalemi, "Lung Volumes," Physiopedia, [Online]. Available: https://www.physio-pedia.com/Lung_Volumes. [Accessed 6 April 2022].
- [37] S. Hallett, F. Toro and J. V. Ashurst, "Physiology, Tidal Volume," StatPearls [Internet], 9 May 2021. [Online]. Available: <https://www.ncbi.nlm.nih.gov/books/NBK482502/>. [Accessed 12 April 2022].
- [38] U. Bhatti, K. Rani and M. Q. Memon, "Variation in lung volumes and capacities among young males in relation to height," *Journal of Ayub Medical College Abbottabad*, vol. 27, no. 2, pp. 200-202, 2014.
- [39] S. W. Littleton, "Impact of obesity on respiratory function," *Respirology*, vol. 17, no. 1, pp. 43-49, 2011.
- [40] C. Rong, H. Bei, M. Yun, W. Yuzhu and Z. Mingwu, "Lung function and cytokine levels in professional athletes," *Journal of Asthma*, vol. 45, no. 4, pp. 343-348, 2008.
- [41] F. Lemaitre, J. Coquart, F. Chavallard, I. Castres, P. Mucci, G. Costalat and D. Chollet, "Effect of additional respiratory muscle endurance training in young well-trained swimmers," *Journal of Sports Science and Medicine*, vol. 12, no. 4, pp. 630-638, 2013.
- [42] P. Myrianthefs and G. Baltopoulos, "A higher tidal volume may be used for athletes according to measured FVC," *The Scientific World Journal*, 2013.
- [43] R. K. C. N. B. V. S. B. Kamal and A. K. Srivastava, "Alterations in Lung Functions Based on BMI and Body Fat % Among Obese Indian Population at National Capital Region," *Nepal Journal of Epidemiology*, vol. 5, no. 2, pp. 470-479, 2015.
- [44] G. Sharma and J. Goodwin, "Effect of aging on respiratory system physiology and immunology," *Clinical Interventions in Aging*, vol. 1, no. 3, pp. 253-260, 2006.
- [45] J. Zeleznik, "Normative aging of the respiratory system," *Clinics in Geriatric Medicine*, vol. 19, no. 1, 2003.
- [46] C. Mittman, N. H. Edelman, A. H. Norris and N. W. Shock, "Relationship between chest wall and pulmonary compliance and age," *Journal of Applied Physiology*, vol. 20, no. 6, pp. 1211-1216, 1965.
-

-
- [47] J. P. Janssens, J. C. Pache and L. P. Nicod, "Physiological changes in respiratory function associated with ageing," *European Respiratory Journal*, vol. 13, no. 1, pp. 197-205, 1999.
- [48] T. R. Martin, R. G. Castile, J. J. Fredberg, M. E. Wohl and J. Mead, "Airway size is related to sex but not lung size in normal adults," *Journal of Applied Physiology*, vol. 63, no. 5, pp. 2042-2047, 1987.
- [49] W. M. Thurlbeck, "Postnatal human lung growth," *Thorax*, vol. 37, no. 8, pp. 564-571, 1982.
- [50] B. Korotzer, S. Ong and J. E. Hansen, "Ethnic differences in pulmonary function in healthy nonsmoking Asian-Americans and European-Americans," *American Journal of Respiratory and Critical Care Medicine*, vol. 161, no. 4, pp. 1101-1108, 2000.
- [51] P. Piriälä, T. Seikkula and P. Välimäki, "Differences between Finnish and European reference values for pulmonary diffusing capacity," *International Journal of Circumpolar Health*, vol. 66, no. 5, pp. 449-457, 2007.
- [52] N. L. Lapp, H. E. Amandus, R. Hall and W. K. C. Morgan, "Lung volumes and flow rates in black and white subjects," *Thorax*, vol. 29, no. 2, pp. 185-188, 1974.
- [53] W. Nystad, S. O. Samuelsen, P. Nafstad and A. Langhammer, "Association between level of physical activity and lung function among Norwegian men and women: the HUNT study," *International Journal of Tuberculosis and Lung Disease*, vol. 10, no. 12, pp. 1399-1405, 2006.
- [54] M. R. Wolfson and T. H. Shaffer, "Respiratory Physiology: Structure, Function, and Integrative Responses to Intervention with Special Emphasis on the Ventilatory Pump," in *Cardiopulmonary Physical Therapy*, Mosby, 2004.
- [55] B. L. Graham, I. Steenbruggen, M. R. Miller, I. Z. Barjaktarevic, B. G. Cooper, G. L. Hall, T. S. Hallstrand, D. A. Kaminsky, K. McCarthy, M. C. McCormack, C. E. Oropez, M. Rosenfeld, S. Stanojevic, M. P. Swanney and B. R. Thompson, "Standardization of Spirometry 2019 Update. An Official American Thoracic Society and European Respiratory Society Technical Statement," *American Journal of Respiratory and Critical Care Medicine*, vol. 200, no. 8, pp. 70-88, 2019.
- [56] B. H. Culver, "Pulmonary Function Testing," in *Clinical Respiratory Medicine*, Saunders, 2012.
- [57] "Air - Composition and Molecular Weight," Engineering ToolBox, 2003. [Online]. Available: https://www.engineeringtoolbox.com/air-composition-d_212.html. [Accessed 15 April 2022].
-

-
- [58] R. G. Castile, "Pulmonary Function Testing in Children," in *Kendig's Disorders of the Respiratory Tract in Children*, Saunders, 2006.
- [59] C. P. Criée, S. Sorichter, H. J. Smith, P. Kardos, R. Merget, D. Heise, D. Berdel, D. Köhler, H. Magnussen, W. Marek, H. Mitfessel, K. Rasche, M. Rolke, H. Worth and R. A. Jörres, "Body plethysmography - Its principles and clinical use," *Respiratory Medicine*, vol. 105, no. 7, pp. 959-971, 2011.
- [60] R. Mehra and K. P. Strohl, "Evaluation and Monitoring of Respiratory Function," in *Sleep Disorders Medicine*, Saunders, 2009.
- [61] A. Aliverti, R. Dellacà, P. Pelosi, D. Chiumello, L. Gattinoni and A. Pedotti, "Compartmental Analysis of Breathing in the Supine and Prone Positions by Optoelectronic Plethysmography," *Annals of Biomedical Engineering*, vol. 29, no. 1, pp. 60-70, 2001.
- [62] A. Aliverti, S. J. Cala, R. Duranti, G. Ferrigno, C. M. Kenyon, A. Pedotti, G. Scano, P. Sliwinski, P. T. Macklem and S. Yan, "Human respiratory muscle actions and control during exercise," *Journal of Applied Physiology*, vol. 83, no. 4, pp. 1256-1269, 1997.
- [63] S. J. Cala, C. M. Kenyon, G. Ferrigno, P. Carnevali, A. Aliverti, A. Pedotti, P. T. Macklem and D. F. Rochester, "Chest wall and lung volume estimation by optical reflectance motion analysis," *Journal of Applied Physiology*, vol. 81, no. 6, pp. 2680-2689, 1996.
- [64] M. C. Khoo, "Determinants of ventilatory instability and variability," *Respiration Physiology*, vol. 122, no. 2-3, pp. 167-182, 2000.
- [65] R. Pool, "Is It Healthy to Be Chaotic?," *Science*, vol. 243, no. 4891, pp. 604-607, 1989.
- [66] T. Brack, A. Jubran and M. J. Tobin, "Effect of Resistive Loading on Variational Activity of Breathing," *American Journal of Respiratory and Critical Care Medicine*, vol. 157, no. 6, pp. 1756-1763, 1998.
- [67] T. Brack, A. Jubran and M. J. Tobin, "Effect of elastic loading on variational activity of breathing," *American Journal of Respiratory and Critical Care Medicine*, vol. 155, no. 4, pp. 1341-1348, 1997.
- [68] A. Jubran, B. J. B. Grant and M. J. Tobin, "Effect of Hyperoxic Hypercapnia on Variational Activity of Breathing," *American Journal of Respiratory and Critical Care Medicine*, vol. 156, no. 4, pp. 1129-1139, 1997.
-

-
- [69] A. Jubran and M. J. Tobin, "Effect of Isocapnic Hypoxia on Variational Activity of Breathing," *American Journal of Respiratory and Critical Care Medicine*, vol. 162, no. 4, pp. 1202-1209, 2000.
- [70] T. Brack, A. Jubran and M. J. Tobin, "Dyspnea and Decreased Variability of Breathing in Patients with Restrictive Lung Disease," *American Journal of Respiratory and Critical Care Medicine*, vol. 165, no. 9, pp. 1260-1264, 2002.
- [71] H. L. Preas, A. Jubran, R. W. Vandivier, D. Reda, P. J. Godin, S. M. Banks, M. J. Tobin and A. F. Suffredini, "Effect of Endotoxin on Ventilation and Breath Variability," *American Journal of Respiratory and Critical Care Medicine*, vol. 164, no. 4, pp. 620-626, 2001.
- [72] R. J. Leigh and D. A. Shaw, "Rapid Regular Respiration in Unconscious Patients," *Archives of Neurology*, vol. 33, no. 5, pp. 356-361, 1976.
- [73] E. Bruce and J. Daubenspeck, "Mechanisms and analysis of ventilatory stability," in *Regulation of breathing*, New York, M. Dekker, 1995, p. 285-313.
- [74] N. Giardino, P. Lehrer and J. Feldman, "The role of oscillations in self- regulation: their contribution to homeostasis," in *Stress and Health: Research and Clinical Applications*, Harwood Academic Publishers, 2000, pp. 27-51.
- [75] E. Vlemincx, I. Van Diest, P. M. Lehrer, A. E. Aubert and O. Van den Bergh, "Respiratory variability preceding and following sighs: A resetter hypothesis," *Biological Psychology*, vol. 84, no. 1, pp. 82-87, 2010.
- [76] G. C. Donaldson, "The chaotic behaviour of resting human respiration," *Respiration Physiology*, vol. 88, no. 3, pp. 313-321, 1992.
- [77] R. L. Hughson, Y. Yamamoto and J. O. Fortrat, "Is the Pattern of Breathing at Rest Chaotic?," *Advances in Experimental Medicine and Biology*, p. 15.19, 1995.
- [78] M. Wysocki, M.-N. Fiamma, C. Straus, C.-S. Poon and T. Similowski, "Chaotic dynamics of resting ventilatory flow in humans assessed through noise titration," *Respiratory Physiology & Neurobiology*, vol. 153, no. 1, pp. 54-65, 2006.
- [79] M. Small, K. Judd, M. Lowe and S. Stick, "Is breathing in infants chaotic? Dimension estimates for respiratory patterns during quiet sleep," *Journal of Applied Physiology*, vol. 86, no. 1, pp. 359-376, 1999.
- [80] E. Vlemincx, J. L. Abelson, P. M. Lehrer, P. W. Davenport, I. Van Diest and O. Van Den Bergh, "Respiratory variability and sighing: a psychophysiological reset model," *Biological Psychology*, vol. 93, no. 1, pp. 24-32, 2013.
-

-
- [81] G. Benchetrit, "Breathing pattern in humans: diversity and individuality," *Respiration Physiology*, vol. 122, no. 2-3, pp. 123-129, 2000.
- [82] M. Modarreszadeh, E. N. Bruce and B. Gothe, "Nonrandom variability in respiratory cycle parameters of humans during stage 2 sleep," *Journal of Applied Physiology*, vol. 69, no. 2, pp. 630-639, 1990.
- [83] M. J. Tobin, K. L. Yang, A. Jubran and R. F. Lodato, "Interrelationship of breath components in neighboring breaths of normal eupneic subjects.," *American Journal of Respiratory and Critical Care Medicine*, vol. 152, no. 6, pp. 1967-1976, 1995.
- [84] M. Wysocki, C. Cracco, A. Teixeira, A. Mercat, J.-L. Diehl, Y. Lefort, J.-P. Derenne and T. Similowski, "Reduced breathing variability as a predictor of unsuccessful patient separation from mechanical ventilation*," *Critical Care Medicine*, vol. 34, no. 8, pp. 2076-2083, 2006.
- [85] B. Suki, A. M. Alencar, M. K. Sujeer, K. R. Lutchen, J. J. Collins, J. S. Andrade, E. P. Ingenito, S. Zapperi and H. E. Stanley, "Life-support system benefits from noise," *Nature*, vol. 393, no. 6681, pp. 127-128, 1998.
- [86] W. A. Mutch, G. M. Eschun, S. E. Kowalski, M. R. Graham, L. G. Girling and G. R. Lefevre, "Biologically variable ventilation prevents deterioration of gas exchange during prolonged anaesthesia," *British Journal of Anaesthesia*, vol. 84, no. 2, pp. 197-203, 2000.
- [87] F. H. Wilhelm, W. Trabert and W. T. Roth, "Characteristics of sighing in panic disorder," *Biological Psychiatry*, vol. 49, no. 7, pp. 606-614, 2001.
- [88] K. Kam, J. W. Worrell, W. A. Janczewski, Y. Cui and J. L. Feldman, "Distinct Inspiratory Rhythm and Pattern Generating Mechanisms in the preBotzinger Complex," *Journal of Neuroscience*, vol. 33, no. 22, pp. 9235-9245, 2013.
- [89] S. P. Lieske, M. Thoby-Brisson, P. Telgkamp and J. M. Ramirez, "Reconfiguration of the neural network controlling multiple breathing patterns: eupnea, sighs and gasps," *Nature Neuroscience*, vol. 3, no. 6, pp. 600-607, 2000.
- [90] A. Ruangkittisakul, S. W. Schwarzacher, L. Secchia, Y. Ma, N. Bobocea, B. Y. Poon, G. D. Funk and K. Ballanyi, "Generation of Eupnea and Sighs by a Spatiochemically Organized Inspiratory Network," *Journal of Neuroscience*, vol. 28, no. 10, pp. 2447-2458, 2008.
- [91] F. H. McCutcheon, "Atmospheric respiration and the complex cycles in mammalian breathing mechanisms," *Journal of Cellular and Comparative Physiology*, vol. 41, no. 2, pp. 291-303, 1953.
-

-
- [92] H. H. Bendixen, G. M. Smith and J. Mead, "Pattern of ventilation in young adults," *Journal of Applied Physiology*, vol. 19, no. 2, pp. 195-198, 1964.
- [93] I. C. Solomon, N. H. Edelman and J. A. Neubauer, "Patterns of Phrenic Motor Output Evoked by Chemical Stimulation of Neurons Located in the Pre-Bötzinger Complex In Vivo," *Journal of Neurophysiology*, vol. 81, no. 3, pp. 1150-1161, 1999.
- [94] F. J. Golder, P. W. Davenport, R. D. Johnson, P. J. Reier and D. C. Bolser, "Augmented breath phase volume and timing relationships in the anesthetized rat," *Neuroscience Letters*, vol. 373, no. 2, pp. 89-93, 2005.
- [95] C. R. Reynolds, K. Vujisic, P. W. Davenport and L. F. Hayward, "Disinhibition of the Dorsomedial Hypothalamus Increases the Frequency of Augmented Breaths in the Anesthetized Rat," *Integration in Respiratory Control: Advances in Experimental Medicine and Biology*, pp. 274-278, 2008.
- [96] R. M. Harper, G. R. Poe, D. M. Rector and M. P. Kristensen, "Relationships between hippocampal activity and breathing patterns," *Neuroscience and Biobehavioral Reviews*, vol. 22, no. 2, pp. 233-236, 1998.
- [97] M. P. Kristensen, G. R. Poe, D. M. Rector and R. M. Harper, "Activity changes of the cat paraventricular hypothalamus during phasic respiratory events," *Neuroscience*, vol. 80, no. 3, pp. 811-819, 1997.
- [98] H. J. Bell, C. Ferguson, V. Kehoe and P. Haouzi, "Hypocapnia increases the prevalence of hypoxia-induced augmented breaths," *American Journal of Physiology - Regulatory, Integrative and Comparative Physiology*, vol. 296, no. 2, pp. 334-344, 2009.
- [99] H. J. Bell and P. Haouzi, "Acetazolamide suppresses the prevalence of augmented breaths during exposure to hypoxia," *American Journal of Physiology - Regulatory, Integrative and Comparative Physiology*, vol. 297, no. 2, pp. 370-381, 2009.
- [100] D. Bartlett, "Origin and regulation of spontaneous deep breaths," *Respiration Physiology*, vol. 12, no. 2, pp. 230-238, 1971.
- [101] L. B. Reynolds, "Characteristics of an inspiration-augmenting reflex in anesthetized cats," *Journal of Applied Physiology*, vol. 17, no. 4, pp. 683-688, 1962.
- [102] M. Glogowska, J. G. Richardson, J. G. Widdicombe and A. J. Winning, "The role of the vagus nerves, peripheral chemoreceptors and other afferent pathways in the genesis of augmented breaths in cats and rabbits," *Respiration Physiology*, vol. 16, no. 2, pp. 179-196, 1972.
-

-
- [103] F. J. Golder, P. J. Reier, P. W. Davenport and D. C. Bolser, "Cervical spinal cord injury alters the pattern of breathing in anesthetized rats," *Journal of Applied Physiology*, vol. 91, no. 6, pp. 2451-2458, 2001.
- [104] N. S. Cherniack, C. Euler, M. Glowgowska and I. Homma, "Characteristics and rate of occurrence of spontaneous and provoked augmented breaths," *Acta Physiologica Scandinavica*, vol. 111, no. 3, pp. 349-360, 1981.
- [105] G. C. Knowlton and M. G. Larrabee, "A unitary analysis of pulmonary volume receptors," *American Journal of Physiology*, vol. 147, no. 1, pp. 100-114, 1946.
- [106] J. Mead and C. Collier, "Relation of volume history of lungs to respiratory mechanics in anesthetized dogs," *Journal of Applied Physiology*, vol. 14, no. 5, pp. 669-678, 1959.
- [107] C. G. Caro, J. Butler and A. B. DuBois, "Some effects of restriction of chest cage expansion on pulmonary function in man: an experimental study," *Journal of Clinical Investigation*, vol. 39, no. 4, pp. 573-583, 1960.
- [108] D. N. Baldwin, B. Suki, J. J. Pillow, H. L. Roiha, S. Minocchieri and U. Frey, "Effect of sighs on breathing memory and dynamics in healthy infants," *Journal of Applied Physiology*, vol. 97, no. 5, pp. 1830-1839, 2004.
- [109] E. Vlemincx, J. Taelman, I. Van Diest and O. Van den Bergh, "Take a deep breath: The relief effect of spontaneous and instructed sighs," *Physiology & Behavior*, vol. 101, no. 1, pp. 67-73, 2010.
- [110] R. Wuyts, E. Vlemincx, K. Bogaerts, I. Van Diest and O. Van den Bergh, "Sigh rate and respiratory variability during normal breathing and the role of negative affectivity," *International Journal of Psychophysiology*, vol. 82, no. 2, pp. 175-179, 2011.
- [111] E. Vlemincx, I. Van Diest and O. Van den Bergh, "A sigh following sustained attention and mental stress: Effects on respiratory variability," *Physiology & Behavior*, vol. 107, no. 1, pp. 1-6, 2012.
- [112] B. G. Ferris and D. S. Pollard, "Effect of deep and quiet breathing on pulmonary compliance in man," *Journal of Clinical Investigation*, vol. 39, no. 1, pp. 143-149, 1969.
- [113] G. Davis and J. Moscato, "Changes in lung mechanics following sighs in premature newborns without lung disease," *Pediatric Pulmonology*, vol. 17, no. 1, pp. 26-30, 1994.
- [114] A. Verrilli, "EPA explains My Air, My Health Sensor Challenge," *Environmental Monitor - Fondriest*, 30 November 2012. [Online]. Available: <https://www.fondriest.com/news/epa-explains-my-air-my-health-sensor-challenge.htm>. [Accessed 19 April 2022].
-

-
- [115] D. T. Kuller, "Breath volume monitoring system and method". United States Patent US20160213287A1, 28 July 2016.
- [116] "Products - Airgo™," MyAir Inc., [Online]. Available: <https://www.myairgo.com/products>. [Accessed 19 April 2022].
- [117] A. Antonelli, A. Stanzi, F. Mazza, M. Venturino, P. Noceti, D. Guilizzoni, A. Aliverti and G. Melloni, "Validation study of the AirGo™ device for continuous monitoring of respiratory function," *European Respiratory Journal*, 2018.
- [118] A. Braghiroli, C. Sacco, A. Giordano, M. Godio, F. Rossato, S. Rossi, S. Carli, B. Balbi, D. Kuller and E. Morrone, "Validation study of a new analysis software to screen sleep respiratory disorders," *European Respiratory Journal*, vol. 58, 2021.
- [119] "Clinical results & Publications - Airgo™," MyAir Inc., [Online]. Available: <https://www.myairgo.com/clinical>. [Accessed 26 April 2022].
- [120] M. I. srl, *Product data sheet - Airgo™*, Milan, 2021.
- [121] "Clinical applications - Airgo™," MyAir Inc., [Online]. Available: <https://www.myairgo.com/use-cases>. [Accessed 22 April 2022].
- [122] S. Biswal, H. Sun, B. Goparaju, M. B. Westover, J. Sun and M. T. Bianchi, "Expert-level sleep scoring with deep neural networks," *Journal of the American Medical Informatics Association*, vol. 25, no. 12, pp. 1643-1650, 2018.
- [123] *MATLAB and Econometrics Toolbox*, Natick, Massachusetts, United States: The MathWorks, Inc., Release 2022a.
- [124] *MATLAB and Statistics and Machine Learning Toolbox*, Natick, Massachusetts, United States: The MathWorks, Inc., Release 2022a.
- [125] S. Stockwell, M. Trott, M. Tully, J. Shin, Y. Barnett, L. Butler, D. McDermott, F. Schuch and L. Smith, "Changes in physical activity and sedentary behaviours from before to during the COVID-19 pandemic lockdown: a systematic review," *BMJ Open Sport & Exercise Medicine*, vol. 7, no. 1, 2021.
- [126] J. Qiu, B. Shen, M. Zhao, Z. Wang, B. Xie and Y. Xu, "A nationwide survey of psychological distress among Chinese people in the COVID-19 epidemic: implications and policy recommendations," *General Psychiatry*, vol. 33, no. 2, 2020.
- [127] L. Sher, "COVID-19, anxiety, sleep disturbances and suicide," *Sleep Medicine*, vol. 70, 2020.
- [128] J. R. Peteet, "COVID-19 Anxiety," *Journal of Religion and Health*, vol. 59, no. 5, pp. 2203-2204, 2020.
-

-
- [129] J. Pinto, M. Van Zeller, P. Amorim, A. Pimentel, P. Dantas, E. Eusébio, A. Neves, J. Pipa, E. Santa Clara, T. Santiago, P. Viana and M. Drummond, "Sleep quality in times of Covid-19 pandemic," *Sleep Medicine*, vol. 74, pp. 81-85, 2020.
- [130] V. Krishnan, R. Gupta, S. Grover, A. Basu, A. Tripathi, A. Subramanyam, A. Nischal, A. Hussain, A. Mehra, A. Ambekar, G. Saha, K. Mishra, M. Bathla, M. Jagiwala, N. Manjunatha, N. Nebhinani, N. Gaur, N. Kumar, P. Dalal, P. Kumar and Midha, "Changes in sleep pattern and sleep quality during COVID-19 lockdown," *Indian Journal of Psychiatry*, vol. 62, no. 4, 2020.
- [131] H. Xiao, Y. Zhang, D. Kong, S. Li and N. Yang, "Social capital and sleep quality in individuals who self-isolated for 14 days during the coronavirus disease 2019 (COVID-19) outbreak in January 2020 in China," *Medical Science Monitor*, vol. 26, 2020.
- [132] E. Vlemincx, I. Van Diest, S. De Peuter, J. Bresseleers, K. Bogaerts, S. Fannes, W. Li and O. Van Den Bergh, "Why do you sigh? Sigh rate during induced stress and relief," *Psychophysiology*, vol. 46, no. 5, pp. 1005-1013, 2009.
- [133] M. Honma, Y. Masaoka, N. Iizuka, S. Wada, S. Kamimura, A. Yoshikawa, R. Moriya, S. Kamijo and M. Izumizaki, "Reading on a smartphone affects sigh generation, brain activity, and comprehension," *Scientific Reports*, vol. 12, no. 1, 2022.
- [134] Z. Nova, H. Skovierova and A. Calkovska, "Alveolar-Capillary Membrane-Related Pulmonary Cells as a Target in Endotoxin-Induced Acute Lung Injury," *International Journal of Molecular Sciences*, vol. 20, no. 4, February 2019.
- [135] "Bronchi, Bronchial Tree, & Lungs," SEER Training, [Online]. Available: <https://training.seer.cancer.gov/anatomy/respiratory/passages/bronchi.html>. [Accessed 15 March 2022].
- [136] E. A. Loiacono, "Empiema pleurico, subdurale, della colecisti: cause e cure," *Medicina Online*, March 2017. [Online]. Available: <https://medicinaonline.co/2017/03/17/empiema-pleurico-subdurale-della-colecisti-cause-e-cure/>. [Accessed 16 March 2022].
- [137] D. C. Dugdale and D. Zieve, "Upper respiratory tract," *MedlinePlus Medical Encyclopedia*, [Online]. Available: <https://medlineplus.gov/ency/imagepages/19378.htm>. [Accessed 14 March 2022].
- [138] D. C. Dugdale and D. Zieve, "Lower respiratory tract," *MedlinePlus Medical Encyclopedia*, [Online]. Available: <https://medlineplus.gov/ency/imagepages/19379.htm>. [Accessed 14 March 2022].
-

-
- [139] "The Amazing Diaphragm," Foundational Concepts, [Online]. Available: <https://www.foundationalconcepts.com/the-pelvic-chronicles-blog/amazing-diaphragm/>. [Accessed 16 March 2022].
- [140] R. L. Drake, W. Vogel and A. W. M. Mitchell, *Gray's Anatomy for Students*, Philadelphia: Elsevier, 2005.
- [141] J. Duffin, "Functional organization of respiratory neurones: a brief review of current questions and speculations," *Experimental Physiology*, vol. 89, no. 5, pp. 517-529, 2004.
- [142] "PubMed results for 'Respiratory Variability'," PubMed, [Online]. Available: <https://pubmed.ncbi.nlm.nih.gov/?term=respiratory+variability>. [Accessed 30 March 2022].
- [143] Kapwatt, "Lung volumes," Wikipedia, [Online]. Available: https://en.wikipedia.org/wiki/Lung_volumes. [Accessed 1 April 2022].
- [144] M. F. Lutfi, "The physiological basis and clinical significance of lung volume measurements," *Multidisciplinary Respiratory Medicine*, vol. 12, no. 1, 2017.
- [145] N. H. L. a. B. I. (NIH), "File: Spirometry NIH.jpg," Wikipedia, 12 November 2013. [Online]. Available: https://en.wikipedia.org/wiki/File:Spirometry_NIH.jpg. [Accessed 8 April 2022].
- [146] V. F. Parreira, D. S. R. Vieira, M. A. C. Myrrha, I. M. B. S. Pessoa, S. M. Lage and R. R. Britto, "Optoelectronic plethysmography: a review of the literature," *Revista Brasileira de Fisioterapia*, vol. 16, no. 6, pp. 439-453, 2012.
- [147] B. M. Koeppen and B. A. Stanton, *Berne & Levy's Physiology*, Philadelphia: Elsevier, 2018.
- [148] H. Ziv and D. Burton, "Respiratory Inductive Plethysmography Band," Patentdocs, 17 March 2011. [Online]. Available: https://www.patentsencyclopedia.com/imgfull/20110066063_02. [Accessed 19 April 2022].
- [149] "NIH, ONC, and EPA award \$100,000 to winner of health and technology challenge," National Institutes of Health (NIH), 4 June 2013. [Online]. Available: <https://www.nih.gov/news-events/news-releases/nih-onc-epa-award-100000-winner-health-technology-challenge>. [Accessed 19 April 2022].
-

Acknowledgements

I would like to thank Kuller David, inventor of the Airgo™ device, for his kindness, his willingness to help me anytime it was needed and for the trust he put in me for this project.

Thanks to Professor Molinari Filippo for passing me the passion for his teachings, and for agreeing to follow me in this thesis project.

Moreover, I would like to thank Professor Pellegrino Riccardo, who had the idea around which my whole thesis was developed.

A special thanks goes to my mother, who taught me discipline and dedication to work, and to my father, who always stood by my side and supported my choices.

Last but not least, I would like to thank my boyfriend, who supported me through these long and difficult five years, putting his needs aside in order to leave me the space I needed to fully dedicate myself to achieving my professional goals.